Enhancing oncolytic adenovirus vector efficacy through co-expression of the p14 fusion-associated small transmembrane protein and adenovirus death protein

Ryan Gregory Clarkin

Submitted to the Faculty of Graduate and Postdoctoral Studies in partial fulfillment of the requirements for the degree of Master of Science in Biochemistry with Specialization in Human and Molecular Genetics

Department of Biochemistry, Microbiology and Immunology

Faculty of Medicine

University of Ottawa

ABSTRACT

Conditionally-replicating adenoviruses (CRAds) have generally demonstrated only modest therapeutic efficacy in human clinical trials, in part due to their poor ability to spread throughout a tumor mass. In these studies, I first examined whether inclusion of an intact early region 3 (E3) and the p14 fusion-associated small transmembrane (FAST) protein in a CRAd vector can enhance oncolytic efficacy by improving viral spread. E3 encodes the adenovirus death protein (ADP), which enhances virus progeny release from infected cells, while p14 FAST can allow spread of the virus through cell-cell fusion. I generated viruses with (CRAdRC109) or without (CRAdRC111) an intact E3 region, which encoded the p14 FAST gene between the fiber coding sequence and E4 region of their viral genomes. In the A549 human lung cancer cell line, both CRAdRC109 and CRAdRC111 expressed p14 FAST at very low levels when compared to CRAdFAST, a similar virus that expressed the protein from within the E3 deletion, and thus had a relatively poor ability to mediate cell-cell fusion. Although inclusion of E3/ADP in CRAdRC109 did result in larger plaques and increased virus spread relative to CRAdRC111, neither virus showed improved oncolytic activity relative to CRAdFAST. I subsequently developed CRAdRC116, in which the E3 region of the viral genome was replaced with a bicistronic expression cassette containing the p14 FAST and ADP coding sequences separated by a self-cleaving 2A peptide sequence. This virus co-expressed p14 FAST and ADP and caused extensive cell-cell fusion in A549 cells. However, expression of ADP from CRAdRC116 did not increase cancer cell killing nor virus spread, and thus did not enhance oncolytic efficacy relative to CRAdFAST. These studies suggest that p14 FAST and ADP do not exhibit synergy when co-expressed from a CRAd vector. Future studies should instead focus on combining other methods of improving viral spread in conjunction with expression of ADP or FAST proteins from CRAd.

ACKNOWLEDGEMENTS

Firstly, I would like to thank my supervisor Dr. Robin Parks for his invaluable advice and support throughout my studies, it is much appreciated. Many thanks to my thesis advisory committee, Dr. Carolina Ilkow and Dr. Tommy Alain, for also providing great insight and guidance. Additionally, I would like to acknowledge and thank the Province of Ontario and University of Ottawa for awarding me with the scholarships that supported my studies.

To my colleagues in the Parks lab, thanks for your support and companionship, particularly JDP for some great mentorship. I wish you all the best!

Lastly, to my family and friends, I am extremely grateful for all of your patience and encouragement whilst listening to me ramble on about the wonders and woes of grad school, especially Mom, Dad, JC, AB, and MP.

TABLE OF CONTENTS

LIST OF ABBREVIATIONS

Δ24: 24 base-pair deletion in conserved region 2 of E1A
β-actin: beta-actin
Ad: adenovirus
ADP: adenovirus death protein
AFP: a-fetoprotein
ANOVA: analysis of variance
BiTEs: bispecific T cell engagers
bp: base-pair
CAR: coxsackie-adenovirus receptor
CMC: carboxymethylcellulose
COX-2: cyclooxygenase 2
CPE: cytopathic effect
CRAd: conditionally-replicating adenovirus
CR2: conserved region 2 of E1A
DNA: deoxyribonucleic acid
dpi: days post-infection
E1: early region 1
E2: early region 2
E3: early region 3
E4: early region 4
ECM: extracellular matrix
ER: endoplasmic reticulum
ERE: estrogen response element
FAST: fusion-associated small transmembrane protein
FBS: fetal bovine serum
GALV: gibbon ape leukemia virus
GFP: green fluorescent protein
GM-CSF: granulocyte-macrophage colony-stimulating factor
HA: hemagglutinin
HAdV-5: human adenovirus C serotype 5
HCC: hepatocellular carcinoma
HIF-1: hypoxia-inducible factor-1
HRP: horseradish peroxidase
hpi: hours post-infection
HSV: herpes simplex virus
HSV-1: herpes simplex virus type 1
IgG: immunoglobulin G
IRES: internal ribosome entry site
ITR: inverted terminal repeats
kDa: kilodalton
mAb: monoclonal antibody
MDSC: myeloid-derived suppressor cell
MEM: minimum essential medium
MHC: major histocompatibility complex

mL: millilitre
MLP: major late promoter
MLTU: major late transcription unit
MOI: multiplicity of infection
MTS: 3-(4,5-dimethylthiazol-2-yl)-5-(3-carboxymethoxyphenyl)-2-(4-sulfophenyl)-2H-tetrazolium
NDV: Newcastle disease virus
NFDM: non-fat dry milk
nm: nanometer
orf: open reading frame
pAb: polyclonal antibody
PBS: phosphate-buffered saline
PFA: paraformaldehyde
PFU: plaque-forming units
PVDF: polyvinylidene fluoride
PSA: prostate-specific antigen
Rb: retinoblastoma protein
RSV: respiratory syncytial virus
SA: splice acceptor
SDS-PAGE: sodium dodecyl sulfate polyacrylamide gel electrophoresis
SV5: simian virus 5
TERT: telomerase reverse transcriptase
TGF-β: transforming growth factor β
TNF-α: tumor necrosis factor alpha
TRAIL: TNF-related apoptosis-inducing ligand
T-reg: regulatory T cell
T-VEC: Talimogene laherparepvec (IMLYGIC®)
VSV: Vesicular stomatitis virus
VV: Vaccinia virus

LIST OF FIGURES

CHAPTER 1: Introduction

1.1. Cancer: a devastating disease of growing prevalence

Cancer is a leading cause of morbidity and mortality worldwide and is responsible for millions of deaths each year. Unfortunately, the negative impact that cancer has on human health is steadily growing as its prevalence is predicted to increase by roughly 75% over the next 20 years (1). It encompasses numerous diseases, all of which are characterized by rapid and/or uncontrolled growth of abnormal cells, which can subsequently invade surrounding tissues.

Hanahan and Weinberg delineate the "hallmarks of cancer" through a series of distinct and integral biological capabilities; of which, sustaining cell proliferation is debatably the most fundamental (2, 3). Cancer cells must also resist cell death, evade growth suppressors, and achieve replicative immortality in order to survive and proliferate. Additionally, tumors induce angiogenesis to fuel their growth, and disease progression can lead to invasion of local tissue and metastatic dissemination to distant sites. More recently, deregulating cellular metabolism and avoiding destruction by the immune system have emerged as core components of cancer pathogenesis, while genomic instability and inflammation have been defined as enabling characteristics in disease progression. The tumor microenvironment, which includes cancer cells, tumor stroma, blood vessels, immune cells, and other associated tissue, also plays a significant role in tumor progression (3, 4).

Conventional treatments for cancer include chemotherapy, radiation therapy, and surgery (5); however, approximately 50% of all cancer patients will ultimately die from the disease (1), clearly illustrating the need for new and more effective therapeutics. In recent years, treatment strategies such as immunotherapy, targeted therapy, stem cell transplants, and precision medicine have shown great promise in improving our ability to treat, and in some cases, cure cancer.

1.2. Oncolytic virotherapy for cancer treatment

Oncolytic virotherapy is an emerging cancer treatment that uses replication-competent viruses, either native or genetically engineered, to selectively infect, replicate in, and kill cancerous tissue, while leaving healthy tissue relatively unharmed (6). Killing of cancer cells by oncolytic viruses can occur through several different mechanisms, including direct virus-mediated cancer cell lysis, disruption of the tumor microenvironment, and induction of a systemic anti-tumour immune response (7, 8). Additionally, genetically engineered oncolytic viruses can be "armed" with therapeutic transgenes to enhance anti-tumor efficacy (9, 10).

The potential of viruses as anti-cancer therapeutics was first recognized during the late 19^{th}-century upon serendipitous observations of tumor regression coinciding with natural virus infection or following vaccination (7, 11, 12). Over the next few decades, several viruses were tested for their ability to infect and replicate in cancer cells. The first clinical studies employing viruses as anti-cancer therapeutics were conducted during the 1950s-70s and included agents such as hepatitis B virus, West Nile virus, adenovirus, and mumps virus (11). The viruses in these early studies, which were wild-type or attenuated in nature, were often eradicated by the immune system and had minimal or no therapeutic efficacy (8). While instances of tumor regression were observed in some cases, the inherent safety risks associated with viral pathogenesis and the inability to restrict viral replication to cancerous tissue rendered the future of oncolytic viruses as useful cancer therapeutics doubtful (13).

Major progress in the field of oncolytic virotherapy was somewhat limited until the 1990s, when researchers began using recombinant DNA technology to modify viral genomes to develop targeted, replication-selective viruses, ushering in a new era of genetically-engineered oncolytic viruses with enhanced cancer-selectivity and reduced pathogenicity (11, 12). Some of the first

genetically engineered oncolytic viruses included herpesvirus, paramyxovirus, poxviruses, and adenoviruses (11, 14-17).

A diverse array of oncolytic viruses has shown promise in preclinical studies and many have recently progressed to clinical trials, including adenoviruses, coxsackieviruses, herpesviruses, paramyxoviruses, parvoviruses, reoviruses, and poxviruses (18-25). As of August 2018, oncolytic viruses are currently listed in 76 clinical trials on clinicaltrials.gov, of which 26 are completed, 28 are recruiting, and 11 are active but not recruiting (26). Three oncolytic viruses have completed clinical trials and been approved for the treatment of cancer. RIGVIR, a wild-type picornavirus ECHO-7, was approved in Latvia in 2004 for treatment of melanoma (27). Following this was Oncorine, an adenoviral vector approved in China in 2005 for the treatment of head and neck cancer (28). Most recently, Imlygic™ (T-VEC or talimogene laherparepvec), a modified herpes simplex virus type 1 (HSV-1) encoding granulocyte-macrophage colony-stimulating factor (GM-CSF), was approved in the USA, Europe, and Australia for the treatment of advanced melanoma (13, 29, 30).

As previously mentioned, oncolytic viruses preferentially infect, replicate in, and kill cancer cells. These viruses exert their anti-cancer activity primarily through tumor-selective viral replication resulting in direct cancer cell lysis and by stimulating an anti-tumor immune response (6). Ensuring selective replication of oncolytic viruses in cancerous tissue and limiting their pathogenicity to surrounding healthy tissue is crucial for their development as safe and effective anti-cancer therapeutics. Cancer cells frequently exhibit deficiencies in antiviral immune response pathways and are thus naturally susceptible to viral infection (9), however, tumor-selectivity can be further increased through several approaches. Viruses that exploit cellular machinery to mediate viral replication can be engineered to contain tumor-specific promoters regulating essential viral

genes, such that viral replication is restricted to cancerous tissue in which the tumor-specific promoter is present (10). Alternatively, essential viral genes can be mutated or deleted such that replication is inhibited or highly attenuated in normal cells, but not in cancerous cells, where the functions of these genes are no longer essential due to inherent changes (i.e. cell cycle deregulation, deficient antiviral response) that occur during carcinogenesis. Tumor-selectivity has also been achieved by engineering oncolytic viruses to target tumor-associated antigens for viral entry, thus restricting viral tropism to cancerous tissue (8, 31).

Translation from the lab to the clinic has revealed that, in most patients, oncolytic viruses exhibit only modest clinical efficacy as monotherapies (32-34). This limited efficacy is likely the result of a variety of factors, including inefficient systemic delivery, poor intratumoral spread, and the immunosuppressive tumor microenvironment. As such, current research is focusing on developing "armed" oncolytic viruses that are engineered to express therapeutic transgenes with the aim of improving their efficacy as anti-cancer agents (35, 36). Importantly, armed oncolytic viruses have the potential to mediate high-level tumor-specific expression of therapeutic transgenes, allowing maximal activity within the tumor microenvironment and while minimizing impact on healthy tissue (10). A variety of transgenes have been investigated for their potential to augment oncolytic activity, including those that encode cytokines, chemokines, antibodies, checkpoint inhibitors, co-stimulatory receptors, bispecific T cell engagers (BiTEs), secreted toxins, prodrug convertases, enzymes targeting the tumor microenvironment, fusogenic membrane glycoproteins, and pro-apoptotic proteins (9, 32, 35, 37). These transgenes ultimately function to enhance viral growth, intratumoral spread, anti-tumor immunity, and/or targeting of the tumor microenvironment of oncolytic viruses (8). Indeed, clinical efficacy has been achieved with armed

oncolytic viruses, including T-VEC (HSV-1) and ONCOS-102 (adenovirus), both of which encode the cytokine GM-CSF (38).

1.3. Oncolytic adenovirus for cancer treatment

1.3.1. Adenovirus biology

Human adenoviruses (Ads) are nonenveloped double-stranded DNA viruses classified within the genus *Mastadenovirus*, family *Adenoviridae* (39). Initially isolated from adenoid tissue in the early 1950s (40), Ads are ubiquitous pathogens that typically cause mild and/or self-limiting illness (41). However, severe disease can occur in pediatric, geriatric, and immunosuppressed populations (42). Clinical manifestations of Ad infection include acute respiratory disease (i.e. bronchitis, pneumonia), conjunctivitis, and gastrointestinal illness.

The Ad virion is characterized by a nonenveloped icosahedral capsid, 70-100 nm in diameter, surrounding a linear double-stranded DNA viral genome of approximately 30-40 kb (43). The icosahedral capsid comprises 252 capsomeres formed from 3 major proteins: II (hexon), III (penton base), and IV (fiber) (44). Trimers of hexon form the 240 nonvertex capsomeres (hexons), whereas pentamers of penton base joined to trimers of fiber protein comprise the 12 vertex capsomeres (pentons) (45). There are also five minor proteins, IIIa, IVa2, VI, VIII, and IX, which mainly function to stabilize the capsid (42, 46). Contained within the Ad virion is the nucleoprotein core which consists of viral DNA bound to protein VII, V, and Mu (42, 47-49).

1.3.2. The adenovirus genome and life cycle

Human Ad C serotype 5 (HAdV-5) is one of the most extensively characterized Ads (43). While the following paragraphs specifically refer to the genome and life cycle of HAdV-5, much of this information is generally true for most Ad serotypes. Its ~36kb genome (Figure 1.1) encodes over 40 proteins and is divided into early and late regions, which are expressed before or after viral

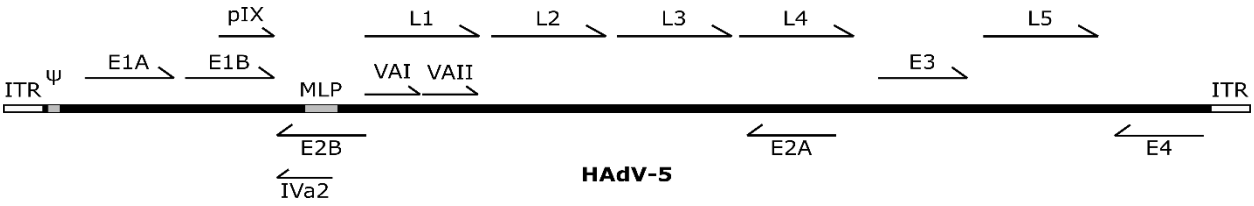
pIX
L1
L2
L3
L4
L5
E1A
E1B
VAI
VAII
E3
ITR
ψ
MLP
ITR
E2B
E2A
E4
IVa2
HAdV-5

Figure 1.1: The human adenovirus C serotype 5 genome. The early regions include E1-E4. The major late promoter (MLP) drives expression of the major late transcription unit (MLTU), consisting of viral late regions L1-L5. ITR denotes the inverted terminal repeats and Ψ represents the packaging element. The genome map is not shown to scale.

DNA replication, respectively (42, 50). Inverted terminal repeats (ITR) located at either end of the Ad genome serve as origins of replication, and the viral packaging sequence is positioned adjacent to the left ITR. The early regions E1A, E1B, E2, E3, and E4 encode ~25 proteins that are maximally expressed shortly after the viral DNA enters the nucleus to ~6 hours post-infection (hpi) (51). The early proteins have 3 main functions: 1) induce S-phase entry and render the cell permissive for viral DNA replication, 2) mediate viral DNA replication, and 3) suppress host antiviral immune responses (50, 52). Ad late gene expression is regulated by the major late promoter (MLP), which is minimally active during the early stages of infection (53) and only fully activated following the onset of viral DNA replication (~8 hpi) (54, 55). The MLP drives expression of the major late transcription unit (MLTU) which through alternative splicing leads to the production of five families of mature mRNAs with co-terminal 3'-ends, designated L1 to L5 (55). The Ad late genes primarily encode structural capsid proteins as well as proteins involved in virion assembly and genome packaging. There are also two non-coding virus-associated RNAs, VA RNA I and II, which are expressed during the late stages of infection and disrupt various cellular processes, including the innate antiviral immune response and microRNA biogenesis (56). Lastly, structural protein IX and the IVa2 protein, which are expressed at intermediate time points (i.e. after early gene expression but before late gene expression), are involved in capsid assembly and packaging of viral DNA into virions (57, 58).

The Ad life cycles takes 24-36h to complete and can lead to the production of ~10,000 progeny virions per infected cell (59). Viral infection and entry begin with binding of the Ad fiber protein to the coxsackie-adenovirus receptor (CAR) on the cell surface (60), followed by interactions between the Ad penton base and cellular integrins (61). Viral internalisation occurs through receptor-mediated endocytosis followed by escape from the early endosome (62).

Subsequent disassembly of the Ad virion occurs during transport to the nucleus via the microtubule network (62, 63). The Ad DNA eventually enters the nucleus via the nuclear pore, where viral DNA replication and virion assembly occur. Finally, host cell lysis during the late stages of infection allows for release of viral progeny (52).

1.3.3. Evolution of conditionally-replicating adenoviruses

Oncolytic or conditionally-replicating Ads (CRAds) have been intensively studied for their use as anti-cancer therapeutics and have shown tremendous promise in preclinical models of cancer (14, 64-67). Ad is well-suited for use as an oncolytic virus for many reasons. For example, Ad has been thoroughly characterized both genetically and biochemically, its double-stranded DNA genome is very stable and can be modified relatively easily through recombinant DNA technology, and large-scale clinical-grade vector stocks can be grown and purified to high titers (68). Furthermore, Ad can infect a wide range of cell types, both dividing and non-dividing (69), and thus has the potential to treat many different forms of cancer. As previously mentioned, up to 10,000 progeny virions can be produced from a single infected cell upon completion of one viral life cycle (70). Progeny virions can then spread to neighbouring cells upon lysis and release, effectively amplifying the therapeutic potential with each round of viral replication (71). Therefore, Ad replication and dissemination of progeny virions should theoretically continue until the tumor has been completely eliminated (14, 72). Ad vectors are also relatively safe as they typically cause mild and/or self-limiting illness in humans and rarely integrate into the genome (73). Taken together, these characteristics clearly illustrate the therapeutic potential of CRAd for the treatment of cancer.

Ensuring tumor-specific replication is of considerable importance in the development of CRAd vectors and has been primarily achieved through two main approaches (74, 75). The first

involves placing expression of E1A, which is required for S-phase entry of the infected cell and transactivation of the viral and cellular machinery necessary for productive viral infection (76), under regulation by tumor-specific promoters. In the second approach, tumor-specific replication can be achieved through the deletion of gene regions, or entire genes, that are essential for viral replication in normal cells, but dispensable in cancer cells.

Replacement of endogenous Ad promoters by tumor- or tissue-specific promoters has been thoroughly investigated as a mechanism to achieve transcriptional regulation of oncolytic Ad replication (75, 77). As previously mentioned, this approach typically involves replacement of the E1A promoter with a heterologous tumor-specific promoter, such that viral replication occurs preferentially in cancer cells in which the heterologous promoter is active (78). For example, insertion of a prostate-specific antigen (PSA) promoter/enhancer sequence upstream of the E1A gene restricted viral replication preferentially to prostate cancer cells expressing PSA (79). Other examples of tumor-specific promoters that have been used to regulate oncolytic Ad replication were reviewed by Toth *et al*. (78) and include, but are not limited to, a-fetoprotein (AFP) (80), estrogen response element (ERE) (81), E2F-1 (82), hypoxia inducible factor-1 (HIF-1) (83), and telomerase reverse transcriptase (TERT) promoters (84).

Tumor-specific replication of CRAd vectors has also been achieved by abolishing gene functions that are necessary for replication in normal cells, but are dispensable in cancer cells (75). This approach largely relies on exploiting the deregulated cell cycle and cell death programs of cancer cells (78). As illustrated by Seymour and Fisher, the "hallmarks of cancer" (3), which define the cellular changes associated with carcinogenesis, are undoubtedly similar to the "hallmarks" of Ad infection (10). For example, carcinogenesis and Ad infection both involve avoiding immune destruction, subverting cell death programs, deregulating cellular metabolism, and deregulating

cell cycle checkpoints. Thus, deletion and/or mutations of viral genes necessary for these functions can impair replication in normal cells, while allowing replication in cancer cells in which these functions are transcomplemented (10). ONYX-015 (*dl*1520) was the first CRAd to employ this gene-deletion approach (64). This vector was designed to selectively replicate in p53-deficient tumor cells through the deletion of the Ad gene encoding the E1B-55kD protein. The rationale for tumor-selectivity in this vector was based on the fact that the E1B-55kD protein functions to bind and inhibit p53, effectively preventing apoptosis of infected cells (78). As the p53 tumor suppressor gene is typically deleted or mutated in most human cancers, this vector should, in theory, only achieve productive replication in p53-deficient cells, but lead to apoptosis or abortive infection in cells with functional p53 (78). Deletions within the Ad E1A region have also been used by several groups to achieve tumor-specific replication (65, 66, 85). Conserved regions 1 (CR1) and 2 (CR2) of the E1A protein function to bind and sequester retinoblastoma protein (pRb) (76). This binding of pRb by E1A causes dissociation of pRb-E2F complexes, which in turn allows E2F to transactivate the viral and cellular genes necessary for the induction of S-phase and viral replication (50, 78). Specifically, a 24 base-pair (bp) deletion within the CR2 domain of the E1A protein abrogates pRb-binding, and thus these vectors replicate poorly in normal cells with an intact G_1-S phase checkpoint, but replicate efficiently in cancer cells in which the pRb pathway is frequently inactive and cell cycle checkpoints are deregulated (65, 66).

Replication-competent Ad vectors can promote cancer cell death through several mechanisms (75). The Ad E1A proteins have demonstrated potent anti-tumor effects in a range of tumor types through various mechanisms, including inhibition of metastasis, sensitization to tumor necrosis factor alpha (TNF-α), and induction of apoptosis (86). Other Ad proteins are also directly cytotoxic; the E4ORF4 protein can induce p53-independent cell death selectively in cancer cells

(87), while the adenovirus death protein (ADP) improves cancer cell lysis and viral release (52, 85). Additionally, viral replication and cell lysis may stimulate a systemic anti-tumor immune response (6).

1.3.4. Cancer clinical trials with unarmed CRAd

CRAd vectors have been extensively studied for their use as anti-cancer therapeutics and represent the most commonly used oncolytic vectors in clinical trials worldwide (38, 71). Results from these studies have illustrated that CRAds have exceptional safety in the clinic; no dose-limiting toxicity has been reported and adverse events were typically mild (78, 88). However, these studies also generally show that, as a stand-alone therapy, CRAd has limited anti-tumor efficacy. Despite this, the first approved oncolytic virus therapy was H101, a CRAd similar to ONYX-015, which has been available in China for the treatment of head and neck squamous cell carcinoma in combination with chemotherapy since 2005 (28). The most recent clinical advancements in oncolytic adenoviruses for treatment of cancer have been review by Pol *et al*. (34).

ONYX-015 (*dl*1520) (64) was the first, and is the most extensively studied, CRAd used in human clinical trials (24, 78, 89, 90). As previously mentioned, this vector contains an E1B-55kDa gene-deletion and was shown to selectively replicate in and kill p53-deficient cancer cells (64). ONYX-015 has been evaluated in over 18 phase I-II clinical trials since 1996 for the treatment of various cancers, including head and neck, hepatocellular, ovarian, prostate, colorectal, lung, pancreatic, and brain cancers (71, 91). Routes of administration included intratumoral, intravenous, intra-arterial, and intraperitoneal injection. ONYX-015 demonstrated excellent safety and was well tolerated at doses of up to 2×10^{12} virus particles (VP) delivered via intratumoral, intraperitoneal, intra-arterial, and intravenous routes of administration (24). Phase I/II trials showed a lack of clinically significant toxicity; adverse events from treatment were generally mild

and most commonly included flu-like symptoms (75). Proof-of-concept for selective viral replication and/or infection in human tumors was also obtained with ONYX-015 (92-94). However, the local tumor regression response rate was only 14% in a phase II trial of intratumoral injection of ONYX-015 in patients with recurrent head and neck cancer (95). No objective responses were observed following intratumoral injection in pancreatic cancer patients (phase I/II) (96), intraperitoneal injection in ovarian cancer patients (phase I) (97), or intravenous administration in patients with metastatic carcinomas (phase I) (92). Thus, results from several clinical studies illustrated that ONYX-015 has limited anti-tumor efficacy (<15% response rate) as a monotherapy. Replication of ONYX-015 is greatly attenuated compared to wild-type Ad (98), which could in part explain the lack of efficacy observed for this virus in human clinical trials. Additionally, the tumor-selectivity of ONYX-015 has been heavily disputed (99), with several studies finding no correlation between p53 status and the extent of viral replication of E1B-55kD-deleted Ads in a range of cancer cell lines (98, 100-103). Results from one study suggested that tumor-selective replication depends on late viral mRNA transport rather than p53 status (104). Collectively, the results obtained with ONYX-015 demonstrated that improved vector design was required to enhance the tumor-selectivity and anti-tumor efficacy of CRAd as a monotherapy, and prompted the discovery and evaluation of other Ad genome mutations that confer tumor-selective replication without attenuating potency (105).

Several groups have explored modulating the expression of E1A in CRAd vectors in an attempt to achieve enhanced anti-tumor efficacy and stringent tumor-selective replication in cancer clinical trials (106-113). OBP-301, a CRAd in which a human telomerase reverse transcriptase (hTERT) promoter drives expression of E1A and E1B linked through an internal ribosome entry site (IRES), was evaluated in a phase I trial in 9 patients with advanced solid cancer (107). Dose-

limiting toxicity was not observed upon intratumoral injection with up to 1 x 10^{12} VP of OBP-301. Disease stabilization was achieved in all patients, with a 6.6-34% reduction in tumor size observed in 6 patients.

CV706 (also referred to as CG7060, CN706), a CRAd in which E1A expression is regulated by the PSA promoter/enhancer, was evaluated in a phase I trial for recurrent prostate cancer (106). Intraprostatic injection with up to 1 x 10^{13} VP of CV706 was well tolerated in all 20 patients, with a ≥50% reduction in PSA levels observed in 5 patients. Evidence of tumor-specific replication was also detected by post-treatment biopsy. CG7870, a similar vector in which the rat probasin promoter drives expression of E1A and the PSA promoter/enhancer drives expression of E1B, was evaluated in a phase I trial for the treatment of metastatic prostate cancer (112). Mild to moderate flulike symptoms and transient hypotension were observed among the 23 patients administered 6 x 10^{12} VP of CG7870 via intravenous injection. A serious adverse event involving grade 3 fatigue was reported, yet was transient and resolved completely. Partial or complete PSA responses were not observed, however, 5 patients had decreases in PSA levels of 25-49%.

A triple modified oncolytic Ad, Ad5/3-Cox2L-D24, which contains an E1AΔ24 mutation, cyclooxygenase 2 (COX-2) promoter regulating E1A expression, and human Ad B serotype 3 fiber knob to enhance transduction, was evaluated in 18 patients with metastatic and refractory solid tumors (111). Grade 1-2 flu-like symptoms were common amongst patients treated with Ad5/3-Cox2L-D24. Grade 3 ileus was observed in one patient. Virus persisted in serum for up to 5 weeks post-treatment and some evidence of anti-tumor efficacy was observed in 11/18 (61%) of patients. Treatment with Ad5/3-Cox2L-D24 showed very promising results in a six-year-old patient with refractory metastatic neuroblastoma (110). Intratumoral injection of 1 x 10^{11} VP lead to a 71% regression of the primary tumor and a reduction of tumor cells detected in the bone marrow.

ICOVIR-7, a CRAd in which an insulator element, modified E2F promoter, and E1AΔ24 deletion confer tumor-selectivity, was evaluated in 21 patients with advanced and refractory solid tumors (109). This vector also contains an RGD-4C modification of the fiber to enhance tumor transduction. Treatment with up to 1 x 10^{12} VP was generally well tolerated. Evidence of anti-tumor activity was reported in 9/17 evaluated patients, with disease stabilization or tumor shrinkage reported in 5 of 12 patients that had undergone radiological evaluation.

DNX-2401, a CRAd containing the E1AΔ24 mutation for tumor-selectivity and an RGD fiber modification for enhanced transduction, was recently evaluated in a phase I trial in patients with recurrent malignant glioma (108). Dose-escalation studies were conducted on one group of 25 patients receiving intratumoral injections of DNX-2401 in recurrent tumors (group A), while a second group of 12 patients received intratumoral injection via permanently implanted catheter followed by *en bloc* resection 14 days post-treatment (group B). No dose-limiting toxicities were reported at doses up to 3 x 10^{10} VP delivered intratumorally. In group B, viral replication was observed in 6/11 (55%) tumor samples at 14 days post-treatment. Tumor shrinkage was reported in 18/25 (72%) patients in group A. Five patients (20%) in group A had >3 years survival, with a ≥95% reduction in the enhancing tumor observed in 3 patients.

Taken together, results from these clinical studies illustrate that oncolytic Ad represents a feasible treatment approach for many types of cancer. Unfortunately, these studies also demonstrate that unarmed CRAds are largely ineffective as monotherapies and suggest that replication-mediated viral oncolysis (cancer cell lysis) alone does not fully eliminate tumors (91).

1.3.5. Limitations of CRAd and strategies to overcome them

A number of physical and immunological factors within the tumor microenvironment can contribute to the limited anti-tumor efficacy of CRAd vectors in the clinic (38, 67, 71, 91). Physical

barriers such as dense stromal tissue, abundant extracellular matrix proteins, increased hydrostatic pressure, and abnormal vascularization can hinder viral spread throughout tumors, while tumor hypoxia can impair Ad replication (38). The tumor microenviroment is also frequently immunosuppressive; elevated levels of cytokines such as transforming growth factor beta (TGF-β) and interleukin 10 (IL-10) recruit myeloid-derived suppressor cells (MDSCs), regulatory T cells (T-regs), and M2 macrophages, which counteract the anti-tumor immune response (114).

One broad strategy to enhance the anti-tumor efficacy of CRAd is the development of vectors armed with therapeutic transgenes which function to improve oncolysis, viral release, intratumoral spread, and/or anti-tumor immune responses (38, 74, 91). When constructing armed CRAd vectors, it is important to ensure that the location in which an exogenous transgene is inserted, and/or its function, does not disrupt viral replication (74). It is also important to consider the cloning capacity of Ad vectors. The genome of HAdV-5 is approximately 36kb. Bett *et al*. showed that genomes of up to 38kb (105%) were stable and efficiently packaged into capsids, while larger genomes were genetically unstable and led to impaired virus growth, thus defining a cloning capacity of approximately 2kb of exogenous DNA (115). Regions nonessential for viral replication, such as the E3 region, can be deleted to further increase cloning capacity.

There are two main approaches for achieving transgene expression from armed CRAd vectors, as described by Cody and Douglas (74). The first involves placing transgene expression under regulation by endogenous viral promoters, which can be achieved by replacing non-essential viral genes with transgenes while retaining the flanking regulatory elements, or by fusing transgenes to viral genes via IRES or 2A peptide sequences which results in co-expression from a single transcript. Alternatively, transgene expression can be regulated through incorporation of exogenous promoters within the viral genome. This approach also typically requires deleting non-

essential viral genes to allow for incorporation of larger expression cassettes. The location at which transgenes are inserted within the viral genome also greatly impacts the kinetics of their expression, which can be exploited to achieve temporal control over expression. For example, expression of transgenes during the early stages of infection can be achieved by fusing transgenes to E1A via IRES or 2A peptide sequences (116). With the exception of ADP, substitution of E3 genes can also allow for early transgene expression (117). In the context of CRAd, transgenes are more commonly expressed during the late stages of infection to ensure replication-dependent, tumor-specific expression and thus minimize toxicity to healthy tissue. Late expression can be achieved by placing the transgene under regulation by the MLP, which drives expression of the MLTU (118). Inclusion of a splice acceptor sequence upstream of the transgene (118, 119), or fusing the transgene to Ad late genes via IRES (116, 120) or 2A peptides (121), allows for expression as a part of the MLTU.

As mentioned previously, CRAds, like many other oncolytic viruses, have a relatively poor ability to spread throughout a tumor mass (122-124). Following intratumoral injection, CRAd typically only diffuses a few millimeters from the injection tract, leaving much of the tumor unaffected (122). Additionally, viral distribution was shown to be uneven and patchy upon intratumoral injection of wild-type Ad in an A549 xenograft mouse model of cancer, suggestive of poor viral spread (123). As a result, CRAd vectors have shown limited therapeutic efficacy in human clinical trials and rarely mediate complete tumor regression (67, 96, 125). Arming CRAds with transgenes that function to enhance oncolysis and viral spread throughout the tumor has been explored as a means to improve overall vector efficacy (38, 67, 77, 78).

Several groups have developed CRAd vectors armed with transgenes targeting the tumor stroma to improve viral spread (126-130). CRAds expressing relaxin, a hormone which decreases

synthesis of extracellular matrix (ECM) proteins, exhibited enhanced viral spread and anti-tumor efficacy compared to non-relaxin-expressing CRAds in xenograft mouse models of cancer (127, 129). Expression of hyaluronidase, an ECM-degrading enzyme, was also shown to enhance intratumoral spread and anti-tumor efficacy of CRAd in a melanoma xenograft mouse model (128). Expression of decorin, which regulates ECM production and assembly, from a CRAd vector was shown to decrease ECM components within the tumor, which improved viral spread and anti-tumor efficacy (126).

Other strategies that have been used to enhance the intratumoral spread of CRAd include overexpression of the adenovirus death protein (ADP) (131) and heterologous expression of fusion-inducing proteins (132). These will be discussed in the following sections.

1.4. CRAd expressing the E3 region and/or adenovirus death protein

The Ad E3 proteins, reviewed by Lichtenstein *et al.*, primarily function to suppress the antiviral immune response and prevent premature killing of infected cells (133). The E3 transcription unit encodes seven proteins: E3-12.5K, E3-6.7K, E3-gp19K, ADP, receptor internalization and degradation protein α (RIDα), RIDβ, and E3-14.7K (133). The E3-gp19K protein inhibits transport of major histocompatibility complex (MHC) class I proteins to the cell surface, which thus prevents killing of infected cells by cytotoxic T cells (134). The RID complex, formed by RIDα and RIDβ, promotes internalization and degradation of proapoptotic receptors such as Fas and TNF-related apoptosis-inducing ligand (TRAIL) receptors (135-137). The E3-6.7K protein also downregulates TRAIL receptors, while E3-14.7K inhibits both TNF- and TRAIL-mediated apoptosis (135, 138). Lastly, ADP is required for efficient virus release during the late stages of infection, while the function of E3-12.5K remains unknown (52, 133).

To increase the cloning capacity of Ad vectors, many are deleted of the E3 region, which is not required for replication in tissue culture. However, previous work has shown that inclusion of the E3 region can improve the oncolytic efficacy of CRAd vectors (139-142). For example, inclusion of the E3 region in a prostate-specific CRAd increased vector efficacy *in vitro* in metabolic activity and plaque assays, and *in vivo* in the LNCaP mouse xenograft model of prostate cancer (140). E3+ CRAdΔ24 vectors have also exhibited improved cell killing *in vitro* in A549, Hs 766T, and SKOV-3 cell lines, and had greater *in situ* propagation and tumor growth inhibition *in vivo* compared to E3-deleted vectors in an A549 xenograft mouse model (142). The immunoregulatory properties of the E3 proteins allow CRAd to persist for longer periods within the tumor and could thereby increase viral replication prior to cell killing (141).

As previously mentioned, the E3 region encodes ADP, an 11.6 kDa nuclear membrane glycoprotein required for efficient cell lysis and release of progeny virions during the late stages of Ad infection (52). Although ADP is encoded within the E3 region, it is minimally expressed from the E3 promoter during early infection, but synthesized in abundance from the MLP during the late stages of infection (143). The exact mechanism by which ADP promotes cell lysis and progeny release remains unknown (131). Tollefson *et al*. showed that Ads expressing ADP began to lyse cells at 2-3 days post-infection (dpi), whereas cell lysis by mutants lacking ADP only began 5-6 dpi (52, 144). Furthermore, ADP-deleted viruses had smaller plaques that developed at a slower rate, which is indicative of impaired cell lysis, progeny release, and spreading of virus to adjacent cells. These studies also showed that cells infected with ADP-expressing viruses exhibited decreased metabolic activity starting at 3 dpi and were completely dead by 5 dpi, whereas cells infected with ADP-deleted viruses retained 90% of their initial metabolic activity at 5 dpi. Thus,

retaining ADP expression, which naturally functions to promote cell lysis and Ad progeny release, would be desirable when trying to maximize cancer cell lysis and intratumoral spread of CRAd.

Several studies have indeed shown that overexpressing ADP (in the absence of other E3 proteins) enhances the oncolytic efficacy of CRAd (85, 145). Doronin *et al.* developed two CRAd vectors, KD1 and KD3, in which overexpression of ADP was achieved by deletion of the E3 region and reinsertion of solely the *adp* gene (85). In A549 human lung cancer cells, KD1 and KD3 lyse cells and spread from cell-to-cell with greater efficiency than wild-type Ad. Furthermore, tumors injected with KD1 or KD3 exhibited reduced growth compared to those injected with a control CRAd vector expressing ADP at wild-type levels. The same group obtained comparable results with two additional vectors overexpressing ADP, named VRX-006 and VRX-007 (145). VRX-006 lacks all other E3 genes, whereas E3-12.5K is retained in VRX-007. VRX-006 and VRX-007 had greater cytopathic effect (CPE), larger plaque size, increased cell lysis, and enhanced cell-cell spread in A549 cancer cell culture compared to viruses that do not overexpress ADP.

Ramachandra *et al*. achieved ADP overexpression from a CRAd vector, termed 01/PEME, through insertion of an additional copy of the MLP within the E3 region immediately upstream of the *adp* gene (146). Compared to viruses that do not overexpress ADP, 01/PEME showed increased CPE *in vitro* in the DLD1 human colon cancer cell line, and exhibited enhanced antitumor efficacy *in vivo* in the PC3, FaDu, and A549 xenograft tumor models.

Yun *et al*. developed two CRAd vectors, designated YKL-cADP and YKL-mADP, in which ADP overexpression was achieved by insertion of a CMV promoter or an extra copy of the MLP upstream of the *adp* gene, respectively (147). With the exception of E3-12.5K and ADP, all other E3 genes were deleted from both vectors. ADP expression from YKL-cADP was detected as early as 12 hpi in A549 cell culture, whereas ADP expression was only detected by 48 hpi in

cells infected with YKL-mADP. Importantly, overexpression of ADP from these vectors did not impair viral replication. Plaques formed by YKL-cADP were slightly larger than those formed by wild-type Ad, and substantially larger than plaques formed by YKL-mADP and YKL-1, an ADP-deleted control vector. YKL-cADP also exhibited a 10 to 100-fold increase in CPE in various cancer cell lines compared to YKL-mADP and YKL-1. Additionally, YKL-cADP had enhanced anti-tumor efficacy relative to YKL-mADP and YKL-1 in the C33A cervical and Hep3B hepatoma xenograft tumor models.

These preclinical studies collectively illustrate that CRAd vectors encoding E3 and/or ADP show great promise as anti-cancer agents. They also provide rationale for evaluating whether ADP expression can increase cancer cell lysis, progeny release, viral spread, and overall anti-tumor efficacy of CRAd in human clinical trials.

1.5. Fusogenic proteins as anti-cancer therapeutics

1.5.1. Viral vectors expressing fusogenic proteins

Many preclinical studies have shown that expression of fusogenic proteins can enhance the anti-tumor efficacy of viral vectors (148). Viral vectors encoding fusogenic proteins cause an infected cell to fuse with adjacent cells leading to the formation of multinucleated syncytia, thereby improving lateral spread of the virus and gene transfer throughout tumors (149-151). Additionally, fusogenic proteins can directly impact tumor viability by reducing cellular metabolic activity, inducing cell death, and promoting systemic anti-tumor immune responses through the release of exosome-like particles called syncytiosomes (149). These syncytiosomes contain tumor antigens and can efficiently prime dendritic cells, leading to cross presentation of tumor antigens and induction of a cancer-specific T cell response (149, 152). Expression of fusogenic proteins has been shown to increase therapeutic efficacy of various oncolytic viruses, including Ad, herpes

simplex virus (HSV), vesicular stomatitis virus (VSV), paramyxovirus, and vaccinia virus (VV) (148, 151, 153-157).

Expression of a modified gibbon ape leukemia virus (GALV) envelope fusogenic membrane glycoprotein from oncolytic HSV was shown to increase killing of Hep3B, U87-MG, and DU-145 cancer cells *in vitro*, and enhance anti-tumor efficacy *in vivo* in the Hep3B xenograft mouse model, relative to a control HSV vector expressing GFP (154). The presence of multinucleated syncytia was also observed in tumors injected with fusogenic HSV, suggesting that cell-cell fusion and syncytiogenesis contribute to the oncolytic effect.

A fusogenic VSV vector expressing a modified fusion protein (F) from Newcastle disease virus (NDV), designated rVSV-NDV/F(L289A), exhibited enhanced oncolytic efficacy in preclinical models of hepatocellular carcinoma (HCC) (153). Infection of HCC cell lines with rVSV-NDV/F(L298A) *in vitro* led to the formation of large multinucleated syncytia and enhanced cytotoxicity relative to a non-fusogenic control vector. Treatment with rVSV-NDV/F(L298A) also caused syncytia formation within tumors and prolonged survival compared to a non-fusogenic control virus in an immunocompetent rat HCC model.

An oncolytic paramyxovirus simian virus 5 (SV5) vector expressing a hyperfusogenic mutant F protein also exhibited enhanced oncolytic efficacy relative to the parental strain (155). The hyperfusogenic vector showed greater efficacy in killing prostate tumor cell lines *in vitro* and was more effective at reducing tumor burden in the LNCaP xenograft mouse model *in vivo*.

1.5.2. Adenovirus vectors armed with fusogenic proteins

Several groups have evaluated the use of Ads encoding fusogenic proteins to improve vector efficacy in preclinical models of cancer (132). Many of the fusogenic proteins examined to date are derived from enveloped viruses, including human immunodeficiency virus (HIV), gibbon

ape leukemia virus (GALV), measles virus (MV), respiratory syncytial virus (RSV), simian virus (SV5), and vesicular stomatitis virus (VSV) (150, 151, 158-163). The function of these proteins for the native virus is to mediate fusion of the virus envelope to the host cell membrane, thus allowing the virus to gain entry into the cell (164). In the context of cancer therapies, expression of these fusion-inducing proteins led to some therapeutic efficacy (i.e. enhanced viral spread, increased cancer cell killing and/or reduced tumor burden) in both replication-deficient and replication-competent Ad vectors (150, 151, 160, 161, 165).

Dewar *et al*. developed an E3-deleted replication-competent Ad vector, designated Ad5env, which contains the HIV-1 envelope gene inserted downstream of the E3 promoter (158). The HIV envelope glycoproteins were expressed in Ad5env-infected HeLa cells at both early and late phases of the Ad life cycle, yet expression was highest during the late phase. Infection of Molt-4 human T-lymphoblast cell culture with Ad5env led to syncytium formation beginning at 5 dpi. Li *et al*. later showed that, in addition to improving release of progeny virions, Ad5env-mediated syncytium formation also enhanced viral replication and spread relative to wild-type Ad5 in HeLa-$CD4^+$ cell culture (151).

Guedan *et al*. developed a replication-competent fusogenic Ad vector, AdwtRGD-GALV, in which expression of a hyperfusogenic GALV envelope glycoprotein was regulated by the MLP (161). This construct allowed for replication-dependent expression of the fusogenic protein which resulted in extensive syncytia formation and enhanced killing of SK-Mel-28 melanoma and A549 lung cancer cells *in vitro*. Interestingly, AdwtRGD-GALV replicated efficiently and had accelerated progeny release compared to non-fusogenic AdwtRGD when delivered at high multiplicity of infection (MOI), yet syncytia formation impaired replication and progeny production in cells infected at low MOI. The same group later developed ICOVIR16, another

CRAd vector expressing a hyperfusogenic GALV envelope glycoprotein (160). This vector contained an E1AΔ24 deletion as well as eight E2F-binding sites and one Sp1-binding site inserted into the E1A promoter to achieve tumor-specific replication. Expression of the fusogenic GALV envelope glycoprotein from this vector led to the formation of large syncytia in SK-Mel-28 melanoma, A549 lung cancer, and NP-18 pancreatic cancer cell lines *in vitro*. ICOVIR16 also demonstrated enhanced killing of SK-Mel-28 and NP-9 cancer cells *in vitro* compared to the parental non-fusogenic CRAd vector ICOVIR15. Intratumoral or intravenous injection of ICOVIR16 led to significantly reduced tumor burden, or even complete tumor eradication in mouse xenograft tumor models of melanoma and pancreatic cancer. Furthermore, expression of the fusogenic GALV envelope glycoprotein was shown to enhance viral spread in ICOVIR16-treated tumors.

These studies illustrate that fusogenic proteins have tremendous potential in improving the anti-tumor efficacy of CRAd vectors. However, fusogenic proteins derived from enveloped viruses are fairly large and, due to Ad DNA packaging limits (115), somewhat difficult to incorporate into Ad vectors, especially in armed vectors encoding additional therapeutic transgenes.

1.5.3. The fusion-associated small transmembrane proteins

The fusion-associated small transmembrane (FAST) proteins, reviewed by Ciechonska and Duncan, are a unique group of non-structural (i.e. not a part of the mature virion) fusogenic proteins derived from several orthoreoviruses (166). Rather than mediating virus-cell fusion and subsequent viral entry, FAST proteins promote cell-cell fusion at later stages of infection, leading to increased viral dissemination, cell lysis, and release of progeny. FAST proteins range from 95-198 amino-acids in size and are thus amenable for cloning into Ad vectors.

Upon being expressed, FAST proteins are shuttled through the endoplasmic reticulum

(ER)-Golgi pathway and accumulate at the plasma membrane, where they multimerize into "fusion platforms" (166). The transmembrane domain of FAST proteins functions as a reverse signal anchor which directs their orientation into the membrane in a $N_{exoplasmic}C_{cytoplasmic}$ topology (167). The process of FAST-mediated cell-cell fusion involves three main stages: pre-fusion, fusion, and post-fusion (166). In the pre-fusion stage, FAST proteins accumulate at the plasma membrane and, with the aid of cellular cofactors, mediate membrane binding and close membrane apposition. During the fusion stage, FAST proteins induce hemifusion (i.e. mixing of the membrane bilayers) and subsequent pore formation. Pore expansion during the post-fusion stage leads to the formation of multinucleated syncytia.

The p14 FAST protein, a 125 amino acid type III transmembrane protein isolated from reptilian reovirus (168), is a promising candidate for enhancing the efficacy of oncolytic vectors. Expression of p14 FAST protein causes extensive syncytium formation and apoptosis-induced membrane instability (169). Previous studies demonstrated that expression of p14 FAST protein from oncolytic VSVΔ51 can improve oncolytic vector efficacy (156, 170). In wild-type VSV, the matrix (M) protein functions to inhibit interferon (IFN) production (171). The oncolytic variant VSVΔ51 harbours a deletion in the matrix (M) protein such that it is unable to inhibit *IFN* gene expression, resulting in a virus that replicates poorly in normal cells with an intact IFN response, but replicates with an efficiency similar to wild-type virus in IFN-deficient cancer cells (156, 171). Oncolytic VSVΔ51 expressing p14 FAST (VSV-p14) increased replication and spread of co-infected double-deleted vaccinia virus, a genetically distinct oncolytic vector containing deletions in the viral thymidine kinase (TK) and VGF genes to confer tumor-selectivity, which led to enhanced oncolytic efficacy *in vitro* in the 786-O kidney cancer cell line and *ex vivo* in human colon tumor samples (156). Relative to VSVΔ51 encoding a GFP reporter gene (VSV-GFP), VSV-

p14 also exhibited increased virus replication and cytolytic activity in MCF-7 and 4T1 breast cancer spheroids *in vitro*, reduced primary tumor growth and prolonged survival in a syngeneic 4T1 mouse model, prolonged survival in a 4T1 metastatic mouse model, and reduced lung metastases in a CT26 metastatic colon cancer mouse model (170). VSV-p14 also enhanced immune cell activation in the tumors, draining lymph nodes, and spleens of 4T1 tumor-bearing mice. Despite showing enhanced efficacy relative to VSV-GFP, complete tumor regression was not observed in any of the tumor-bearing mice treated with VSV-p14, thus illustrating the need for further improvements to achieve complete cure. From these studies, it is evident that the ability of p14 FAST to enhance efficacy of oncolytic viruses, along with its small size, make it an attractive candidate in the development of CRAd vectors armed with fusogenic proteins.

1.6. Rationale, hypothesis, and objectives

Previously, we described a non-replicating, E1-deleted Ad vector expressing p14 FAST protein, which we named AdFAST (172, 173). AdFAST caused cell-cell fusion, reduced metabolic activity and membrane stability, and induced apoptosis in A549 human lung cancer and 4T1 mouse breast cancer cells *in vitro*, but unfortunately did not show therapeutic efficacy in the A549 xenograft nor 4T1 syngeneic mouse models of cancer *in vivo*. We subsequently developed a replication-competent CRAd vector, named CRAdFAST, in which the E3 region of the viral genome was removed and replaced with a p14 FAST expression cassette, which was placed under transcriptional regulation by the MLP (174). CRAdFAST was extremely efficient at fusing cancer cells, showed improved oncolytic activity compared to a non-fusogenic CRAd in A549 and 4T1 cells in culture, and caused a statistically significant reduction in tumor growth rate *in vivo*, but the effect was only modest and did not improve mouse survival.

The purpose of my studies is to investigate whether ADP expression can further enhance

oncolytic efficacy of a fusogenic CRAd vector encoding the p14 FAST protein. I hypothesize that co-expression of the ADP and p14 FAST protein from CRAd will enhance cancer cell killing and viral spread, thereby improving oncolytic efficacy. My objectives include:

I) Develop CRAd vectors, both with and without the ADP gene, that encode the p14 FAST protein.

II) Evaluate the oncolytic activity of these vectors *in vitro* (i.e. viral replication, cell-cell fusion, virus spread, cancer cell killing).

CHAPTER 2: Materials and methods

2.1. Cell culture

293 (175), 293N3S (176) and A549 human lung adenocarcinoma cells (177) were grown in Minimum Essential Medium (MEM) (Sigma Aldrich) containing 10% (v/v) Fetal Bovine Serum (FBS) (Sigma Aldrich), 2mM GlutaMAX (Invitrogen) and 1x antibiotic-antimycotic (Invitrogen). All cells, including Ad-infected cells, were incubated at 37◦C in 5% CO_2.

2.2. Adenoviral constructs and adenovirus purification

Viruses used in this study (depicted in Fig 3.1 and 4.1) are based on HAdV-5 and were generated through conventional and RecA-mediated cloning (178). All oncolytic or CRAd vectors are based on CRAdΔ24 and contain a 24-bp deletion in the conserved region 2 (CR2) of the E1A gene which encodes a region of the protein crucial for retinoblastoma (pRb) binding (65, 66). CRAd is E3-deleted and has been described previously (65). CRAdFAST is also E3-deleted and contains the p14 FAST gene with an upstream splice acceptor site inserted within the E3 deletion, to allow for replication-dependent expression of the p14 FAST protein (174). Vectors containing the p14 FAST gene inserted in the engineered L6 region of the virus were constructed using an approach similar to (161, 179, 180), as follows. pRP2015 is an Ad genomic plasmid deleted of the E1 region but containing an intact E3 region. pRP2015 was digested with XbaI, to generate a plasmid containing the right end of the HAdV-5 genome (nucleotides 30471 to 35938), designated pRC103. The p14 FAST gene was amplified from pCW102 (181) using synthetic oligonucleotides RC102F 5'-gcggaatt ctactaagcggtgatgtttctgatcaatggggagtggaccctctaatttcgtc-3’ and RC102R 5'-gcggaattcaaaaataaatttatt aagcgtagtctgggacgtcgtatggg-3’, which places a splice acceptor site upstream of the p14 FAST gene containing a 3’hemagglutinin (HA)-epitope tag, all flanked by EcoRI restriction sites. The splice acceptor was derived from the Ad40 long fiber gene, as

described previously (119, 182). The resulting PCR fragment was digested with EcoRI, cloned into pGEM7, verified by sequencing, and designated pRC102. The EcoRI fragment from pRC102 was cloned into MfeI digested pRC103, which places the p14 FAST expression cassette downstream of the fiber gene at position 32826 bp of the conventional Ad genome, designated pRC105. pRC105 was recombined into pCW130 (181) to generate pRC111, an Ad genomic plasmid comprised of the E1AΔ24 mutation, E3-deletion, and p14 FAST-HA gene in the L6 region. pRC111 was recovered as a virus in 293 cells, and designated CRAdRC111. A 5.8 kb NheI fragment from pRP2015 was cloned into NheI/XbaI digested pRC105, designated pRC107, which restores the E3 region and flanking sequence in its native position relative to fiber. pRC107 was recombined with pCW130, generating pRC109 an Ad genomic plasmid comprised of the E1AΔ24 mutation, intact E3, and p14 FAST-HA gene in the L6 region. pRC109 was recovered as a virus in 293 cells, designated CRAdRC109.

Vector encoding the p14 FAST and ADP genes, separated by a "self-cleaving" 2A peptide sequence from porcine teschovirus-1 (referred to as P2A) (183), in place of the E3 region was constructed as follows. The p14 FAST gene was amplified from pCW102 (181) using synthetic oligonucleotides CW100F 5'-ccgccatggggagtggacc-3' and FAST-R 5'-cacgtctccagcctgcttcagcaggctgaagttagtagctccgcttccagcgtagtctgggacgtcgtatggg-3', which places an HA-epitope tag, a short Gly-Ser-Gly linker sequence, and approximately two-thirds of the 5-prime sequence encoding the P2A self cleaving peptide downstream of the p14 FAST gene. A second PCR reaction was performed with synthetic oligonucleotides ADP-F 5'-ttcagcctgctgaagca ggctggagacgtggaggagaaccctggacctatgaccaacacaaccaacgcggccgccg-3' and ADP-R 5'-cggactagtcta cttatcgtcgtcatccttgtaatctccgcttcctactgtaagagaaaagaacatgtgtttcagtccg-3', which adds approximately two-thirds of the 3-prime sequence encoding the P2A sequence onto the 5' end of the HAdV-5

ADP gene (nucleotides 29491 to 29769 of the HAdV-5 genome), and a sequence encoding a FLAG-epitope tag onto the 3' end of the ADP gene. The resulting PCR fragments were used as template in an overlap PCR reaction using synthetic oligonucleotide primers CW100F and ADP-R. The p14 FAST-HA/P2A/ADP-FLAG PCR fragment was digested with NcoI and SpeI and cloned into NcoI/SpeI digested pCW102 to generate pRC112, which places the fusion gene downstream of the splice acceptor site derived from the Ad40 long fiber gene (119, 182). Plasmid integrity was verified by sequencing. The 928 bp PvuI fragment from pRC112 was cloned into PacI-digested pDC9 (182) to generate pRC114. The E3 expression cassette from pRC114 was recombined with pCW148 to generate pRC116, an Ad genomic plasmid comprised of the E1AΔ24 mutation and a bicistronic p14 FAST-HA/P2A/ADP-FLAG expression cassette replacing the E3 region. pRC116 was recovered as a virus in 293 cells, designated CRAdRC116. Large-scale purified Ad vector stocks were generated and titered using standard virological techniques (184). Vector titers in particles/millilitre were determined by the OD_{260} assay (184). Infectious titers in plaque-forming units (PFU)/millilitre were determined by plaque assay in 293 cells (184).

2.3. Immunoblotting

All immunoblots were developed with Immobilon Classico Western HRP substrate (MilliporeSigma, WBLUC0500). Densitometry of blots was performed using Image Studio ™ Lite (LI-COR Biosciences).

2.3.1. Immunoblot analysis of purified Ad virions

Ad virus particles ($1x10^9$-$1x10^{10}$ VP) were mixed at a 1:1 ratio with 2 × SDS-PAGE protein loading buffer (62.5 mM Tris HCl pH 6.8, 25% glycerol, 2% SDS, 0.01% bromophenol blue, 5% β-mercaptoethanol), heated for 5 min at 95◦C, separated by electrophoresis on a 12% SDS-PAGE, and transferred onto a polyvinylidene fluoride (PVDF) membrane (MilliporeSigma, IPVH00010).

Membranes were blocked for 1h in 5% w/v non-fat dry milk (NFDM) in TBS-T, then probed with rabbit anti-Ad type 5 polyclonal antibody (pAb) (1:10 000, Abcam #ab6982) and horseradish peroxidase (HRP) conjugated goat anti-rabbit IgG secondary antibody (1:10 000, Bio-RAD #1706515). Membranes were also probed with monoclonal antibody (mAb) to Ad5 fiber (1:10 000, mouse anti-fiber mAb, clone 4D2, Neomarkers) and goat anti-mouse IgG secondary antibody (1:10 000, Bio-RAD #1706515).

2.3.2. Immunoblot analysis of viral protein expression *in vitro*

A549 cells were seeded in 12-well plates at a density of $0.4x10^6$ cells per well. The cells were infected the following day with CRAdFAST, CRAdRC111, CRAdRC109, or CRAdRC116 at an MOI of 1 and 3 plaque-forming units (PFU)/cell for 1h. Whole cell lysates were collected at 24 and 48 hpi in 2 × SDS-PAGE protein loading buffer, separated by 12% or 15% SDS-PAGE, and transferred to PVDF membrane as described above. Membranes were probed with rabbit anti-Ad type 5 pAb (1:10 000, Abcam #ab6982) and horseradish peroxidase (HRP) conjugated goat anti-rabbit IgG secondary antibody (1:10 000, Bio-RAD #1706515) to analyze expression of capsid proteins. Membranes were also probed with mAb to Ad5 fiber (1:10 000, mouse anti-fiber mAb, clone 4D2, Neomarkers) and goat anti-mouse IgG secondary antibody (1:10 000, Bio-RAD #1706515) to assess viral replication. Expression of HA epitope-tagged p14 FAST protein was analyzed by probing with mouse anti-HA tag mAb (1:5000, Cell signaling #2367) and goat anti-mouse IgG secondary antibody (1:10 000, Bio-RAD #1706515). Mouse anti-FLAG mAb (1:1000, Rockland #200-301-383S) and goat anti-mouse IgG secondary antibody (1:10 000, Bio-RAD #1706515) were used to probe for expression of FLAG epitope-tagged ADP. Membranes were also probed with anti-β-actin mouse mAb (1:10 000, Sigma-Aldrich #A1978) as a loading control.

2.4. Analysis of virus spread *in vitro*

2.4.1. Plaque assays

A549 cells were seeded at 1.0 x 10^6 cells per well in 6-well plates. The following day, the cells were infected with serial dilutions of HAdV-5, CRAd, CRAdFAST, CRAdRC111, CRAdRC109, or CRAdRC116 virus stocks for 1h. Plates were rinsed with phosphate-buffered saline (PBS) and 4mL of overlay medium was added to each well. Overlay medium was prepared as follows: 3% carboxymethylcellulose (CMC) (w/v) diluted in water was mixed with equal volumes of 2x MEM containing 20% (v/v) FBS, 4mM GlutaMAX and 2x antibiotic-antimycotic. At 7 dpi, overlay medium was aspirated and the cells were fixed with 4% paraformaldehyde (PFA) in PBS for 30 min and stained with 0.1% crystal violet (w/v) in water for 10 min. Plates were then rinsed with a gentle stream of cold tap water and left to dry overnight. Bright-field images of viral plaques were acquired with Zeiss Axiovert 200 M microscope (10 × objective) and ZEN imaging software (Zeiss).

2.4.2. CPE assays

A549 cells were seeded at 0.15 x 10^6 cells per well in 24-well plates. The cells were infected the following day with HAdV-5, CRAd, CRAdFAST, CRAdRC111, CRAdRC109, or CRAdRC116 at MOI ranging from 0.01-10 PFU/cell for 1h. Media was removed 7 dpi, at which time the cells were fixed with PFA and stained with crystal violet as described above.

2.5. Microscopy

Phase-contrast and bright-field images were acquired with Zeiss Axiovert 200 M microscope (10 × objective). Images were processed with ZEN imaging software (Zeiss) and figures were generated using Inkscape software (www.inkscape.org).

2.6. MTS metabolic activity assays

A549 cells were seeded in 96 well plates at a density of $4x10^4$ cells per well and infected the following day at an MOI of 1 and 10 PFU/cell with CRAd, CRAdFAST, CRAdRC111, CRAdRC109, or CRAdRC116 for 1h. Cellular metabolic activity was measured 24 and 48 hpi using the CellTiter 96 AQueous Non-Radioactive Cell Proliferation Assay (Promega, G5430). Infected cells were incubated with MTS reagent [3-(4,5-dimethylthiazol-2-yl)-5-(3-carboxymethoxyphenyl)-2-(4-sulfophenyl)-2H- tetrazolium] for 1h and absorbance at 490nm was measured using a SpectraMax 190 plate spectrophotometer (Molecular Devices).

2.7. Statistical analysis

Statistical analysis was performed using Graphpad Prism 6.0 ($p=0.05$). One-way ANOVA and Tukey's multiple comparisons tests were conducted on log-transformed viral titer data and densitometric data generated from immunoblot analysis of purified virions. Two-way ANOVA and Tukey's multiple comparisons tests were conducted for metabolic activity studies and densitometric analysis of p14 FAST protein expression.

CHAPTER 3: Evaluating the impact of the E3 region on oncolytic activity of fusogenic CRAd vectors expressing the p14 FAST protein *in vitro*

3.1. Introduction

Although we achieved efficient, replication-dependent p14 FAST protein expression from our CRAdFAST vector, in which a p14 FAST expression cassette replaced the E3 region (174), oncolytic activity was only modestly improved relative to an E3-deleted non-fusogenic CRAd. Previous studies have show that inclusion of the E3 region in CRAd can enhance efficacy of the vector (139-142); this effect is due in part to the ability of the E3-encoded ADP to enhance virus progeny release from the cell, which ultimately enhances virus spread (145). We thus proposed that expression of p14 FAST in an E3-encoding CRAd vector would further improve cell lysis and viral spread, thereby enhancing overall oncolytic efficacy. To test this hypothesis, we generated E3+ and E3- CRAd vectors encoding the p14 FAST protein and evaluated their oncolytic activity *in vitro* in A549 human lung cancer cells.

3.2. Results

3.2.1. Developing fusogenic CRAd vector with p14 FAST expression cassette in the viral late 6 (L6) region

Since our original CRAdFAST construct contained the p14 FAST gene within the E3-deletion, we needed to redesign our construct to encode FAST within an alternative location. Due to its inherent cytotoxicity, we wished to retain replication-dependent expression of p14 FAST protein so that it was not expressed from the CRAd in cells in which the virus cannot replicate (i.e. in non-cancerous tissues). This is achieved by placing transgene expression under regulation of the endogenous MLP, which is minimally expressed before DNA replication (53) and only fully-activated following the onset of Ad DNA replication (54, 55). Aside from within the E3 region (as

in CRAdFAST), several other positions have been identified for insertion of transgenes, including between the viral late 5 (L5) sequence, which encodes fiber, and the E4 coding region (refer to Fig 1.1 for HAdV-5 genome structure) (117, 118). Indeed, insertion of expression cassettes after the L5 region has been used to achieve replication-dependent transgene expression driven by the MLP (51, 179, 180). Notably, this approach was used by Guedan *et al.* to express a hyperfusogenic GALV envelope glycoprotein from a replication-competent Ad vector (161). Thus, insertion of the p14 FAST gene downstream of L5 fiber could be a promising approach for the development of fusogenic CRAd vectors containing an intact E3 region.

We first developed CRAdRC111, an E3-deleted CRAdΔ24 in which the p14 FAST gene and upstream splice acceptor were relocated to a position after the L5 region, which we will refer to as an L6 transcription unit (Fig 3.1). This vector would allow us to test p14 FAST expression from the L6 region relative to our original vector (CRAdFAST) that contained p14 FAST replacing the E3 region. Generation of viral stocks of CRAdRC111 in 293 cells resulted in a high particle yield of ~$1.1x10^{13}$ VP/mL (Fig 3.2A). Interestingly, a plaque-forming assay in 293 cells revealed that the infectious titer of this virus preparation was only ~$1.05x10^{7}$ PFU/mL (Fig 3.2B), indicating that most of the virus particles in our stock were non-infectious. Typically, Ad vectors have a VP/PFU ratio of about 10 (185), and a ratio of between 1 and 100 is generally considered "normal". In contrast, the average VP/PFU ratio for our CRAdRC111 preparation was ~$1.2x10^{6}$ to 1 (Fig 3.2C). To ensure reproducibility of this unexpected result, a second transfection of pRC111 Ad genomic plasmid was performed to generate another preparation of CRAdRC111 vector stock. Titration of the second CRAdRC111 virus preparation revealed that it also had an abnormally high average VP/PFU ratio of ~$4.6x10^{4}$ to 1 (Fig 3.2C). Thus, in our hands, placement of the p14 FAST gene within the L6 region results in a dramatic reduction in the recovery of viable virus.

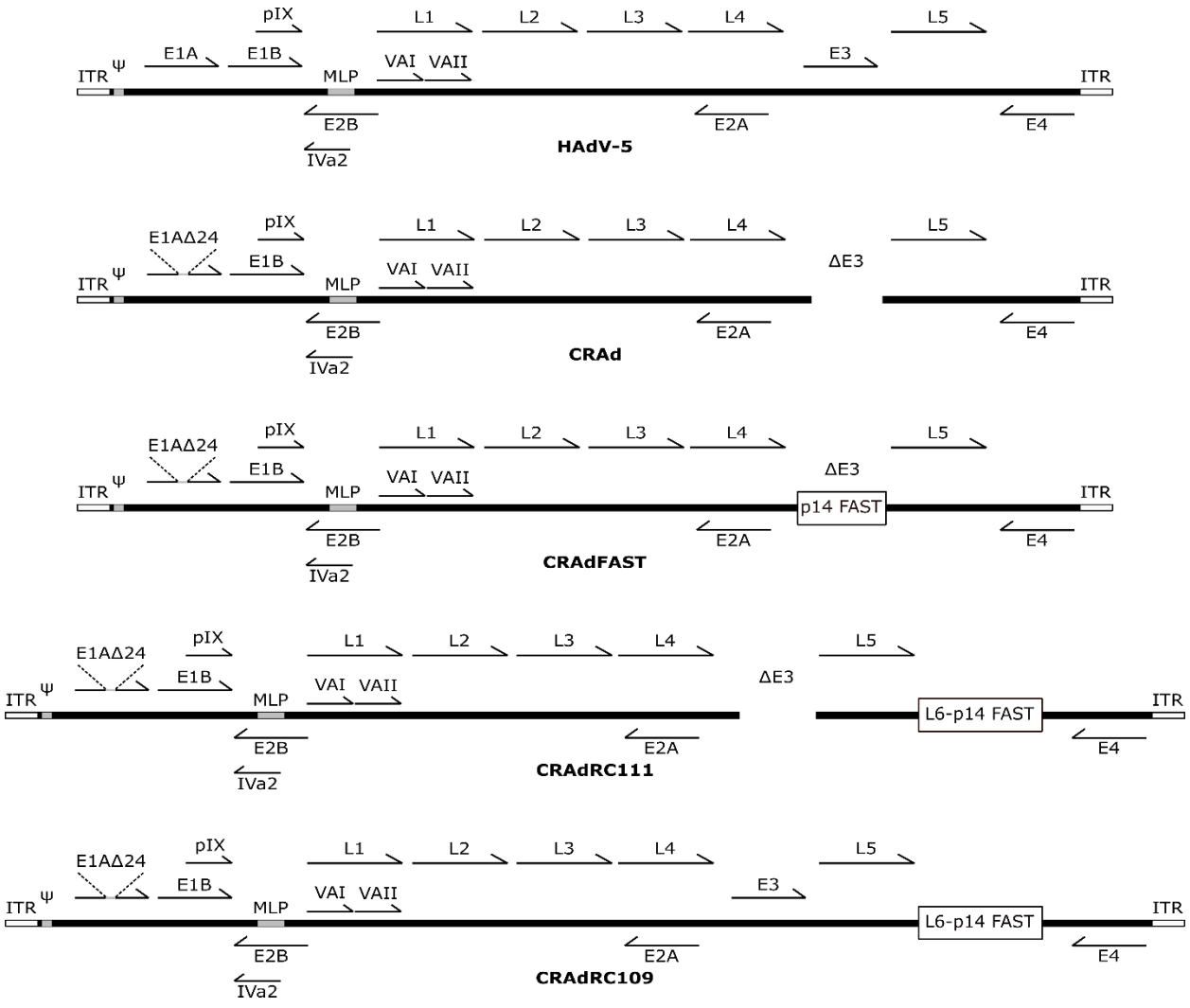
pIX
L1
L2
L3
L4
L5
E1A
E1B
VAI VAII
E3
ITR
Ψ
MLP
ITR
E2B
E2A
E4
IVa2
HAdV-5
E1AΔ24
ΔE3
CRAd
p14 FAST
CRAdFAST
L6-p14 FAST
CRAdRC111
CRAdRC109

Figure 3.1: Viral genome structure of the adenovirus vectors used in chapter 3. HAdV-5 = wild-type human adenovirus C serotype 5. The E1AΔ24 mutation allows for preferential replication in cancer cells deficient in the Rb tumor-suppressor pathway. The E3 region in CRAdFAST is removed and replaced with an HA-tagged p14 FAST expression cassette. The presence of a splice acceptor (SA) DNA element upstream of the p14 FAST gene allows for replication-dependent expression of the protein. CRAdRC111 is E3-deleted, with an HA-tagged p14 FAST placed downstream of the L5 region, creating an L6 region. The p14 FAST gene contains an upstream SA for replication-dependent expression. CRAdRC109 contains E3 and an L6-encoded HA-tagged p14 FAST expression cassette identical to CRAdRC111. ITR denotes the inverted terminal repeats, MLP denotes the major late promoter, and Ψ represents the packaging element. The genome maps are not shown to scale.

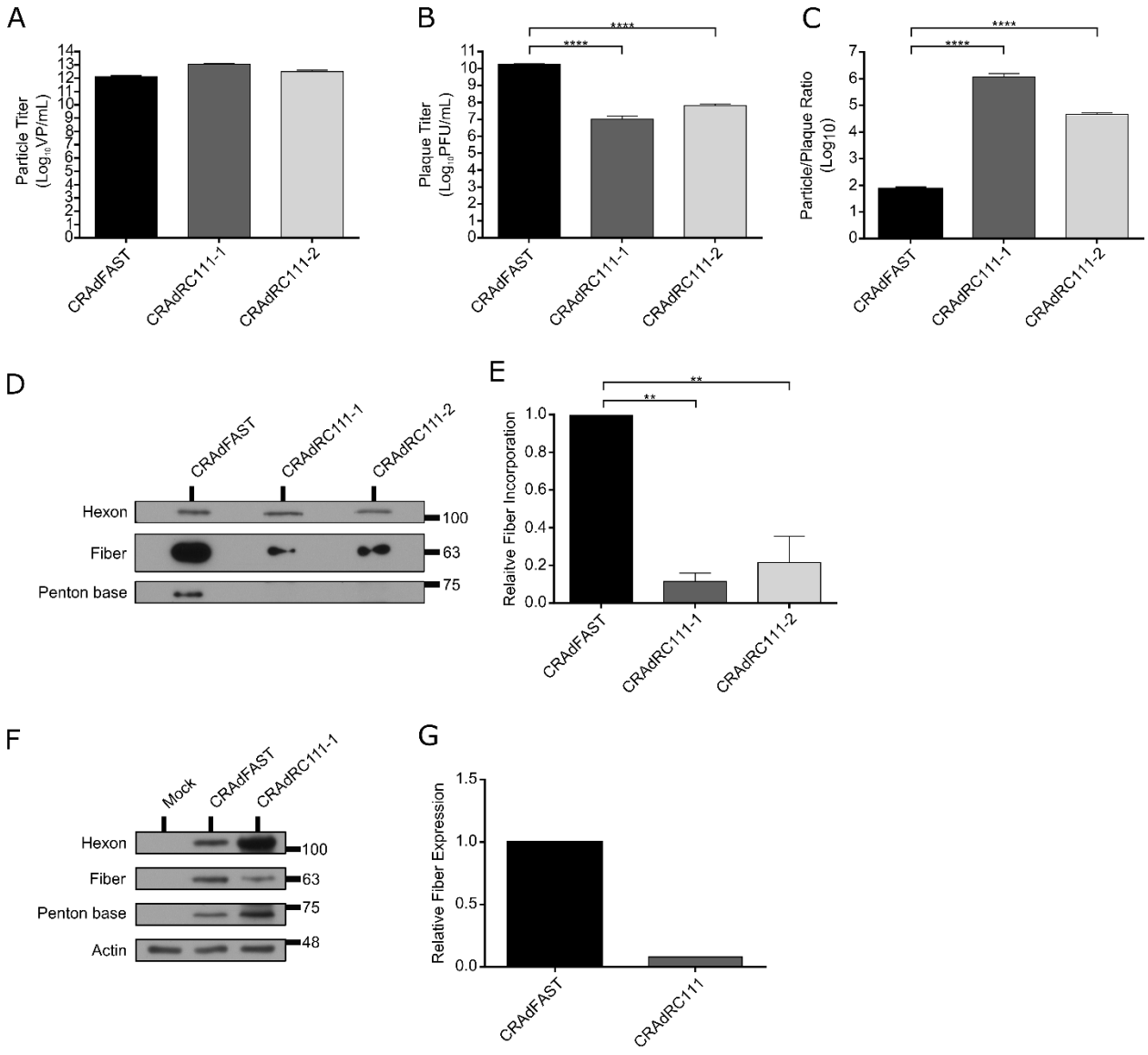
A
Particle Titer
(Log10VP/mL)
CRAdFAST
CRAdRC111-1
CRAdRC111-2
B
Plaque Titer
(Log10PFU/mL)
****
****
C
Particle/Plaque Ratio
(Log10)
****
****
D
Hexon
Fiber
Penton base
100
63
75
E
Relaitve Fiber Incorporation
**
**
F
Mock
Actin
48
G
Relative Fiber Expression
CRAdRC111

Figure 3.2: CRAdRC111 vector stocks have low infectious titer due to deficiencies in fiber and penton base. Viral titers of purified vector stocks are shown in A) virus particles per mL and B) infectious units by plaque-forming units (PFU) per mL. ***p=0.0008, ****p<0.0001). C) Virus particle/mL to PFU/mL ratio of vector stocks. ****p<0.0001. Values graphed in panels A-C represent the average from three separate measurements for each stock (n=3), with error bars denoting standard deviation. Please note that the Y axis for graphs in panels A-C are in $\log_{10}$ scale. CRAdRC111-1 and CRAdRC111-2 denote two independent preparations of purified CRAdRC111 vector stocks. D) Immunoblot analysis of $1x10^9$ virus particles of CRAdFAST and two independent vector stocks of CRAdRC111 was conducted to measure expression of viral capsid proteins. Fiber and penton base signals are markedly reduced in CRAdRC111 virions relative to CRAdFAST virions. E) Densitometric analysis showing reduction of fiber signal intensities in CRAdRC111 virions relative to CRAdFAST virions. Fiber signal intensity was normalized to hexon signal intensity. Averages and standard deviation are shown (n=2). **p<0.006 F) Immunoblot analysis of A549 cells 24 hpi with CRAdFAST or CRAdRC111 at an MOI of 3 PFU/cell. G) Densitometric analysis showing reduction of fiber signal intensity in CRAdRC111-infected cells relative to CRAdFAST-infected cells. Fiber signal intensity was normalized to hexon signal intensity.

3.2.2. CRAdRC111 has reduced infectivity due to deficiencies in fiber and penton base

To begin to elucidate why CRAdRC111 had an extremely high VP/PFU ratio, $1.0x10^9$ purified virus particles of each CRAdRC111 preparation and our original CRAdFAST vector were analyzed by immunoblot. As shown in Fig 3.2D, this analysis revealed that both penton base and fiber appeared to be under-represented in CRAdRC111 relative to CRAdFAST virions. Indeed, the quantity of fiber incorporated into the CRAdRC111 virions was only ~10-20% of that present in CRAdFAST (Fig 3.2E). These data indicate that virions of CRAdRC111 showed reduced incorporation of Ad penton base and fiber, which results in aberrantly high recovery of non-infectious virions in virus stocks. We subsequently analyzed structural protein expression in CRAdRC111-infected cells. A549 cells were infected with CRAdFAST or CRAdRC111 at an MOI of 3 PFU/cell and harvested at 24 hpi for immunoblot analysis. As shown in Fig 3.2F and 3.2G, fiber expression was drastically reduced in CRAdRC111-infected cells compared to CRAdFAST-infected cells, when normalized to hexon expression. Of note, penton base does not appear to be aberrantly expressed within the cell. During virion assembly within the cell, trimers of fiber attach to pentamers of penton base to form penton capsomere complexes in the cytoplasm, which are then shuttled into the nucleus (186, 187). Reduced expression of fiber likely results in reduced formation of penton capsomeres within the cell, leading to reduced availability for virion assembly. Thus, inclusion of the p14 FAST expression cassette in the L6 region of CRAdRC111 led to reduced expression of the L5-fiber protein, resulting in reduced incorporation of the penton capsomeres in the progeny virions and a high proportion of non-infectious particles in our vector preparations.

3.2.3. p14 FAST protein is poorly expressed from the L6 region of CRAd

Despite its high VP/PFU ratio, we proceeded to evaluate replication and p14 FAST protein expression of CRAdRC111 in cancer cells. A549 cells were infected with either CRAdFAST or CRAdRC111 at an MOI of 1 and 3 PFU/cell. Of note, an MOI of 1 infectious particle (PFU) per cell corresponds to ~72 and ~46,000 total particles (i.e. infectious and non-infectious particles) per cell for CRAdFAST and CRAdRC111, respectively. Immunoblot analysis of cell lysates harvested 24 and 48 hpi confirmed that both viruses replicate in A549 cells, as indicated by the expression of fiber, a structural viral protein expressed only after viral DNA replication (Fig 3.3). Levels of fiber protein appear elevated in A549 cells infected with CRAdRC111 at an MOI of 3 relative to cells infected with CRAdFAST at the same dose. When normalized to expression of the abundant capsid protein hexon, however, fiber expression in CRAdRC111-infected cells was markedly reduced relative to CRAdFAST-infected cells (data not shown), consistent with our results from Fig 3.2. Unexpectedly, expression of the p14 FAST protein was drastically reduced in cells infected with CRAdRC111 relative to those infected with CRAdFAST (Fig 3.3). Indeed, under conditions in which p14 FAST protein was readily detectable in cells infected with CRAdFAST, the protein was not detectable in CRAdRC111-treated cells. However, upon longer exposure, we could detect expression of p14 FAST protein in the CRAdRC111-treated cells, although at a level less than 50-fold below that observed for CRAdFAST. Thus, relocation of the p14 FAST gene from the E3 region in CRAdFAST to the L6 region in CRAdRC111 resulted in a dramatic reduction in the expression level of the protein.

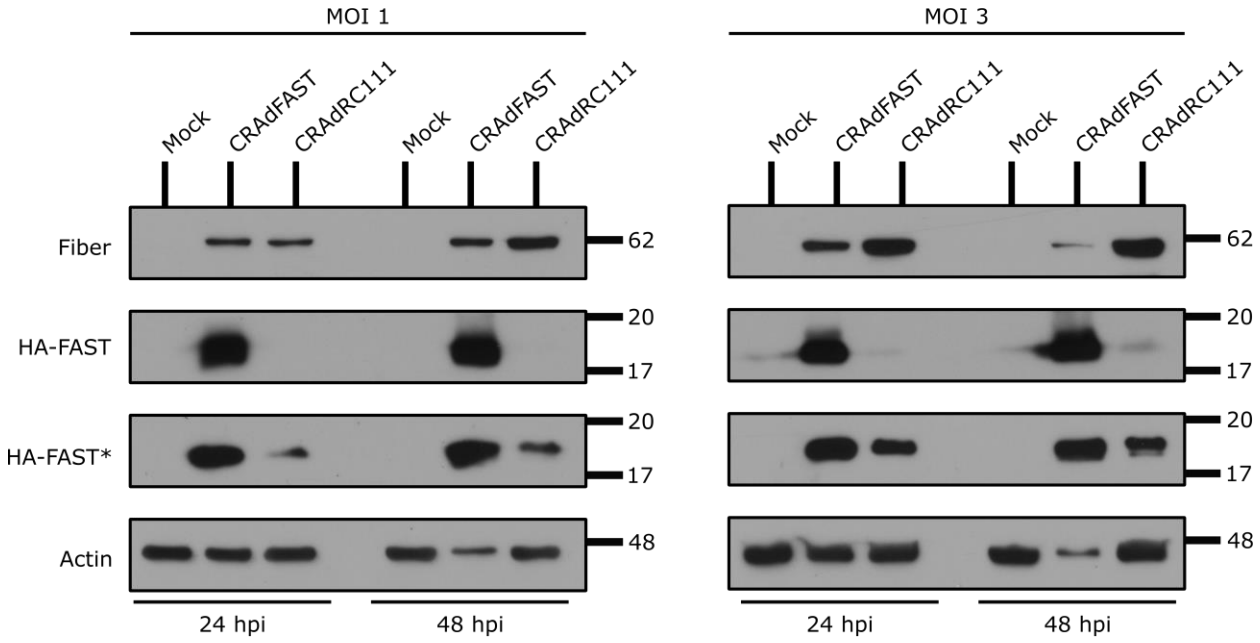

*CRAdFAST samples were diluted 50x

Figure 3.3: CRAdRC111 has reduced p14 FAST expression relative to CRAdFAST. A549 cells were infected with CRAdFAST or CRAdRC111 at an MOI of 1 and 3 PFU/cell, or mock-treated with PBS. Whole cell lysates were collected at 24 and 48 hpi and analyzed via immunoblot. Samples were probed for fiber, HA epitope-tagged p14 FAST, and actin as loading control. Expression of p14 FAST is drastically reduced in CRAdRC111-infected cells compared to CRAdFAST-infected cells. *CRAdFAST samples were diluted 50x.

3.2.4. Restoring the E3 region improves recovery of functional virus but does not improve expression of L6-encoded p14 FAST protein

Previous studies have shown that the "context" of Ad genes can impact their expression. For example, although a codon-optimized Ad fiber protein was expressed more efficiently in mammalian cells during plasmid-based transient transfection assays, when incorporated into a virus, the codon optimized fiber was expressed with poor efficiency (188). Moreover, the codon optimized fiber gene impacted/reduced expression of an L6-encoded transgene, similar to what we observed when p14 FAST was relocated from the E3 region to the L6 region of the viral genome. Since our ultimate goal was to examine potential synergy between p14 FAST and co-expression of E3 proteins, which would in part place fiber in a more natural context within the virus, we generated a new CRAd vector that restored the E3 region and contained p14 FAST within the L6 region, designated CRAdRC109 (Fig 3.1). A high yield of ~$4.4x10^{12}$ VP/mL was obtained upon large-scale virus purification (Fig 3.4A). Plaque-forming assay in 293 cells revealed a relatively high infectious titer of ~$2.1x10^{11}$ PFU/mL (Fig 3.4B), giving an average VP/PFU ratio of ~23 (Fig 3.4C), consistent with what is normally observed for Ad vector stocks. Immunoblot analysis of purified virions showed that incorporation of penton base and fiber protein was improved in CRAdRC109 compared to CRAdRC111 (Fig 3.4D and 3.4E). An analysis of fiber expression in CRAdRC109- and CRAd111-infected cells showed that inclusion of the E3 region improved fiber expression (Fig 3.4F and 3.4G). Thus, restoration of E3 in our CRAd containing the L6-FAST expression cassette appeared to restore fiber expression and normal virus viability.

To determine whether including the E3 region in CRAdRC109 would improve expression of the L6-encoded p14 FAST protein, A549 cells were infected with CRAdFAST, CRAdRC111, or CRAdRC109 at an MOI 1 and 3 PFU/cell, and immunoblot analysis was conducted on whole

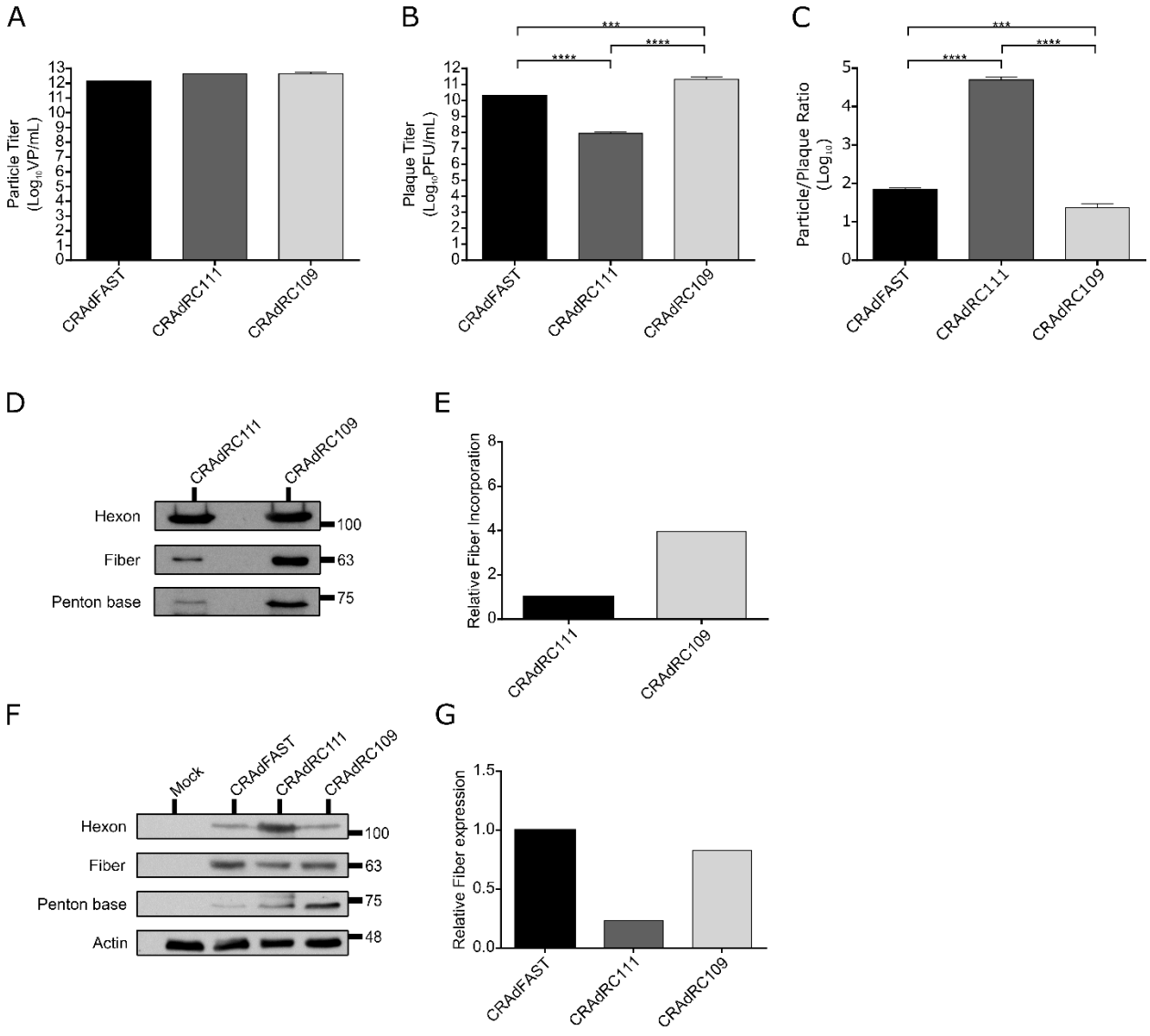
A
Particle Titer
(Log10VP/mL)
CRAdFAST
CRAdRC111
CRAdRC109
B
Plaque Titer
(Log10PFU/mL)
***
****
****
CRAdFAST
CRAdRC111
CRAdRC109
C
Particle/Plaque Ratio
(Log10)
***
****
****
CRAdFAST
CRAdRC111
CRAdRC109
D
CRAdRC111
CRAdRC109
Hexon
Fiber
Penton base
100
63
75
E
Relative Fiber Incorporation
CRAdRC111
CRAdRC109
F
Mock
CRAdFAST
CRAdRC111
CRAdRC109
Hexon
Fiber
Penton base
Actin
100
63
75
48
G
Relative Fiber expression
CRAdFAST
CRAdRC111
CRAdRC109

Figure 3.4: Restoring E3 region in CRAdRC109 improves recovery of functional virus. Viral titers of purified vector stocks in A) Virus particles per mL B) Infectious units by plaque-forming units (PFU) per mL. ***p=0.0005, ****p<0.0001. C) Virus particle/mL to PFU/mL ratio. ***p=0.0008, ****p<0.0001. Values graphed in panels A-C represent the average from three separate measurements for each virus stock (n=3), with error bars denoting standard deviation. Please note that the Y axis for graphs in panels A-C are in $\log_{10}$ scale. D) Immunoblot analysis of $1x10^{10}$ virus particles of CRAdRC111 and CRAdRC109 was conducted to measure expression of viral capsid proteins. Fiber and penton base signal intensities are increased in CRAdRC109 virions relative to CRAdRC111. E) Densitometric analysis showing a ~4-fold increase in fiber signal intensity of CRAdRC109 virions relative to CRAdRC111 virions. Fiber signal intensity was normalized to hexon signal intensity. F) Immunoblot analysis of A549 cells 24 hpi with CRAdFAST, CRAdRC111, or CRAdRC109 at an MOI of 3 PFU/cell. G) Densitometric analysis showing fiber expression is improved in CRAdRC109-infected cells relative to CRAdRC111-infected cells. Fiber signal intensity was normalized to hexon signal intensity.

cell lysates harvested at 24 and 48 hpi (Fig 3.5). Of note, a slight decrease in fiber was observed at the 48 hpi timepoint for CRAdFAST-infected cells with an accompanying decrease in actin, likely due to cell loss resulting from FAST-mediated CPE at this time point. As observed previously (Fig 3.3), p14 FAST protein expression was drastically reduced in CRAdRC111-infected lysates, compared to CRAdFAST. Although inclusion of the E3 region was able to restore expression of the fiber protein in CRAdRC109 (Fig 3.4D and 3.4E), it did not improve expression of p14 FAST protein encoded in the downstream L6 region, as demonstrated by the absence of a detectable signal in Fig 3.5A. To more accurately determine the relative decrease in protein expression when the p14 FAST expression cassette was relocated from the E3 region to the L6 region of the viral genome, whole cell lysates of A549 cells infected with CRAdFAST at an MOI of 3 PFU/cell were diluted 100x-800x and compared to undiluted samples of A549 cells infected with CRAdRC111 or CRAdRC109 at the same MOI (Fig 3.5B). Comparison of signal intensities shows that expression of p14 FAST protein was reduced approximately 400-fold in CRAdRC111 and CRAdRC109-infected cell lysates at 24 hpi, and 100 to 200-fold by 48 hpi relative to CRAdFAST. Thus, in our constructs, placement of p14 FAST within the L6 region led to dramatically lower expression of the protein compared to virus expressing the gene from the E3 region.

3.2.5. CRAds expressing p14 FAST protein from the L6 region show a reduced ability to mediate cell-cell fusion

Since both CRAdRC109 and CRAdRC111 express reduced levels of the p14 FAST protein, we would expect these vectors to have a reduced ability to cause cell-cell fusion relative to CRAdFAST. As shown in Fig 3.5C, infection of A549 cells with CRAdFAST at an MOI of 3 PFU/cell resulted in complete monolayer fusion as early as 24 hpi. In contrast, no cell fusion was

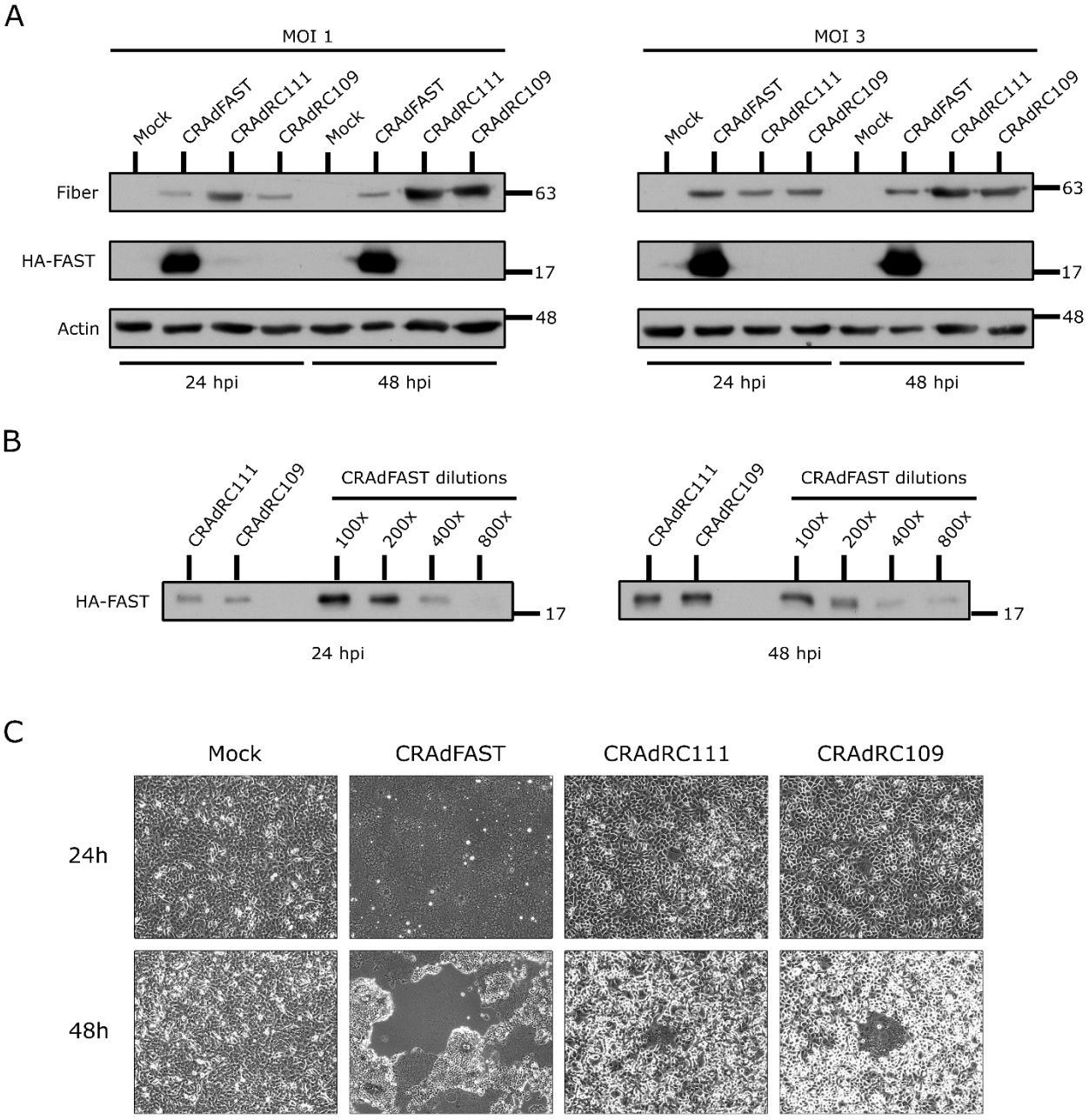
A
MOI 1
MOI 3
Mock
CRAdFAST
CRAdRC111
CRAdRC109
Fiber
HA-FAST
Actin
63
17
48
24 hpi
48 hpi
B
CRAdFAST dilutions
100x
200x
400x
800x
24 hpi
48 hpi
C
24h
48h

Figure 3.5: CRAdRC111 and CRAdRC109 have reduced fusogenic properties in A549 cells compared to CRAdFAST. A) A549 cells were infected with CRAdFAST, CRAdRC111, or CRAdRC109 at an MOI of 1 and 3 PFU/cell, or mock-treated with PBS. Whole cell lysates were collected at 24 and 48 hpi and analyzed via immunoblot. Two independent experiments were performed (n=2) and representative results are shown. B) Whole cell lysates of A549 cells infected with CRAdFAST at an MOI of 3 PFU/cell were diluted 100x-800x. Undiluted samples of A549 cells infected with CRAdRC111 or CRAdRC109 at an MOI of 3 PFU/cell were compared against diluted CRAdFAST samples via immunoblot to determine the relative decrease in p14 FAST expression. Expression of p14 FAST protein was reduced approximately 400-fold in CRAdRC111 and CRAdRC109-infected cells at 24 hpi, and 100 to 200-fold at 48 hpi relative to CRAdFAST-infected cells. Two independent experiments were performed (n=2) and representative results are shown. C) Phase-contrast microscopy images of A549 cells 24 and 48 hpi with CRAdRC109, CRAdRC111, or CRAdFAST at an MOI of 3 PFU/cell. CRAdFAST-infected monolayers are extensively fused at 24 hpi and exhibit complete cytopathic effect at 48 hpi. In contrast, small fusion spots are rarely observed at 48 hpi in CRAdRC111 and CRAdRC109-infected cells. Two independent experiments were performed (n=2) and representative results are shown.

evident at 24 hpi in cells treated with CRAdRC109 or CRAdRC111, but small regions of fused cells were observed at 48 hpi. Taken together, these results show that although the p14 FAST protein is poorly expressed from the L6 position, this level of expression is sufficient to promote cell fusion, albeit much less efficiently than our original CRAdFAST vector.

3.2.6. Inclusion of the E3 region in CRAdRC109 improves viral lysis and cell-cell spread relative to E3-deleted CRAd and CRAdRC111

Several studies have shown that inclusion of the E3 region in CRAd can enhance vector efficacy relative to vector lacking E3 (139-142). This effect is due in part to the ability of the E3-encoded ADP to enhance virus progeny release from the cell, which ultimately enhances virus spread (145). To determine whether inclusion of E3 alters virus spread for our constructs, we first examined plaque morphology. A549 cells were infected for 1 hr with serial dilutions of HAdV-5, CRAd, CRAdFAST, CRAdRC111, or CRAdRC109, and the infected cells were overlayed with semi-viscous CMC overlay media to limit viral spread to immediately adjacent cells, allowing plaque formation (189). At 7 dpi, overlay media was removed and cells were stained with crystal violet to aid in visualization of the viral plaques. Consistent with previous studies (52, 85, 144), HAdV-5 and CRAdRC109, which contain the entire E3 region, form large comet-shaped plaques in A549 cells, whereas the E3-deletion mutants CRAd, CRAdFAST, and CRAdRC111 have a small plaque phenotype (Fig 3.6A). We also examined plaque morphology at higher magnification. HAdV-5 showed a large plaque morphology, whereas CRAd, which lacks E3, showed a small plaque morphology (Fig 3.6B). CRAdFAST formed atypical syncytial plaques consisting of regions of fused cells surrounded by acellular regions reminiscent of conventional viral plaques (Fig 3.6B), similar to what was observed for a fusogenic oncolytic herpesvirus (190). Relocating the p14 FAST gene to L6 in CRAdRC111, which resulted in a significant reduction in the level of

A

HAdV-5 E3+ | **CRAd** E3- | **CRAdFAST** FAST/E3- | **CRAdRC111** L6 FAST/E3- | **CRAdRC109** L6 FAST/E3+

B

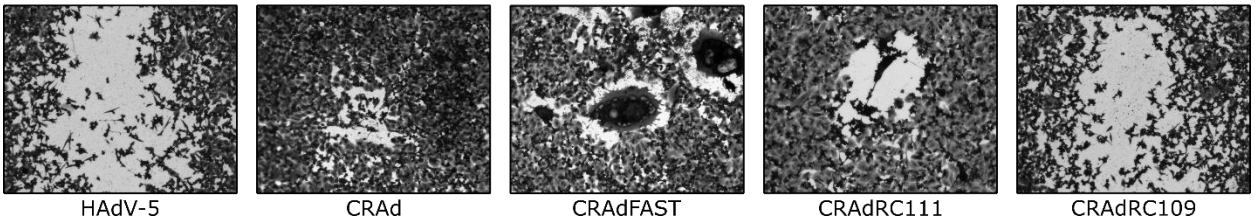

HAdV-5 | CRAd | CRAdFAST | CRAdRC111 | CRAdRC109

Figure 3.6: Inclusion of E3/ADP in CRAdRC109 increases viral plaque size compared to E3-deleted vectors. A) Plaque-forming assay of Ad vectors under carboxymethylcellulose (CMC) overlay. A549 cells were infected with ten-fold serial dilutions of various Ad vectors. Infected cells were fixed and stained with crystal violet 7 dpi. Plaque sizes (depicted by unstained regions) were notably larger in cells infected with human adenovirus C serotype 5 (HAdV-5) or CRAdRC109, which encode E3/ADP. B) Bright-field microscopy images of viral plaques showing increased plaque size of E3-encoding vectors at 7 dpi. CRAdFAST formed syncytial plaques.

p14 FAST protein expression, caused this virus to no longer produce syncytial plaques, but instead produce small plaques similar to CRAd. In contrast, the E3+ CRAdRC109 produced large plaques similar to HAdV-5. Syncytial plaques were very rarely observed in CRAdRC111 and CRAdRC109-infected monolayers. Thus, for CRAdRC111 and CRAdRC109, in which the p14 FAST protein is poorly expressed, plaque size and morphology is dictated by the presence or absence of E3.

We next evaluated vector efficacy through an *in vitro* CPE assay, which provides a measure of viral lysis, progeny release, and cell-cell spread. At high MOI (i.e. 10 PFU/cell), all cells in the monolayer are infected, resulting in complete CPE after a single round of replication (85). At low MOI, multiple rounds of viral replication, cell lysis, release of progeny, and re-infection of neighbouring cells are required to achieve complete monolayer CPE. In this assay, the efficiency of virus spread is reflected in the quantity of virus required to achieve complete CPE. A549 cells were infected with HAdV-5, CRAd, CRAdFAST, CRAdRC111, or CRAdRC109 at MOI ranging from 0.01-10 PFU/cell and overlayed with liquid medium to permit maximal virus diffusion and spread. Seven days later, the monolayers were with stained with crystal violet to qualitatively evaluate the extent of virus-induced CPE. As shown in Fig 3.7, virus containing E3 (HAdV-5 and CRAdRC109) showed significant CPE at an MOI of 0.1, and almost complete CPE at an MOI of 1. CRAdRC111, which lacks E3, required approximately a 10-fold higher amount of virus to achieve complete CPE. The efficient expression of p14 FAST protein from our CRAdFAST vector allowed this virus to mediate complete CPE with only very small amounts of virus (MOI = 0.1), despite the lack of E3.

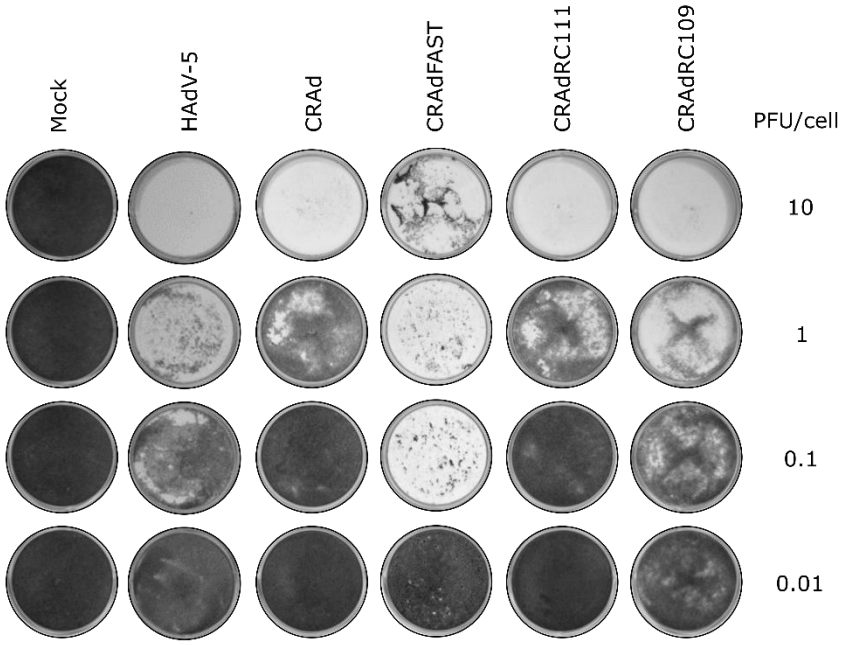
Mock
HAdV-5
CRAd
CRAdFAST
CRAdRC111
CRAdRC109
PFU/cell
10
1
0.1
0.01

Figure 3.7: Inclusion of E3/ADP in CRAdRC109 improves cell-cell spread relative to CRAd and CRAdRC111, but not CRAdFAST. *In vitro* cytopathic effect (CPE) assay in A549 cells. A549 cells were infected with HAdV-5, CRAd, CRAdFAST, CRAdRC111, or CRAdRC109 at an MOI of 0.01-10 PFU/cell. Infected cells were fixed and stained with crystal violet 7 dpi. Vectors containing E3/ADP (HAdV-5 and CRAdRC109) cause extensive CPE, which is indicative of cell death, at low MOI. Evidence of virus-induced CPE was reduced ~10-fold in cells infected with CRAd and CRAdRC111, which lack E3/ADP. CRAdFAST causes extensive CPE at low MOI, despite lacking E3/ADP, likely due to its fusogenic properties. Three independent experiments were performed (n=3) and representative results are shown.

3.2.7. Inclusion of E3 in CRAd expressing p14 FAST from the L6 region does not enhance cell killing relative to CRAdFAST

We have previously shown that treatment of A549 cells with non-replicating AdFAST or replication-competent CRAdFAST vectors caused significantly greater decreases in cellular metabolic activity compared to non-fusogenic control vectors (173, 174). The reduction in metabolic activity was associated with induction of apoptosis and death of the cancer cells. We asked whether our new CRAd vectors that express p14 FAST from the L6 region with (CRAdRC109) or without (CRAdRC111) the E3 region also impact metabolic activity of cancer cells. A549 cells were infected at an MOI of 1 and 10 PFU/cell with a non-fusogenic CRAd, CRAdFAST, CRAdRC111, or CRAdRC109, and metabolic activity was measured 24 and 48 hpi by MTS assay (Fig 3.8). At 24 hpi, all virus-treated cells showed similar metabolic activity relative to mock-treated cells, regardless of dose. At 48 hpi, both CRAd and CRAdFAST showed a significant reduction in metabolic activity, with a trend towards a greater decline in cells treated with CRAdFAST relative to CRAd at the lower MOI; both viruses were able to reduce metabolic activity to a similar extent at the higher MOI of 10. A549 cells treated with CRAdRC111 or CRAdRC109 also showed a reduction in metabolic activity at 48 hpi, at both vector doses, but the effect was statistically less than that observed for CRAdFAST. No statistically significant differences in metabolic activity were observed between CRAd- and CRAdRC111-infected cells at 48 hpi. CRAd-infected cells did, however, show statistically greater decreases in metabolic activity relative to CRAdRC109-infected cells at 48 hpi, but only at an MOI of 10. Metabolic activity of CRAdRC111- and CRAdRC109-infected cells did not statistically differ from one another at any given time point or dose. Thus, in the context of CRAd expressing p14 FAST from the L6 region, the presence of an intact E3 region can enhance cancer cell lysis, progeny release,

and virus spread after several rounds of viral replication (i.e. 7 dpi), but does not enhance cancer cell killing at earlier time points (i.e. 24-48 hpi).

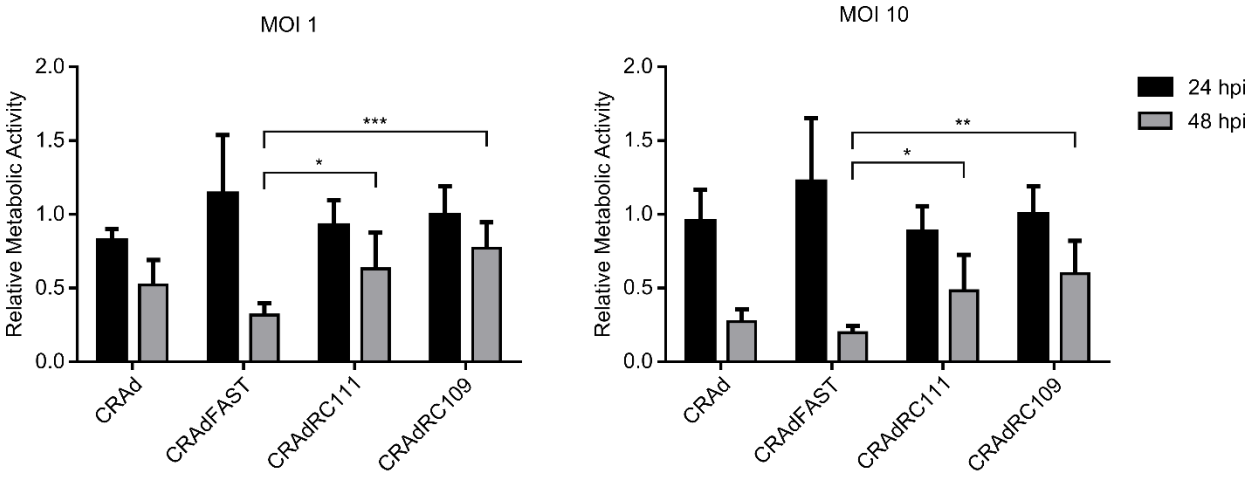
MOI 1
MOI 10
Relative Metabolic Activity
2.0
1.5
1.0
0.5
0.0
***
*
**
*
CRAd
CRAdFAST
CRAdRC111
CRAdRC109
24 hpi
48 hpi

Figure 3.8: CRAdRC111 and CRAdRC109 are less cytotoxic than CRAdFAST. Metabolic activity of A549 cells was measured 24 and 48 hpi with CRAd, CRAdFAST, CRAdRC111, or CRAdRC109 by MTS assay. Values were normalized to mock-infected cells. Three independent experiments (n=3) were performed in triplicate. The values graphed represent the average with error bars denoting standard deviation. *$p<0.05$, **$p=0.0022$, ***$p=0.0001$.

3.3. Discussion

In chapter 3 we developed two CRAds, designated CRAdRC111 (E3-) and CRAdRC109 (E3+), in which the p14 FAST gene was located downstream of the L5 region of the viral genome, creating an L6 transcription unit (Fig 3.1). The p14 FAST expression cassette contained an upstream splice acceptor site to allow for replication-dependent gene expression driven by the MLP, an approach that worked very well for our original CRAdFAST construct (174). Comparing CRAdRC111 and CRAdRC109 vectors to CRAdFAST provided valuable insight regarding the design and construction of "armed" CRAd vectors, in which therapeutic genes are co-expressed from the CRAd with the hope of further improving efficacy. Such knowledge is of particular importance when designing vectors where there is a specific need for higher or lower transgene expression levels, or temporal control of expression.

We observed aberrantly high VP/PFU ratios for our CRAdRC111 virus preparations (Fig 3.2C), indicating that most of the recovered virus was non-infectious. The capsid proteins fiber and penton base were under-represented in the CRAdRC111 purified virus preparations and fiber expression was also decreased in CRAdRC111-infected A549 cells (Fig 3.2D–3.2G). During formation of new virions within the cell, newly synthesized fiber and penton base proteins self-associate in the cytoplasm into trimers and pentamers, respectively, before assembling into the intact penton capsomere that is imported into the nucleus (186, 187). Thus, a reduction in the levels of fiber protein in the cytoplasm may have led to less penton capsomere available to complete the virion, resulting in the excess of defective particles obtained in our virus preparations. It is possible that insertion of the p14 FAST gene as an L6 transcription unit adversely affected expression of the adjacent upstream fiber protein. Previous work has shown that transgene insertion can significantly impact the expression and activity of adjacent viral genes, and that these effects can

vary between different insertions sites within the Ad genome (116). In the case of our CRAdRC111 construct, the L6-encoded p14 FAST protein appeared to be a contributing factor in the substantial reduction of fiber expression. Insertion of the p14 FAST expression cassette could have impacted mRNA splicing and/or stability within the Ad MLTU, leading to reduced expression of the fiber protein.

Previous studies in which the expression of L6-encoded transgenes was regulated by the MLP did not observe reductions in fiber expression or overall viral replication of their Ad vectors (161, 179). For example, insertion of a hyperfusogenic GALV envelope glycoprotein expression cassette in the L6 region of the fusogenic Ad vector developed by Guedan *et al.* did not impair effective virus production, as both the fusogenic Ad and a non-fusogenic control vector were efficiently propagated in 293 cells and had similar infectious titers (161). Fiber expression was also unaffected, as no differences in capsid proteins were detected between purified virions of the fusogenic Ad and the non-fusogenic control vectors. Viral replication in 293 cells was also unchanged between an Ad vector expressing an L6-encoded thymidine kinase and a wild-type control virus (179). As the impact on adjacent viral genes can depend on the nature of the nucleotide sequence of the transgene itself (116), the decrease in fiber expression observed for our CRAdRC111 vector could be specific to the p14 FAST sequence, but not L6-encoded transgenes in general. It is also important to note that the vectors in both of the aforementioned studies contained intact E3 regions upstream of the fiber coding sequence, whereas our CRAdRC111 vector was E3-deleted. As the E3 region is located within the MLTU (191), its presence or absence could potentially have a significant impact on Ad late gene expression. Similar to our CRAdRC111 construct, virus preparations of an E3-deleted CRAd vector containing an L6-encoded immunoRNase also exhibited aberrantly high proportions of defective particles (51). Thus, it is

evident that Ad gene expression can be affected by both upstream and downstream genomic elements flanking the fiber gene, and that there may be some undescribed interplay between the two.

Interestingly, we observed a recovery in fiber expression and a normal VP/PFU ratio for our CRAdRC109 vector, in which the E3 region was reintroduced upstream of the fiber coding sequence and the p14 FAST gene retained in the downstream L6 region (Fig 3.4). This suggests that the decrease in fiber expression for CRAdRC111 was not specific to the p14 FAST nucleotide sequence, but perhaps due to the combined impact of the upstream E3-deletion and the downstream L6-encoded transgene. Inclusion of the E3 region in CRAdRC109 thus provided a genomic context which restored proper fiber expression and improved recovery of infectious virus particles.

Characterization of CRAdRC111 and CRAdRC109 vectors in A549 human lung cancer cells revealed that p14 FAST protein expression was drastically reduced in both viruses relative to CRAdFAST and, as a result, these viruses had a relatively poor ability to cause cell-cell membrane fusion and syncytia formation (Fig 3.5). This observation suggests that relocating p14 FAST from within the E3-deletion in CRAdFAST to the L6 region of the viral genome in CRAdRC111 and CRAdRC109 negatively impacted transgene expression, emphasizing the importance of transgene location on protein expression and overall vector efficacy. These results also show that although reinsertion of the E3 region in CRAdRC109 was able to improve fiber expression and overall viral replication, it had no impact on expression of the L6-encoded p14 FAST protein. Efficient expression from the MLP for transgenes inserted between the L5 fiber and E4 coding regions, including GFP (180), thymidine kinase (179), and a hyperfusogenic GALV envelope glycoprotein (161), has been previously achieved via inclusion of adenoviral splice acceptor sequences upstream of the transgene, similar to the structure of our viruses. Heterologous splice acceptors

(51) and promoters (192) have also been used to achieve expression from this region. In the context of fusogenic Ad vectors, insertion of the Ad IIIa splice acceptor and a hyperfusogenic GALV envelope glycoprotein gene within the L6 region resulted in transgene expression levels that were sufficient to mediate extensive cell-cell fusion in 293 cells (161), however, it is possible that GALV can cause cell fusion at lower concentrations than p14 FAST. In the case of our CRAdRC111 and CRAdRC109 vectors, p14 FAST protein expression from the L6 region might be improved by "fusing" the p14 FAST sequence to the fiber gene via IRES or "self-cleaving" 2A peptides, such that both proteins are co-expressed from a single polycistronic mRNA (116, 121). The use of alternative splice acceptor sequences (117) or inclusion of a heterologous promoter might also improve p14 FAST protein expression (192). Alternatively, insertion of the p14 FAST gene at other positions within the Ad MLTU may allow for superior protein expression (118). These cloning strategies will be important to consider when developing future fusogenic CRAd vector constructs.

As previously mentioned, CRAdRC109 and CRAdRC111 caused minimal cell-cell fusion in A549 cancer cells, due to poor p14 FAST protein expression from the L6 region in these vectors (Fig 3.5). These observations are consistent with the results obtained with our non-replicating AdFAST vector construct, which only caused fusion of A549 cells at relatively high MOI (173), suggesting that a certain threshold of p14 FAST expression is required for cell-cell membrane fusion and syncytia formation. The p14 FAST protein oligomerizes into homomultimeric "fusion platforms" (166, 193), which could potentially explain why relatively high-level protein expression is required for efficient cell-cell fusion and syncytia formation.

Plaque-forming assays in A549 cells revealed that vectors containing the E3 region had notably larger plaque-sizes than E3-deleted vectors at 7 dpi (Fig 3.6). CRAdRC109 also exhibited

increased oncolytic activity relative to the E3-deleted CRAd and CRAdRC111 in a CPE assay (Fig 3.7). These results indicate that inclusion of the E3 region did improve viral lysis and cell-cell spread in A549 cancer cells at later time points. It is important to note that, aside from ADP, proteins encoded by the E3 region have immunomodulatory properties (133), and should thus only significantly impact vector efficacy in an immunocompetent cancer model. As some of the E3 proteins can affect the innate antiviral immune response of infected cells (134), we cannot completely exclude that E3 proteins other than ADP also contribute to increased viral lysis and cell-cell spread in A549 cell culture. However, our findings are consistent with previous work showing that the small plaque phenotype is specific to ADP-deletion mutants (144), and is also consistent with studies in which overexpression of ADP in the absence of other E3 proteins improved the efficacy of oncolytic Ad vectors (85, 145). Therefore, the improved viral spread and cancer cell killing of CRAdRC109 relative to CRAd and CRAdRC111 are likely attributed to the expression of ADP from this vector. As previously mentioned, ADP is required for efficient virus-mediated cell lysis, release of progeny, and subsequent spreading to neighbouring cells (52). Ads containing ADP lyse cells beginning at 2-3 dpi, whereas cells infected with ADP-deleted vectors began to lyse only at 5-6 dpi (52, 144), which is consistent with the reduced cytotoxicity of our ADP-deleted vectors CRAd and CRAdRC111 at 7 dpi. Despite lacking ADP and having a smaller plaque size, CRAdFAST exhibited superior efficacy in CPE assays, suggesting that extensive cell-cell fusion and syncytia formation causes greater cytotoxicity to cancer cells than ADP expression.

We have previously shown that treatment of A549 cells with CRAdFAST results in significant reductions in cellular metabolic activity (174). In this study, CRAdRC111 and CRAdRC109 were significantly less effective at reducing metabolic activity of A549 cells than CRAdFAST (Fig 3.8). These results illustrate that the effects of our fusogenic CRAd vectors on

cellular metabolic activity are largely determined by the level of p14 FAST protein expression and the extent of virus-mediated cell-cell fusion. Furthermore, we show that the E3-encoded proteins did not significantly impact metabolic activity of infected cells, at least at time points ≤ 48 hpi. Other studies have shown that A549 cells infected with Ad vectors encoding E3 and/or ADP exhibit greater decreases in metabolic activity compared to those infected with E3- and/or ADP-deleted vectors, however, only at very late time points (≥ 3 dpi) (52, 141, 142). Suzuki *et al.* showed that A549 cells infected with E3+ vectors exhibited greater decreases in metabolic activity at 9 dpi than those infected with E3-deleted vectors (142). Tollefson *et al*. showed that A549 cells infected with ADP-expressing viruses exhibited decreased metabolic activity starting at 3 dpi and were completely dead by 5 dpi, whereas cells infected with ADP-deleted viruses retained 90% of their initial metabolic activity at 5 dpi (52). Additionally, Zou *et al.* reported that treatment of A549 cells with Ad vectors overexpressing ADP caused greater reductions in cellular metabolic than wild-type or ADP-deleted vectors at 5-6 dpi (194). Consistent with these studies, the impact of E3 and/or ADP expression on the oncolytic activity of our vectors was apparent at 7 dpi in plaque-forming (Fig 3.6) and CPE assays (Fig 3.7), but not during analysis of cellular metabolic activity at 1-2 dpi (Fig 3.8). Thus, while ADP expression improves oncolytic activity at later time points, it appears that extensive cell-cell fusion and syncytia formation mediated by p14 FAST expression provides a faster and superior oncolytic effect.

Our results described in chapter 3 illustrate how the context in which viral genes are placed greatly impacts their expression and overall vector efficacy. Specifically, we showed that L6-encoded transgenes had substantially reduced expression relative to transgenes inserted within the E3-deletion. In the context of our CRAdRC111 and CRAdRC109 vectors, poor expression of the L6-encoded p14 FAST protein led to a substantial decrease in the ability of these viruses to fuse

cells, which thereby reduced overall vector efficacy relative to CRAdFAST. However, we observed that inclusion of the E3 region in CRAdRC109 significantly improved viral lysis and spread relative to the E3-deleted CRAdRC111 and non-fusogenic CRAd vectors, and therefore increased overall oncolytic activity; an effect which was likely attributed to the expression of ADP. Thus, improved vector design is required to achieve efficient co-expression of both p14 FAST and ADP from CRAd in order to truly evaluate potential synergistic efficacy, which we explore in the following chapter.

CHAPTER 4: Evaluating the oncolytic efficacy of an E3-deleted CRAd vector co-expressing p14 FAST and ADP *in vitro*

4.1. Introduction

Studies have shown that overexpression of ADP from oncolytic Ad vectors (in the absence of other E3 proteins) improves cancer cell lysis, release of progeny virions, and viral spread, which ultimately enhances oncolytic vector efficacy (85, 145). As p14 FAST protein was efficiently expressed from our CRAdFAST vector (174), we hypothesized that a similar vector construct encoding both p14 FAST and ADP within the E3-deletion would allow for efficient co-expression of both proteins, and lead to enhanced vector efficacy. We thus developed a CRAd vector encoding a bicistronic p14 FAST/ADP expression cassette in place of the E3 region and evaluated its oncolytic activity in the A549 human lung cancer cell line.

4.2. Results

4.2.1. Developing a fusogenic CRAd vector with a bicistronic expression cassette encoding p14 FAST and ADP within the E3-deletion

In an attempt to achieve efficient co-expression of ADP and p14 FAST from a CRAd vector, we developed CRAdRC116, a fusogenic CRAd vector in which the E3 region of the viral genome was removed and replaced with a bicistronic expression cassette containing HA epitope-tagged p14 FAST and FLAG epitope-tagged ADP coding sequences separated by a "self-cleaving" P2A peptide sequence derived from porcine teschovirus-1 (Fig 4.1). The "self-cleaving" 2A peptides were first identified in viral polyproteins from picornaviruses and range from 18-22 amino acids in length (183, 195). Studies have shown that 2A peptides function through a ribosomal-skipping mechanism, in which formation of the Gly-Pro peptide bond at the C-terminus of the 2A peptide is impaired, causing the ribosome to "skip" to the next codon and continue downstream

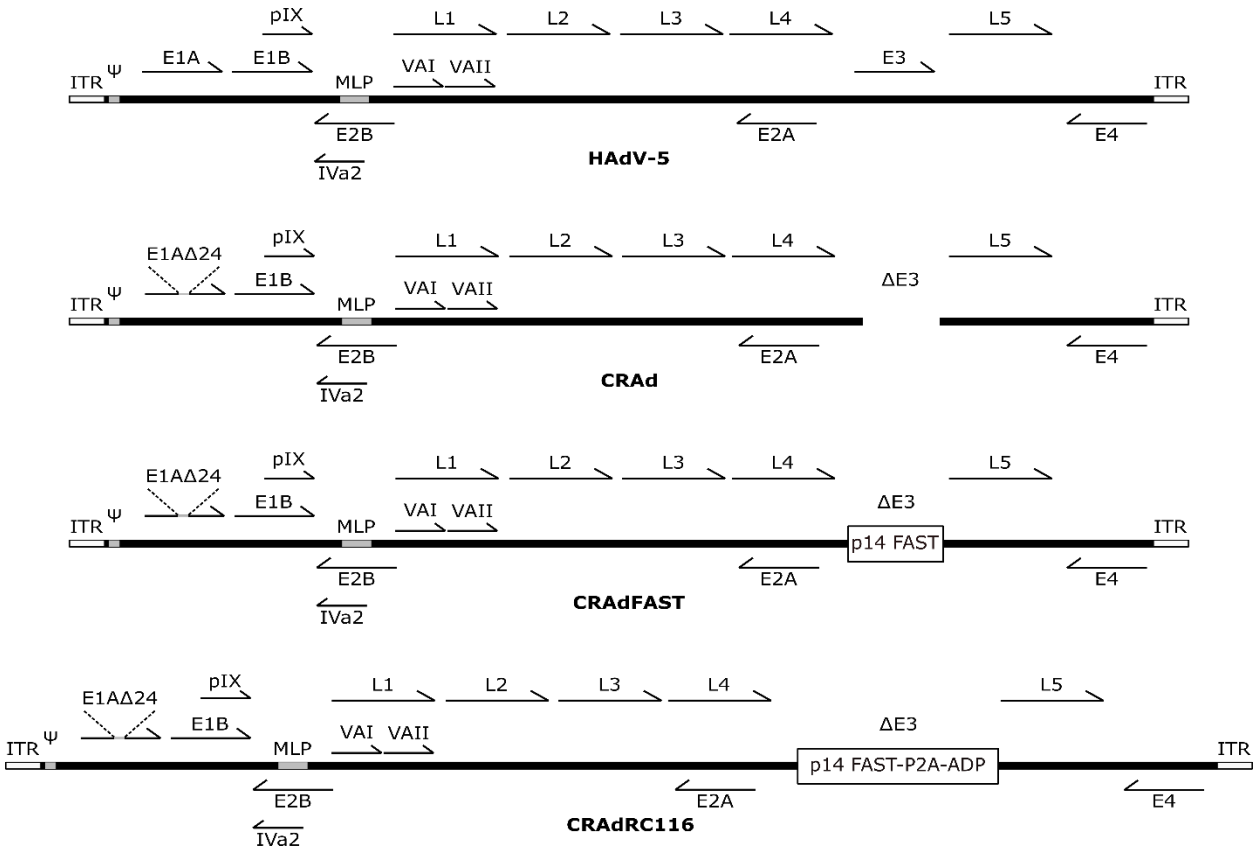
pIX
L1
L2
L3
L4
L5
E1A
E1B
VAI
VAII
E3
ITR
Ψ
MLP
ITR
E2B
E2A
E4
IVa2
HAdV-5
E1AΔ24
ΔE3
CRAd
p14 FAST
CRAdFAST
p14 FAST-P2A-ADP
CRAdRC116

Figure 4.1: Viral genome structure of the adenovirus vectors used in chapter 4. HAdV-5 = wild-type human adenovirus C serotype 5. The E1AΔ24 mutation allows for preferential replication in cancer cells deficient in the Rb tumor-suppressor pathway. The E3 region in CRAdFAST is removed and replaced with an HA-tagged p14 FAST expression cassette. The presence of a splice acceptor (SA) DNA element upstream of the p14 FAST gene allows for replication-dependent expression of the protein. The E3 region in CRAdRC116 is removed and replaced with a bicistronic expression cassette containing HA-tagged p14 FAST and FLAG-tagged ADP genes, separated by a "self-cleaving" P2A peptide. The bicistronic expression cassette also contains an upstream SA for replication-dependent expression. ITR denotes the inverted terminal repeats, MLP denotes the major late promoter, and Ψ represents the packaging element. The genome maps are not shown to scale.

translation, effectively "cleaving" the upstream and downstream peptides (196). Although internal ribosome entry sites (IRES) have been extensively used in multigene expression systems, they are fairly large (>500 bp in length), and expression of the gene downstream of the IRES is considerably lower relative to the upstream gene (183). We chose to use a 2A peptide instead of an IRES as they are much smaller in size (~60-70 bp), have a cleavage efficiency of nearly 100%, and allow equimolar expression of the flanking proteins (197). Several groups have also used 2A peptides to achieve multigene expression from Ad vectors (121, 198, 199).

CRAdRC116 was easily rescued upon transfection of 293 cells with linearized plasmid containing the genomic viral DNA. Large-scale purification of CRAdRC116 generated a vector stock with an infectious titer of $5.4x10^9$ plaque-forming units (PFU) per mL and VP/PFU ratio of 79, which was sufficient for *in vitro* characterization.

4.2.2. CRAdRC116 efficiently replicates in A549 cells and co-expresses p14 FAST and ADP

To investigate viral replication and transgene expression of CRAdRC116, A549 cells were infected with CRAdFAST or CRAdRC116 at an MOI of 1, cell lysates were harvested 24 and 48 hpi and subjected to immunoblot analysis. As shown in Fig 4.2, expression of fiber, a viral structural protein expressed only after viral DNA replication, was detected in both CRAdFAST and CRAdRC116-infected cells and increased from 24 to 48 hpi. Fiber protein levels were slightly elevated in CRAdRC116-infected cells relative to CRAdFAST-infected cells at both time points, which could be due to small differences in the titers of the two virus stocks, or could indicate that CRAdRC116 replicates with greater efficiency compared to CRAdFAST. When normalized to fiber expression, expression of p14 FAST protein was reduced approximately 12- and 4.5-fold in CRAdRC116-infected cells relative to CRAdFAST-infected cells at 24 and 48 hpi, respectively. Importantly, the increase in molecular weight of the p14 FAST signal observed in CRAdRC116-

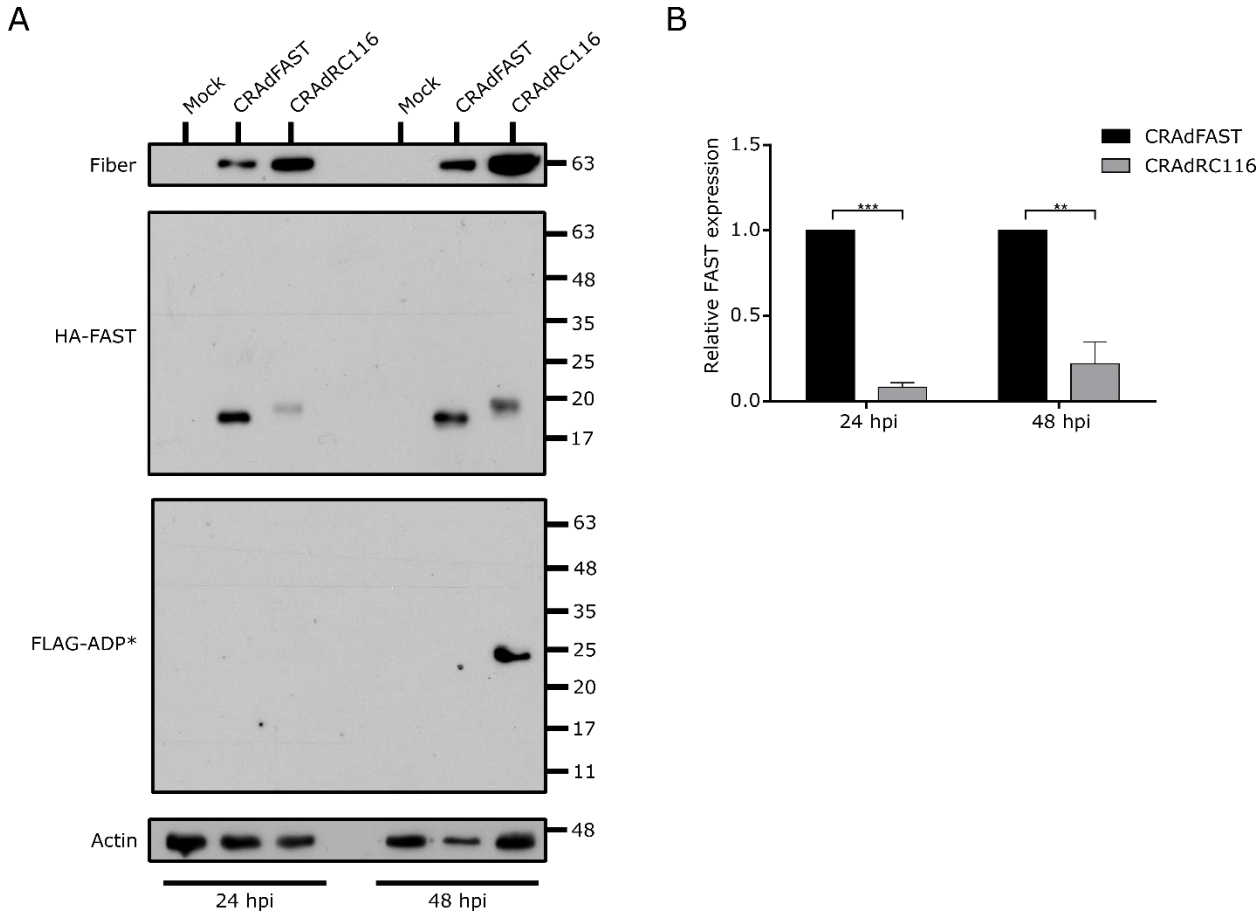
A
Mock
CRAdFAST
CRAdRC116
Mock
CRAdFAST
CRAdRC116
Fiber
63
HA-FAST
63
48
35
25
20
17
FLAG-ADP*
63
48
35
25
20
17
11
Actin
48
24 hpi
48 hpi
B
CRAdFAST
CRAdRC116
Relative FAST expression
1.5
1.0
0.5
0.0
***
**
24 hpi
48 hpi

Figure 4.2: CRAdRC116 efficiently replicates in A549 cells and co-expresses both p14 FAST and ADP. A) A549 cells were infected with CRAdFAST or CRAdRC116 at an MOI of 1 PFU/cell, or mock-treated with PBS. Immunoblot analysis was conducted on whole cell lysates harvested at 24 and 48 hpi. Samples were probed for fiber, HA epitope-tagged p14 FAST, FLAG epitope-tagged ADP, and actin as a loading control. Expression of p14 FAST is reduced in CRAdRC116-infected cells relative to CRAdFAST-infected cells. Expression of ADP from CRAdRC116 is detectable by 48 hpi. Uncleaved p14 FAST/ADP fusion protein was not detected. Two independent experiments were performed (n=2) and representative results are shown. *In order to obtain a detectable signal, blots probed for FLAG epitope-tagged ADP were loaded with twice as much sample relative to blots probed for fiber, actin, and HA-tagged FAST. B) Densitometric analysis showing decreased p14 FAST expression from CRAdRC116 relative to CRAdFAST. p14 FAST signal intensities were normalized to fiber signal intensities. ***p=0.0005, **p=0.001.

infected cells likely results from the addition of residual P2A peptide onto the C-terminus of p14 FAST, suggesting that the P2A peptide is indeed "cleaving" at its C-terminal Gly-Pro peptide bond. Previous studies have shown that although ADP has a predicted size of 10.5kDa in HAdV-5 (200), it undergoes extensive post-translational modification (i.e. glycosylation) resulting in protein products that migrate as higher molecular weight bands of ~20-30kDa on SDS-PAGE (201). Expression of the FLAG-tagged ADP from our CRAdRC116 construct was detectable by 48 hpi at a molecular weight of ~20-25kDa, which is consistent with its cleavage from the upstream p14 FAST protein via the P2A peptide and subsequent post-translational modification. These results confirm that our CRAdRC116 vector can replicate efficiently in A549 cancer cells, and that the bicistronic expression cassette permits co-expression of both p14 FAST protein and ADP.

4.2.3. Bicistronic expression of p14 FAST and ADP from CRAdRC116 alters the kinetics of cell-cell fusion compared to CRAdFAST

Expression of p14 FAST protein from CRAdRC116 was reduced relative to CRAdFAST (Fig 4.2), which could negatively impact the fusogenic activity of the virus. As shown in Fig 4.3, both CRAdFAST and CRAdRC116 were able to induce cell-cell fusion and syncytia formation in A549 cells at an MOI of 1 PFU/cell, although the kinetics of fusion differed between the two viruses. CRAdFAST-infected monolayers were extensively fused by 24 hpi and exhibited complete cytopathic effect by 48 hpi. In contrast, small regions of fusion were observed in CRAdRC116-infected cells at 24 hpi, and while CRAdRC116-infected cells were extensively fused by 48 hpi, syncytia were still largely intact and adherent to the plate at this time point. Complete cytopathic effect (CPE) was, however, achieved in CRAdRC116-infected cells by 72 hpi (data not shown). These results are consistent with the observed decrease in p14 FAST protein

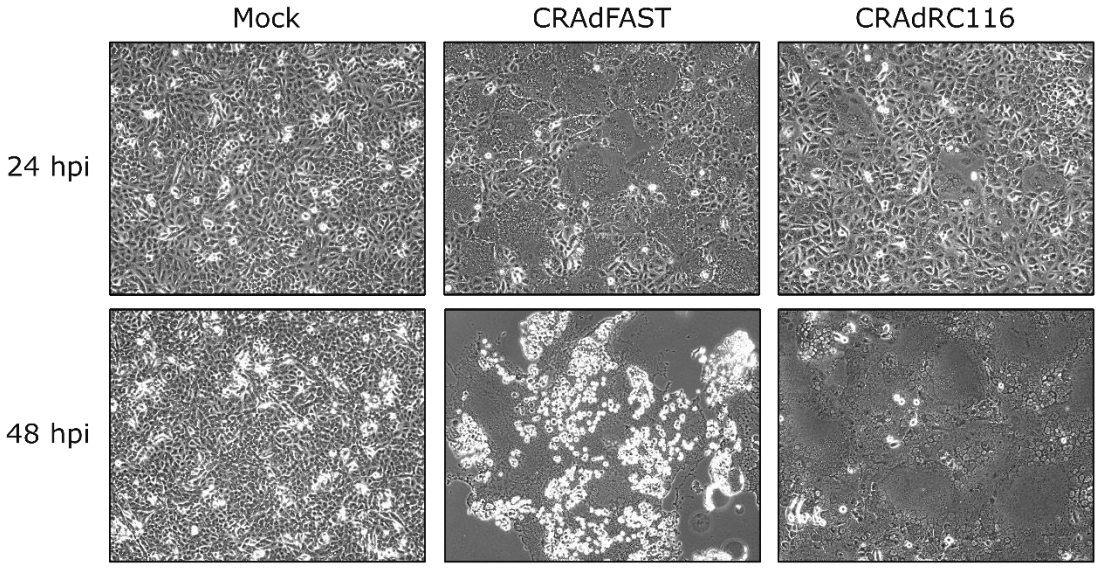
Mock
CRAdFAST
CRAdRC116
24 hpi
48 hpi

Figure 4.3: Bicistronic expression of p14 FAST and ADP from CRAdRC116 alters the kinetics of cell-cell fusion compared to CRAdFAST. Phase-contrast microscopy images of A549 cells 24 and 48 hpi with CRAdFAST or CRAdRC116 at an MOI of 1 PFU/cell, or mock-treated with PBS. CRAdFAST-infected monolayers were extensively fused by 24 hpi and exhibited complete cytopathic effect by 48 hpi. In contrast, minimal fusion was observed in CRAdRC116-infected cells at 24 hpi. Extensive fusion and syncytia formation were observed by 48 hpi in CRAdRC116-infected cells, however, syncytia remained intact and adherent at this time point. Two independent experiments were performed (n=2) and representative results are shown.

expression from CRAdRC116 relative to CRAdFAST (Fig 4.2), and also suggest that expression of ADP from CRAdRC116 did not cause any marked increase in CPE of infected cells. In summary, p14 FAST protein was expressed less efficiently from the bicistronic p14 FAST-P2A-ADP expression cassette of CRAdRC116 relative to CRAdFAST, which reduced the rate of cell-cell fusion and syncytia formation in A549 cell culture, and co-expression of ADP did not appear to have a noticeable effect on vector efficacy in this assay.

4.2.4. ADP expression does not improve cell-cell spread of fusogenic CRAd encoding the p14 FAST protein

Several studies have shown that overexpression of ADP enhances oncolytic Ad vector efficacy (85, 145, 194). ADP improves lysis and release of progeny virions from infected cells, which ultimately enhances viral spread (52). To determine whether expression of ADP improves viral spread of our CRAd vectors, plaque assays were conducted in A549 cells infected with HAdV-5, CRAd, CRAdFAST, or CRAdRC116. Infected cells were overlayed with semi-viscous CMC overlay media to limit viral spread to adjacent cells, thus allowing plaque formation (189). Consistent with our results from chapter 3, and several other studies (52, 85, 144), the ADP-expressing human Ad C serotype 5 (HAdV-5) formed large comet-shaped plaques at 7 dpi in A549 cells, whereas the ADP-deleted, non-fusogenic CRAd exhibited a small plaque phenotype (Fig 4.4). Unexpectedly, ADP expression did not impact plaque morphology in the context of our fusogenic CRAd vectors, as both CRAdFAST and CRAdRC116 formed relatively small plaques at 7 dpi in A549 cells (Fig 4.4A). Analysis of plaque morphology at higher magnification by bright-field microscopy showed that both CRAdFAST and CRAdRC116 formed syncytial plaques of relatively similar morphology and size (Fig 4.4B). Results from this assay demonstrate that ADP increases plaque size of non-fusogenic Ad when expressed at wild-type levels, but has no impact

A

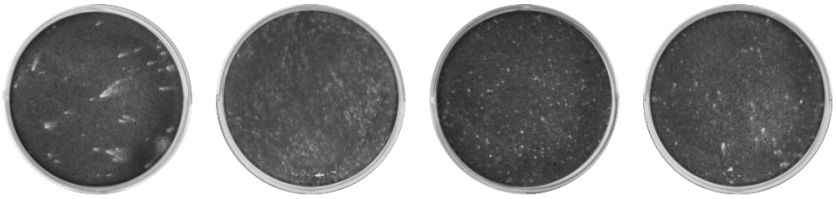

HAdV-5
ADP+/FAST-

CRAd
ADP-/FAST-

CRAdFAST
ADP-/FAST+

CRAdRC116
ADP+/FAST+

B

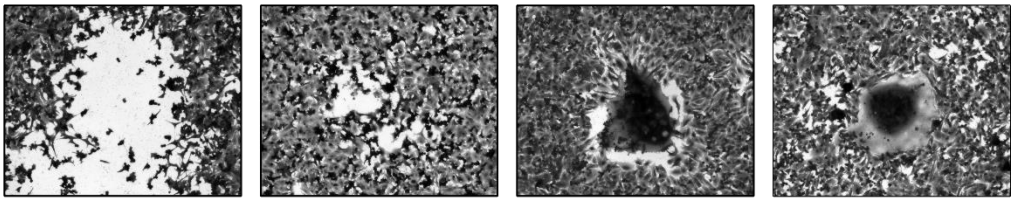

HAdV-5 CRAd CRAdFAST CRAdRC116

Figure 4.4: CRAdFAST and CRAdRC116 have similar plaque morphology. A) Plaque-forming assay of Ad vectors under carboxymethylcellulose (CMC) overlay. A549 cells were infected with ten-fold serial dilutions of various Ad vectors. Infected cells were fixed and stained with crystal violet 7 dpi. Only HAdV-5 formed large comet-shaped plaques. B) Bright-field microscopy images of viral plaques showing that ADP expression increase plaque size of non-fusogenic Ad, but does not impact syncytial plaque morphology of the fusogenic CRAdFAST or CRAdRC116.

on plaque morphology of fusogenic CRAd in which p14 FAST is co-expressed at levels sufficient to induce syncytia formation, at least at the level of ADP expression achieved with CRAdRC116.

We further examined the impact of ADP expression on virus spread through an *in vitro* CPE assay. A549 cells were infected with HAdV-5, CRAd, CRAdFAST, or CRAdRC116 at MOI ranging from 0.01-10 PFU/cell, overlayed with liquid medium, followed by crystal violet staining at 7 dpi. When delivered at low MOI, Ad must undergo multiple cycles of infection, replication, lysis, and spread to adjacent cells in order to achieve complete CPE of the monolayer, whereas complete CPE can be achieved after one round of replication at high MOI (85). This assay thus measures cell lysis, progeny release, and virus spread by identifying and comparing the dose at which complete monolayer CPE is obtained between various vectors. At an MOI of 1, HAdV-5 caused significant CPE and exhibited greater potency than the ADP-deleted non-fusogenic CRAd in A549 cells (Fig 4.5). CRAdFAST (ADP-) was able to mediate complete CPE of the monolayer at an MOI of 0.1. CRAdRC116, which expresses both p14 FAST and ADP, achieved complete monolayer CPE at an MOI of 1. At an MOI of 0.1, the monolayer in CRAdRC116-infected cells remained largely intact, yet appeared extensively fused when examined by phase-contrast microscopy (data not shown). Thus, while co-expression of ADP and p14 FAST from CRAdRC116 improves virus spread relative to non-fusogenic HAdV-5 (ADP+) and CRAd (ADP-), it does not improve virus spread relative to CRAdFAST, which only encodes p14 FAST.

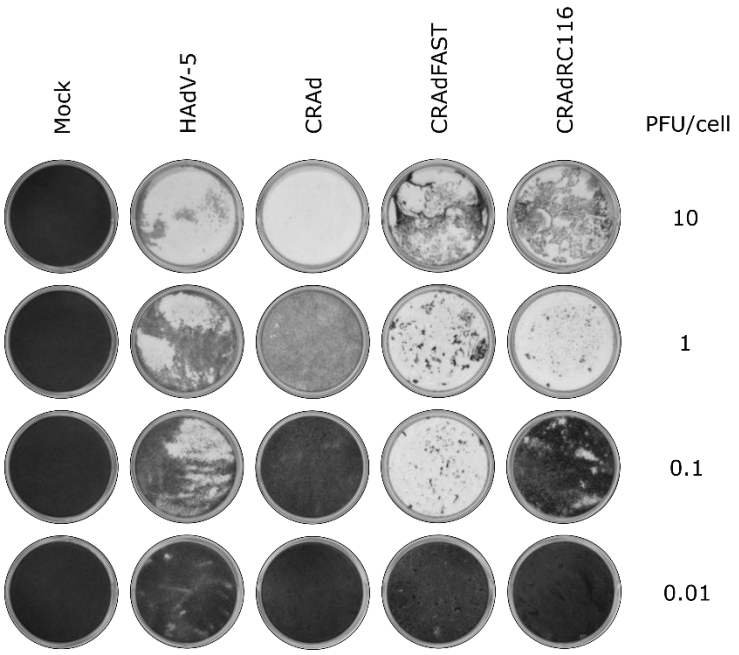
Mock
HAdV-5
CRAd
CRAdFAST
CRAdRC116
PFU/cell
10
1
0.1
0.01

Figure 4.5: ADP expression does not improve cell-cell spread of CRAdRC116 relative to CRAdFAST. *In vitro* CPE assay in A549 cells. A549 cells were infected with HAdV-5, CRAd, CRAdFAST, or CRAdRC116 at an MOI of 0.01-10 PFU/cell. Infected cells were fixed and stained with crystal violet 7 dpi. Evidence of virus-induced cytopathic effect was ~10-fold lower in cells infected with ADP-deleted CRAd, relative to cells infected with ADP-expressing HAdV-5. CRAdFAST caused complete CPE of the monolayer at an MOI of 0.1, whereas the monolayer in CRAdRC116-infected cells is mostly adherent at this dose. Three independent experiments were performed (n=3) and representative results are shown.

4.2.5. ADP expression does not enhance cytotoxicity of fusogenic CRAd encoding p14 FAST

Our lab previously reported that treatment of A549 cells with a non-replicating Ad vector encoding p14 FAST (i.e. AdFAST) led to significant reductions in cellular metabolic activity (173). We subsequently showed that replication-competent CRAdFAST decreased metabolic activity of A549 cells to a significantly greater extent than non-fusogenic CRAd (174). To determine if expression of ADP would enhance cytotoxicity of a fusogenic CRAd vector in which p14 FAST is expressed at levels sufficient to induce extensive cell-cell fusion and syncytia formation, we treated A549 cells with non-fusogenic CRAd, CRAdFAST, or CRAdRC116 at an MOI of 10 PFU/cell, and measured metabolic activity at 24, 48 and 72 hpi via MTS assay. As shown in Fig 4.6, no significant decreases in metabolic activity were observed in any of the infected cells relative to mock-treated cells at 24 hpi. By 48 hpi, CRAdFAST-infected cells exhibited the greatest decrease in metabolic activity at ~23% relative to mock-treated cells, which was significantly lower than the relative metabolic activity of CRAd- and CRAdRC116-infected cells, which were ~68% and ~74%, respectively. By 72 hpi, metabolic activity of all infected cells was less than 30% relative to mock-treated cells, with no statistically significant differences observed between any of the three viruses. These results illustrate that inclusion of ADP does not further improve cytotoxicity of a CRAd vector with modest fusogenic activity mediated by p14 FAST expression.

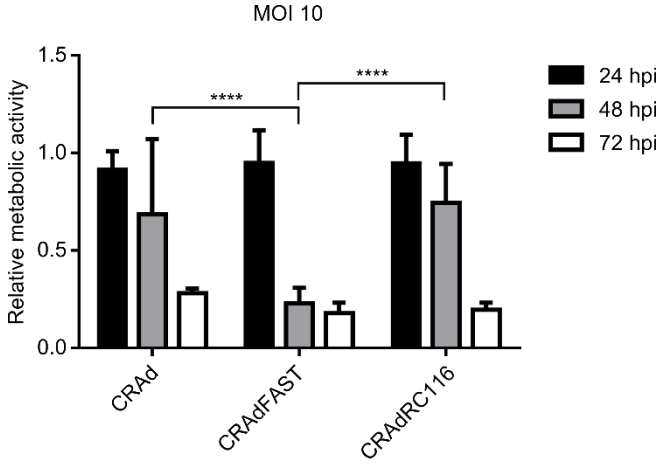
MOI 10
Relative metabolic activity
1.5
1.0
0.5
0.0
****
****
24 hpi
48 hpi
72 hpi
CRAd
CRAdFAST
CRAdRC116

Figure 4.6: ADP expression does not increase cytotoxicity of CRAdRC116 relative to CRAdFAST. Metabolic activity of A549 cells was measured by MTS assay at 24 and 48 hpi with CRAd, CRAdFAST, or CRAdRC116 at an MOI of 10 PFU/cell. Values were normalized to mock-infected cells. Three independent experiments (n=3) were performed in triplicate. The values graphed represent the average with error bars denoting standard deviation. ****$p<0.0001$.

4.3 Discussion

In chapter 4, we developed an oncolytic Ad vector, designated CRAdRC116, in which the E3 region of the viral genome was removed and replaced with a bicisctronic expression cassette containing the p14 FAST and ADP genes separated by a "self-cleaving" P2A peptide. Similar to our CRAdFAST construct (174), a splice acceptor sequence was included at the 5' end of the bicistronic expression cassette in CRAdRC116 to allow for replication-dependent gene expression regulated by the MLP. Results from this study provide general insight regarding the molecular design of "armed" CRAd vectors and illustrate that replication-dependent, multigene expression can be achieved from within an E3-deletion through the use of expression cassettes containing a splice acceptor and 2A peptides.

Although replication-dependent co-expression of p14 FAST and ADP was achieved from our CRAdRC116 vector construct (Fig 4.2), p14 FAST protein expression was notably reduced relative to our original CRAdFAST construct. Furthermore, CRAdRC116 induced cell-cell membrane fusion and syncytia formation in A549 cancer cells, yet with a somewhat poorer efficiency (i.e. at a slower rate) than CRAdFAST (Fig 4.3). This observation demonstrates that the altered kinetics of fusion in CRAdRC116-infected cells are likely attributable to reduced p14 FAST expression from this virus. These findings are consistent with our previous work in which the fusogenic activity of p14 FAST was tightly correlated with the level of its expression. In A549 cells, our E1-deleted, replication-defective AdFAST vector only caused fusion of A549 cells at relatively high MOI (173). Similarly, minimal cell-cell fusion was observed in A549 cells treated with our replication-competent CRAdRC111 and CRAdRC109 vectors described in chapter 3, in which p14 FAST was poorly expressed from the L6 region (Fig 3.5). This suggests that p14 FAST protein functions in a stoichiometric manner, which is in accordance with the theory that a certain

threshold of expression is required to induce cell-cell membrane fusion and syncytia formation. Previous work has shown that the p14 FAST-mediated fusion pathway involves oligomerization of p14 FAST protein into homomultimeric "fusion platforms"(166, 193). Perhaps the formation of these p14 FAST protein complexes and their ability to mediate cell-cell fusion requires relatively high concentrations of p14 FAST protein.

It is unclear why p14 FAST protein was expressed with lower efficiency from CRAdRC116 relative to CRAdFAST. The p14 FAST gene is encoded within the same position of the viral genome (i.e. the E3-deletion) and expressed as a part of the major late transcription unit (MLTU), which is regulated by the MLP, in both vectors. Furthermore, the p14 FAST gene in both constructs is preceded by an upstream Ad40 long fiber splice acceptor sequence, which should ensure efficient splicing in both constructs. ADP activity could have negatively impacted p14 FAST expression, as Tollefson *et al.* showed that Ad late protein synthesis declined ~2 dpi and was undetectable by ~3 dpi in wild-type Ad-infected cells which express endogenous levels of ADP, whereas late protein synthesis was still increasing at ~3 dpi in cells infected with an ADP-deleted Ad vector (52). In our studies, reduced expression of p14 FAST from CRAdRC116 was observed at 24 hpi (Fig 4.2), which is well before the decline in late protein synthesis observed by Tollefson *et al.* Additionally, fiber expression in CRAdRC116-infected cells increased from 24 to 48 hpi, illustrating that late protein synthesis was still increasing at these time points. Unsuccessful ribosomal-skipping in 2A peptide constructs can lead to the production of a fusion protein (202), which in our case could account for the reduced detection of a discrete p14 FAST protein product. However, we did not detect any uncleaved p14 FAST/ADP protein products in our studies, suggesting that unsuccessful cleavage and production of FAST/ADP fusion protein is not a contributing factor. Therefore, it is likely that the inherent properties of the bicistronic expression

cassette strategy employed in CRAdRC116 are responsible for the reduction in p14 FAST protein expression. Perhaps mRNA stability or translation efficiency of the bicistrionic p14 FAST-P2A-ADP mRNA is reduced relative to the monocistronic p14 FAST mRNA, which led to decreased p14 FAST protein expression from the former.

Several studies have shown that ADP enhances oncolytic Ad vector efficacy (85, 145, 194), however, this was not observed in our CRAdRC116 construct. As there are no antibodies commercially-available for ADP, we attached a FLAG epitope to the C-terminus of ADP in CRAdRC116 to allow for its detection by immunoblot. Addition of a FLAG epitope to the C-terminus of ADP could have negatively impacted protein function, which would explain why we did not observe any enhanced vector efficacy from ADP expression in CRAdRC116. ADP is a $N_{endo}C_{exo}$ nuclear membrane glycoprotein, with the N-terminal half of the protein residing in the lumen, and the C-terminal half residing in the cytoplasm/nucleoplasm (143). Mutation studies have shown that viruses containing deletions within the cytoplasmic-nucleoplasmic domain of ADP typically retain their lytic capacity, whereas mutations in the lumenal domain greatly reduced cell lysis (203). We strategically placed the FLAG epitope at the C-terminus of ADP in our construct to minimize any potential impact on cell lysis. However, ADP containing mutations within the cytoplasmic-nucleoplasmic domain can exhibit aberrant subcellular localization (203). Thus, we cannot exclude that the addition of a FLAG epitope to the C-terminus of ADP in our construct impacted subcellular localization and/or protein activity. Placing the ADP gene downstream of the P2A peptide sequence in our construct results in the C-terminal proline of the P2A peptide being incorporated on to the N-terminus of ADP. This N-terminal proline might impact the function of ADP, yet this is unlikely as there are no previous reports of deleterious effects resulting from this addition in 2A peptide-sequence containing constructs developed by other investigators (197).

The order in which p14 FAST and ADP are arranged in our bicistronic 2A expression cassette may have impaired ADP function by impacting its subcellular localization. An effect known as "slipstreaming" can occur in 2A constructs, in which targeted proteins containing a signal sequence, when encoded upstream of the 2A peptide sequence, lead to aberrant shuttling of the downstream protein through the ribosome-translocon complex formed by the N-terminal signal sequence (197). For example, a polycistronic construct containing a protein with an N-terminal signal sequence encoded upstream and protein without signal sequence positioned downstream of the 2A peptide sequence resulted in both proteins being translocated into the endoplasmic reticulum (ER) (204). Despite lacking a cleavable N-terminal signal peptide, the transmembrane domain of FAST proteins serves as a reverse signal anchor and directs insertion into ER membrane in an $N_{exo}C_{cyto}$ orientation (205), which may cause mislocalization of downstream proteins in the context of a bicistronic 2A construct. ADP is a $N_{endo}C_{exo}$ integral membrane protein and has been shown to localize to the Golgi apparatus and ER, where it undergoes extensive post-translational modification (143). From >30 hpi, ADP accumulates at the nuclear membrane, where it is thought to exert its function in promoting cell death (52). Therefore, it is possible that in the context of our bicistronic 2A expression cassette, p14 FAST is negatively impacting the localization and/or post-translational processing of ADP, ultimately preventing its ability to promote cell lysis. In support of this, cells infected with ADP mutants which had aberrant post-translational processing and/or localization also frequently exhibited altered kinetics of cell lysis (203). While switching the gene order in our construct such that ADP is positioned upstream of the 2A peptide sequence may rescue ADP function, it may similarly reduce p14 FAST function and fusogenic activity of the vector.

Alternatively, the lack of enhanced oncolytic efficacy in our CRAdRC116 construct relative to CRAdFAST could be due to insufficient expression of ADP. Although expression of

p14 FAST was detected in CRAdRC116-infected cells at 24 hpi, FLAG-tagged ADP was only detected at 48 hpi (Fig 4.2), which might indicate that ADP is inefficiently expressed from the bicistronic p14 FAST-P2A-ADP expression cassette of our CRAdRC116 construct. While 2A peptides are typically described as providing stoichiometric or equimolar expression of flanking proteins (197), one of the possible outcomes of the 2A peptide-mediated cleavage process is translation of the upstream protein and successful ribosomal skipping, but subsequent ribosomal dissociation and discontinued translation of the downstream sequence (202). This could explain why expression of p14 FAST, but not ADP, is detected at 24 hpi. Indeed, a systematic comparison of 2A peptides conducted by Liu *et al*. found that proteins positioned downstream of the 2A peptide sequence exhibited reductions in expression of 70-95% relative to the upstream protein (202).

In wild-type Ad, ADP is produced in small amounts from the E3 promoter during the early stages of infection, yet synthesized abundantly from the MLP during the late stages of infection (52), and is thus thought to function in a stoichiometric manner (203). This suggests that relatively high levels of ADP expression are required to promote cell lysis and progeny release. Due to a lack of commercially-available antibody for ADP, we do not know how ADP expression from CRAdRC116 compares to HAdV-5, which represents a major limitation of our studies. We are currently developing a wild-type HAdV-5 vector containing a FLAG-epitope tagged ADP to address this issue.

Tollefson *et al.* showed that ADP expression was detected in abundance by 20-25 hpi through immunoprecipitation and immunoblot analyses of KB cells infected with *rec*700, a wild-type-like recombinant HAdV-5 which contains the HAdV-2 version of ADP (201). However, the KB cells in this study were infected at very high MOI (50-200 PFU/cell), whereas the A549 cells in our study were infected with our CRAdRC116 construct at much lower MOI (1 PFU/cell).

Doronin *et al*. later showed that expression of ADP was detectable by immunoblot at 24 hpi in A549 cells infected with CRAd vectors KD1 and KD3, which overexpress ADP relative to wild-type Ad, however, cells in this study were also infected at high MOI (50 PFU/cell) (85). It is also important to note that in both of the aforementioned studies (85, 201), and several other studies (143, 145, 147, 194, 206), ADP expression was probed with a rabbit polyclonal antibody raised against ADP from HAdV-2. In contrast, ADP in our CRAdRC116 construct was FLAG-conjugated to allow for detection with mouse anti-FLAG monoclonal antibody. Thus, differences in antibody specificity and/or sensitivity may account for the observed variability in detecting ADP expression by immunoblot in our study relative to previous work.

In agreement with our results, Yun *et al.* showed that ADP expression was detected at 48 hpi, but not at 24 hpi, in A549 cells infected with YKL-mADP, a CRAd vector in which ADP expression was achieved by insertion of an extra copy of the MLP promoter upstream of the ADP gene. With the exception of E3-12.5K and ADP, all other E3 genes were deleted from this vector. Furthermore, plaques formed by YKL-mADP were much smaller than those formed by wild-type Ad, which is consistent with the results obtained for CRAdRC116 in our plaque assays (Fig. 4.4) and provides additional evidence that ADP must be expressed in abundance to achieve efficient cell lysis, progeny release, and virus spread.

It is also possible that the extensive syncytia formation induced by expression of p14 FAST from CRAdRC116 abrogates the lytic activity of ADP, which would also explain why ADP expression did not improve vector efficacy. In support of this, we previously showed in chapter 3 that ADP expression did improve the oncolytic efficacy of CRAdRC109, which only expressed p14 FAST at relatively low levels and thus caused minimal cell-cell fusion.

In summary, while expression of fusogenic proteins or the ADP have been independently shown to enhance the oncolytic efficacy of CRAd vectors, our results demonstrate that expression of the fusogenic p14 FAST protein from the ADP-deleted CRAdFAST provided greater oncolytic effect than co-expression of both ADP and p14 FAST protein from CRAdRC116. We showed that this is partly due to a reduction in p14 FAST protein expression from CRAdRC116, and a resulting decrease in the fusogenic activity of this vector, relative to CRAdFAST. Additionally, the bicistronic p14 FAST-P2A-ADP expression cassette in CRAdRC116 may have led to relatively poor expression, alterations in post-translational processing, and/or aberrant subcellular localization of ADP, which would also explain why ADP expression did not enhance oncolytic efficacy of this vector.

CHAPTER 5: Conclusions and future directions

Taken together, the results from our studies illustrate that ADP expression, in the context of fusogenic CRAd vectors encoding FAST proteins, enhanced oncolytic efficacy when FAST was expressed at lower levels (i.e. CRAdRC109 vs CRAdRC111), however, it did not enhance oncolytic efficacy when FAST was expressed at levels sufficient to mediate extensive cell-cell fusion and syncytia formation (i.e. CRAdRC116 vs CRAdFAST). Furthermore, while the newly developed vectors described in this study, namely CRAdRC111, CRAdRC109, and CRAdRC116, had improved oncolytic efficacy relative to non-fusogenic CRAd, none exhibited further improvements in efficacy when compared to our original CRAdFAST construct.

It is possible that the mechanisms by which we achieved co-expression of FAST and ADP from our various vectors either did not allow for sufficient expression of both proteins, or perhaps negatively impacted their activity, such that they did not further enhance oncolytic activity relative to CRAdFAST. If this is true, future studies should focus on improving vector design in order to achieve efficient co-expression of ADP and FAST from CRAd, while ensuring that the function of these proteins is not impaired. This could involve placing FAST and ADP in alternate regions of the viral genome and/or using different approaches to achieve protein co-expression, such as IRES or inclusion of heterologous promoters.

Alternatively, it could be that ADP and FAST proteins simply do not act synergistically, in terms of enhancing oncolytic efficacy, when co-expressed from CRAd vectors. For example, FAST-mediated cell-cell fusion and syncytia formation might impair the ability of ADP to enhance cell lysis, progeny release, and virus spread. Similarly, expression of ADP might impair the fusogenic activity of FAST proteins. If this is indeed the case, future studies should perhaps focus on combining other methods of improving efficacy of oncolytic Ad, including the use of CRAd

vectors encoding extracellular matrix-degrading enzymes, junction-opening peptides, or pro-apoptotic proteins (124, 132), in conjunction with ADP or FAST protein expression.

REFERENCES

1. **Stewart BW, Wild CP.** 2014. World cancer report 2014. Lyon, France: International Agency for Research on Cancer. World Health Organization**:**630.
2. **Hanahan D, Weinberg RA.** 2000. The hallmarks of cancer. Cell **100:**57-70.
3. **Hanahan D, Weinberg RA.** 2011. Hallmarks of cancer: the next generation. Cell **144:**646-674.
4. **Whiteside TL.** 2008. The tumor microenvironment and its role in promoting tumor growth. Oncogene **27:**5904.
5. **World Health Organization.** 2018. Cancer. [Online.]
6. **Kaufman HL, Kohlhapp FJ, Zloza A.** 2015. Oncolytic viruses: a new class of immunotherapy drugs. Nat Rev Drug Discov **14:**642.
7. **Keller BA, Bell JC.** 2016. Oncolytic viruses—immunotherapeutics on the rise. J Mol Med **94:**979-991.
8. **Russell SJ, Peng K-W, Bell JC.** 2012. Oncolytic virotherapy. Nat Biotechnol **30:**658.
9. **de Graaf JF, de Vor L, Fouchier RAM, van den Hoogen BG.** 2018. Armed oncolytic viruses: a kick-start for anti-tumor immunity. Cytokine Growth Factor Rev **41:**28-39.
10. **Seymour LW, Fisher KD.** 2016. Oncolytic viruses: finally delivering. Br J Cancer **114:**357.
11. **Kelly E, Russell SJ.** 2007. History of oncolytic viruses: genesis to genetic engineering. Mol Ther **15:**651-659.
12. **Liu T-C, Galanis E, Kirn D.** 2007. Clinical trial results with oncolytic virotherapy: a century of promise, a decade of progress. Nat Clin Pract Oncol **4:**101.
13. **Fukuhara H, Ino Y, Todo T.** 2016. Oncolytic virus therapy: a new era of cancer treatment at dawn. Cancer science **107:**1373-1379.
14. **Alemany R, Balagué C, Curiel DT.** 2000. Replicative adenoviruses for cancer therapy. Nat biotechnol **18:**723.
15. **Latchman DS.** 2005. Herpes simplex virus-based vectors for the treatment of cancer and neurodegenerative disease. Curr Opin Mol Ther **7:**415-418.
16. **Nakamura T, Russell SJ.** 2004. Oncolytic measles viruses for cancer therapy. Expert Opin Biol Ther **4:**1685-1692.
17. **Shen Y, Nemunaitis J.** 2005. Fighting cancer with vaccinia virus: teaching new tricks to an old dog. Mol ther **11:**180-195.
18. **Aghi MK, Chiocca EA.** 2009. Phase ib trial of oncolytic herpes virus G207 shows safety of multiple injections and documents viral replication. Mol Ther **17:**8-9.
19. **Andtbacka RHI, Curti BD, Kaufman H, Daniels GA, Nemunaitis JJ, Spitler LE, Hallmeyer S, Lutzky J, Schultz SM, Whitman ED, Zhou K, Karpathy R, Weisberg JI, Grose M, Shafren D.** 2015. Final data from CALM: A phase II study of Coxsackievirus A21 (CVA21) oncolytic virus immunotherapy in patients with advanced melanoma. J Clin Oncol **33:**9030-9030.
20. **Comins C, Spicer J, Protheroe A, Roulstone V, Twigger K, White CL, Vile R, Melcher A, Coffey M, Mettinger K.** 2010. Reo-10: a phase 1 study of intravenous reovirus and docetaxel in patients with advanced cancer. Clin Cancer Res **16:**5564-5572.
21. **Downs-Canner S, Guo ZS, Ravindranathan R, Breitbach CJ, O'malley ME, Jones HL, Moon A, McCart JA, Shuai Y, Zeh HJ.** 2016. Phase 1 study of intravenous oncolytic poxvirus (vvDD) in patients with advanced solid cancers. Mol Ther **24:**1492-1501.

22. **Geletneky K, Hajda J, Angelova AL, Leuchs B, Capper D, Bartsch AJ, Neumann J-O, Schöning T, Hüsing J, Beelte B.** 2017. Oncolytic H-1 parvovirus shows safety and signs of immunogenic activity in a first phase I/IIa glioblastoma trial. Mol Ther **25:**2620-2634.
23. **Heinzerling L, Künzi V, Oberholzer PA, Kündig T, Naim H, Dummer R.** 2005. Oncolytic measles virus in cutaneous T-cell lymphomas mounts antitumor immune responses in vivo and targets interferon-resistant tumor cells. Blood **106:**2287-2294.
24. **Kirn D.** 2001. Oncolytic virotherapy for cancer with the adenovirus dl1520 (Onyx-015): results of Phase I and II trials. Expert Opin Biol Ther **1:**525-538.
25. **Ungerechts G, Bossow S, Leuchs B, Holm PS, Rommelaere J, Coffey M, Coffin R, Bell J, Nettelbeck DM.** 2016. Moving oncolytic viruses into the clinic: clinical-grade production, purification, and characterization of diverse oncolytic viruses. Mol Ther Methods Clin Dev **3:**16018.
26. **National Institutes of Health.** 2018. [Online.]
27. **Babiker HM, Riaz IB, Husnain M, Borad MJ.** 2017. Oncolytic virotherapy including Rigvir and standard therapies in malignant melanoma. Oncolytic Virother **6:**11-18.
28. **Garber K.** 2006. China approves world's first oncolytic virus therapy for cancer treatment. J Natl Cancer Inst **98:**298-300.
29. **Greig SL.** 2016. Talimogene laherparepvec: first global approval. Drugs **76:**147-154.
30. **Rehman H, Silk AW, Kane MP, Kaufman HL.** 2016. Into the clinic: talimogene laherparepvec (T-VEC), a first-in-class intratumoral oncolytic viral therapy. J Immunother Cancer **4:**53.
31. **Verheije MH, Rottier P.** 2012. Retargeting of viruses to generate oncolytic agents. Adv Virol **2012:**798526.
32. **Meyers DE, Wang AA, Thirukkumaran CM, Morris DG.** 2017. Current immunotherapeutic strategies to enhance oncolytic virotherapy. Front Oncol **7:**114.
33. **Patel MR, Kratzke RA.** 2013. Oncolytic virus therapy for cancer: the first wave of translational clinical trials. Transl Res **161:**355-364.
34. **Pol J, Buqué A, Aranda F, Bloy N, Cremer I, Eggermont A, Erbs P, Fucikova J, Galon J, Limacher J-M.** 2016. Trial Watch—Oncolytic viruses and cancer therapy. Oncoimmunology **5:**e1117740.
35. **Maroun J, Muñoz-Alía M, Ammayappan A, Schulze A, Peng K-W, Russell S.** 2017. Designing and building oncolytic viruses. Future Virol **12:**193-213.
36. **Martin NT, Bell JC.** 2018. Oncolytic Virus Combination Therapy: Killing One Bird with Two Stones. Mol Ther **26:**1414-1422.
37. **Sampath P, Thorne SH.** 2014. Arming viruses in multi-mechanistic oncolytic viral therapy: current research and future developments, with emphasis on poxviruses. Oncolytic Virother **3:**1-9.
38. **Shaw AR, Suzuki M.** 2016. Recent advances in oncolytic adenovirus therapies for cancer. Curr Opin Virol **21:**9-15.
39. **van Regenmortel MH, Fauquet C, Bishop D, Carstens E, Estes M, Lemon S, Maniloff J, Mayo M, McGeoch D, Pringle C.** 2000. Virus taxonomy: classification and nomenclature of viruses. Seventh report of the International Committee on Taxonomy of Viruses. Academic Press.

40. **Rowe WP, Huebner RJ, Gilmore LK, Parrott RH, Ward TG.** 1953. Isolation of a cytopathogenic agent from human adenoids undergoing spontaneous degeneration in tissue culture. Proc Soc Exp Biol Med **84:**570-573.
41. **Ghebremedhin B.** 2014. Human adenovirus: viral pathogen with increasing importance. Eur J Microbiol Immunol **4:**26-33.
42. **Saha B, Wong CM, Parks RJ.** 2014. The adenovirus genome contributes to the structural stability of the virion. Viruses **6:**3563-3583.
43. **Kennedy MA, Parks RJ.** 2009. Adenovirus virion stability and the viral genome: size matters. Mol Ther **17:**1664-1666.
44. **Russell WC.** 2009. Adenoviruses: update on structure and function. J Gen Virol **90:**1-20.
45. **Van Oostrum J, Burnett RM.** 1985. Molecular composition of the adenovirus type 2 virion. J Virol **56:**439-448.
46. **Rux JJ, Burnett RM.** 2004. Adenovirus structure. Hum Gene Ther **15:**1167-1176.
47. **Chatterjee PK, Vayda ME, Flint S.** 1986. Identification of proteins and protein domains that contact DNA within adenovirus nucleoprotein cores by ultraviolet light crosslinking of oligonucleotides 32P-labelled in vivo. J Mol Biol **188:**23-37.
48. **Maizel Jr JV, White DO, Scharff MD.** 1968. The polypeptides of adenovirus: II. Soluble proteins, cores, top components and the structure of the virion. Virology **36:**126-136.
49. **Russell W, Laver W, Sanderson P.** 1968. Internal components of adenovirus. Nature **219:**1127.
50. **Guimet D, Hearing P.** 2016. Adenovirus replication, p. 59-84, Adenoviral vectors for gene therapy (Second Edition). Elsevier.
51. **Fernández-Ulibarri I, Hammer K, Arndt MA, Kaufmann JK, Dorer D, Engelhardt S, Kontermann RE, Hess J, Allgayer H, Krauss J.** 2015. Genetic delivery of an immuno RNase by an oncolytic adenovirus enhances anticancer activity. Int J Cancer **136:**2228-2240.
52. **Tollefson AE, Scaria A, Hermiston TW, Ryerse JS, Wold LJ, Wold W.** 1996. The adenovirus death protein (E3-11.6 K) is required at very late stages of infection for efficient cell lysis and release of adenovirus from infected cells. J Virol **70:**2296-2306.
53. **Akusjärvi G, Persson H.** 1981. Controls of RNA splicing and termination in the major late adenovirus transcription unit. Nature **292:**420.
54. **Thomas GP, Mathews MB.** 1980. DNA replication and the early to late transition in adenovirus infection. Cell **22:**523-533.
55. **Larsson S, Svensson C, Akusjärvi G.** 1992. Control of adenovirus major late gene expression at multiple levels. J Mol Biol **225:**287-298.
56. **Vachon VK, Conn GL.** 2016. Adenovirus VA RNA: an essential pro-viral non-coding RNA. Virus Res **212:**39-52.
57. **Christensen JB, Byrd SA, Walker AK, Strahler JR, Andrews PC, Imperiale MJ.** 2008. Presence of the adenovirus IVa2 protein at a single vertex of the mature virion. J Virol **82:**9086-9093.
58. **Parks RJ.** 2005. Adenovirus protein IX: a new look at an old protein. Mol ther **11:**19-25.
59. **Giberson AN, Davidson AR, Parks RJ.** 2011. Chromatin structure of adenovirus DNA throughout infection. Nucleic acids Res **40:**2369-2376.
60. **Bergelson JM, Cunningham JA, Droguett G, Kurt-Jones EA, Krithivas A, Hong JS, Horwitz MS, Crowell RL, Finberg RW.** 1997. Isolation of a common receptor for Coxsackie B viruses and adenoviruses 2 and 5. Science **275:**1320-1323.

61. **Wickham TJ, Mathias P, Cheresh DA, Nemerow GR.** 1993. Integrins αvβ3 and αvβ5 promote adenovirus internalization but not virus attachment. Cell **73:**309-319.
62. **Leopold PL, Ferris B, Grinberg I, Worgall S, Hackett NR, Crystal RG.** 1998. Fluorescent virions: dynamic tracking of the pathway of adenoviral gene transfer vectors in living cells. Hum Gene Ther **9:**367-378.
63. **Greber UF, Willetts M, Webster P, Helenius A.** 1993. Stepwise dismantling of adenovirus 2 during entry into cells. Cell **75:**477-486.
64. **Bischoff JR, Kirn DH, Williams A, Heise C, Horn S, Muna M, Ng L, Nye JA, Sampson-Johannes A, Fattaey A.** 1996. An adenovirus mutant that replicates selectively in p53-deficient human tumor cells. Science **274:**373-376.
65. **Fueyo J, Gomez-Manzano C, Alemany R, Lee PS, McDonnell TJ, Mitlianga P, Shi Y-X, Levin V, Yung WA, Kyritsis AP.** 2000. A mutant oncolytic adenovirus targeting the Rb pathway produces anti-glioma effect in vivo. Oncogene **19:**2.
66. **Heise C, Hermiston T, Johnson L, Brooks G, Sampson-Johannes A, Williams A, Hawkins L, Kirn D.** 2000. An adenovirus E1A mutant that demonstrates potent and selective systemic anti-tumoral efficacy. Nat Med **6:**1134.
67. **Yamamoto M, Curiel DT.** 2010. Current issues and future directions of oncolytic adenoviruses. Mol Ther **18:**243-250.
68. **Parks RJ, Chen L, Anton M, Sankar U, Rudnicki MA, Graham FL.** 1996. A helper-dependent adenovirus vector system: removal of helper virus by Cre-mediated excision of the viral packaging signal. Proc Natl Acad Sci U S A **93:**13565-13570.
69. **Wilson JM.** 1996. Adenoviruses as gene-delivery vehicles. N Engl J Med **334:**1185-1187.
70. **Green M, Daesch GE.** 1961. Biochemical studies on adenovirus multiplication: II. Kinetics of nucleic acid and protein synthesis in suspension cultures. Virology **13:**169-176.
71. **Choi I, Yun C.** 2013. Recent developments in oncolytic adenovirus-based immunotherapeutic agents for use against metastatic cancers. Cancer Gene Ther **20:**70.
72. **Curiel DT.** 2000. The development of conditionally replicative adenoviruses for cancer therapy. Clin Cancer Res **6:**3395-3399.
73. **Wold WS, Ison MG.** 2013. Adenovirus, Fields Virology 6th Edition. Lippincott, Williams & Wilkins.
74. **Cody JJ, Douglas JT.** 2009. Armed replicating adenoviruses for cancer virotherapy. Cancer Gene Ther **16:**473.
75. **Kirn D.** 2000. Replication-selective oncolytic adenoviruses: virotherapy aimed at genetic targets in cancer. Oncogene **19:**6660.
76. **Whyte P, Ruley H, Harlow E.** 1988. Two regions of the adenovirus early region 1A proteins are required for transformation. J Virology **62:**257-265.
77. **Choi J-W, Lee J-S, Kim SW, Yun C-O.** 2012. Evolution of oncolytic adenovirus for cancer treatment. Adv Drug Deliv Rev **64:**720-729.
78. **Toth K, Dhar D, Wold WS.** 2010. Oncolytic (replication-competent) adenoviruses as anticancer agents. Expert Opin Biol Ther **10:**353-368.
79. **Rodriguez R, Schuur ER, Lim HY, Henderson GA, Simons JW, Henderson DR.** 1997. Prostate attenuated replication competent adenovirus (ARCA) CN706: a selective cytotoxic for prostate-specific antigen-positive prostate cancer cells. Cancer Res **57:**2559-2563.

80. **Hallenbeck PL, Chang Y-N, Hay C, Golightly D, Stewart D, Lin J, Phipps S, Chiang YL.** 1999. A novel tumor-specific replication-restricted adenoviral vector for gene therapy of hepatocellular carcinoma. Hum Gene Ther **10:**1721-1733.
81. **Hernandez-Alcoceba R, Pihalja M, Wicha MS, Clarke MF.** 2000. A novel, conditionally replicative adenovirus for the treatment of breast cancer that allows controlled replication of E1a-deleted adenoviral vectors. Hum Gene Ther **11:**2009-2024.
82. **Johnson L, Shen A, Boyle L, Kunich J, Pandey K, Lemmon M, Hermiston T, Giedlin M, McCormick F, Fattaey A.** 2002. Selectively replicating adenoviruses targeting deregulated E2F activity are potent, systemic antitumor agents. Cancer Cell **1:**325-337.
83. **Hernandez-Alcoceba R, Pihalja M, Qian D, Clarke M.** 2002. New oncolytic adenoviruses with hypoxia- and estrogen receptor-regulated replication. Hum Gene Ther **13:**1737-1750.
84. **Huang TG, Savontaus MJ, Shinozaki K, Sauter BV, Woo SLC.** 2003. Telomerase-dependent oncolytic adenovirus for cancer treatment. Gene Ther **10:**1241.
85. **Doronin K, Toth K, Kuppuswamy M, Ward P, Tollefson AE, Wold WS.** 2000. Tumor-specific, replication-competent adenovirus vectors overexpressing the adenovirus death protein. J Virol **74:**6147-6155.
86. **Hubberstey AV, Pavliv M, Parks RJ.** 2002. Cancer therapy utilizing an adenoviral vector expressing only E1A. Cancer Gene Ther **9:**321.
87. **Shtrichman R, Sharf R, Barr H, Dobner T, Kleinberger T.** 1999. Induction of apoptosis by adenovirus E4orf4 protein is specific to transformed cells and requires an interaction with protein phosphatase 2A. Proc Natl Acad Sci U S A **96:**10080-10085.
88. **Toth K, Wold W.** 2010. Increasing the Efficacy of Oncolytic Adenovirus Vectors. Viruses **2:**1844-1866.
89. **Kirn D.** 2001. Clinical research results with dl1520 (Onyx-015), a replication-selective adenovirus for the treatment of cancer: what have we learned? Gene Ther **8:**89.
90. **Kirn D, Hermiston T, Mccormick F.** 1998. ONYX-015: Clinical data are encouraging. Nat Med **4:**1341.
91. **Pesonen S, Kangasniemi L, Hemminki A.** 2010. Oncolytic adenoviruses for the treatment of human cancer: focus on translational and clinical data. Mol Pharm **8:**12-28.
92. **Nemunaitis J, Cunningham C, Buchanan A, Blackburn A, Edelman G, Maples P, Netto G, Tong A, Randlev B, Olson S, Kirn D.** 2001. Intravenous infusion of a replication-selective adenovirus (ONYX-015) in cancer patients: safety, feasibility and biological activity. Gene Ther **8:**746.
93. **Nemunaitis J, Ganly I, Khuri F, Arseneau J, Kuhn J, McCarty T, Landers S, Maples P, Romel L, Randlev B, Reid T, Kaye S, Kirn D.** 2000. Selective replication and oncolysis in p53 mutant tumors with ONYX-015, an E1B-55kD gene-deleted adenovirus, in patients with advanced head and neck cancer: a phase II trial. Cancer Res **60:**6359.
94. **Reid T, Galanis E, Abbruzzese J, Sze D, Wein LM, Andrews J, Randlev B, Heise C, Uprichard M, Hatfield M, Rome L, Rubin J, Kirn D.** 2002. Hepatic arterial infusion of a replication-selective oncolytic adenovirus (dl1520): phase II viral, immunologic, and clinical endpoints. Cancer Res **62:**6070.
95. **Nemunaitis J, Khuri F, Ganly I, Arseneau J, Posner M, Vokes E, Kuhn J, McCarty T, Landers S, Blackburn A.** 2001. Phase II trial of intratumoral administration of ONYX-015, a replication-selective adenovirus, in patients with refractory head and neck cancer. J Clin Oncol **19:**289-298.

96. **Hecht JR, Bedford R, Abbruzzese JL, Lahoti S, Reid TR, Soetikno RM, Kirn DH, Freeman SM.** 2003. A phase I/II trial of intratumoral endoscopic ultrasound injection of ONYX-015 with intravenous gemcitabine in unresectable pancreatic carcinoma. Clin Cancer Res **9:**555-561.
97. **Vasey PA, Shulman LN, Campos S, Davis J, Gore M, Johnston S, Kirn DH, O'Neill V, Siddiqui N, Seiden MV, Kaye SB.** 2002. Phase I trial of intraperitoneal injection of the E1B-55-KD-gene–deleted adenovirus ONYX-015 (dl1520) given on days 1 through 5 every 3 weeks in patients with recurrent/refractory epithelial ovarian cancer. J Clin Oncol **20:**1562-1569.
98. **Harada JN, Berk AJ.** 1999. p53-Independent and-dependent requirements for E1B-55K in adenovirus type 5 replication. J Virol **73:**5333-5344.
99. **Dix BR, Edwards SJ, Braithwaite AW.** 2001. Does the antitumor adenovirus ONYX-015/dl1520 selectively target cells defective in the p53 pathway?. J Virol **75:**5443-5447.
100. **Goodrum FD, Ornelles DA.** 1998. p53 status does not determine outcome of E1B 55-kilodalton mutant adenovirus lytic infection. J Virol **72:**9479-9490.
101. **Rothmann T, Hengstermann A, Whitaker NJ, Scheffner M, zur Hausen H.** 1998. Replication of ONYX-015, a potential anticancer adenovirus, is independent of p53 status in tumor cells. J Virol **72:**9470-9478.
102. **Steegenga WT, Riteco N, Bos JL.** 1999. Infectivity and expression of the early adenovirus proteins are important regulators of wild-type and ΔE1B adenovirus replication in human cells. Oncogene **18:**5032.
103. **Turnell AS, Grand RJA, Gallimore PH.** 1999. The replicative capacities of large E1B-null group A and group C adenoviruses are independent of host cell p53 status. J Virol **73:**2074-2083.
104. **O'Shea CC, Johnson L, Bagus B, Choi S, Nicholas C, Shen A, Boyle L, Pandey K, Soria C, Kunich J.** 2004. Late viral RNA export, rather than p53 inactivation, determines ONYX-015 tumor selectivity. Cancer cell **6:**611-623.
105. **Jiang H, Gomez-Manzano C, Rivera-Molina Y, Lang FF, Conrad CA, Fueyo J.** 2015. Oncolytic adenovirus research evolution: from cell-cycle checkpoints to immune checkpoints. Curr Opin Virol **13:**33-39.
106. **DeWeese TL, van der Poel H, Li S, Mikhak B, Drew R, Goemann M, Hamper U, DeJong R, Detorie N, Rodriguez R.** 2001. A phase I trial of CV706, a replication-competent, PSA selective oncolytic adenovirus, for the treatment of locally recurrent prostate cancer following radiation therapy. Cancer res **61:**7464-7472.
107. **Fujiwara T, Tanaka N, Nemunaitis JJ, Senzer NN, Tong A, Ichimaru D, Shelby SM, Hashimoto Y, Kawamura H, Urata Y.** 2008. Phase I trial of intratumoral administration of OBP-301, a novel telomerase-specific oncolytic virus, in patients with advanced solid cancer: Evaluation of biodistribution and immune response. J Clin Oncol **26:**3572-3572.
108. **Lang FF, Conrad C, Gomez-Manzano C, Yung WKA, Sawaya R, Weinberg JS, Prabhu SS, Rao G, Fuller GN, Aldape KD, Gumin J, Vence LM, Wistuba I, Rodriguez-Canales J, Villalobos PA, Dirven CMF, Tejada S, Valle RD, Alonso MM, Ewald B, Peterkin JJ, Tufaro F, Fueyo J.** 2018. Phase I study of DNX-2401 (Delta-24-RGD) oncolytic adenovirus: replication and immunotherapeutic effects in recurrent malignant glioma. J Clin Oncol **36:**1419-1427.

109. **Nokisalmi P, Pesonen S, Escutenaire S, Ristimaeki A, Joensuu T, Guse K, Saerkioja M, Hemminki A.** 2008. Clinical data from cancer patients treated with triple modified oncolytic adenovirus Ad5/3-Cox2L-D24. Hum Gene Ther **19:**1076-1097.
110. **Pesonen S, Helin H, Nokisalmi P, Escutenaire S, Ribacka C, Sarkioja M, Cerullo V, Guse K, Bauerschmitz G, Laasonen L, Kantola T, Ristimaki A, Rajecki M, Oksanen M, Haavisto E, Kanerva A, Joensuu T, Hemminki A.** 2010. Oncolytic adenovirus treatment of a patient with refractory neuroblastoma. Acta Oncol **49:**120-122.
111. **Pesonen S, Nokisalmi P, Escutenaire S, Särkioja M, Raki M, Cerullo V, Kangasniemi L, Laasonen L, Ribacka C, Guse K, Haavisto E, Oksanen M, Rajecki M, Helminen A, Ristimäki A, Karioja-Kallio A, Karli E, Kantola T, Bauerschmitz G, Kanerva A, Joensuu T, Hemminki A.** 2010. Prolonged systemic circulation of chimeric oncolytic adenovirus Ad5/3-Cox2L-D24 in patients with metastatic and refractory solid tumors. Gene Ther **17:**892.
112. **Small EJ, Carducci MA, Burke JM, Rodriguez R, Fong L, van Ummersen L, Yu DC, Aimi J, Ando D, Working P, Kirn D, Wilding G.** 2006. A phase I trial of intravenous cg7870, a replication-selective, prostate-specific antigen-targeted oncolytic adenovirus, for the treatment of hormone-refractory, metastatic prostate cancer. Mol Ther **14:**107-117.
113. **Tejada S, Díez-Valle R, Domínguez PD, Patiño-García A, González-Huarriz M, Fueyo J, Gomez-Manzano C, Idoate MA, Peterkin J, Alonso MM.** 2018. DNX-2401, an oncolytic virus, for the treatment of newly diagnosed diffuse intrinsic pontine gliomas: a case report. Front Oncol **8:**61.
114. **Loskog A.** 2015. Immunostimulatory gene therapy using oncolytic viruses as vehicles. Viruses **7:**5780-5791.
115. **Bett A, Prevec L, Graham F.** 1993. Packaging capacity and stability of human adenovirus type 5 vectors. J Virol **67:**5911-5921.
116. **Rivera AA, Wang M, Suzuki K, Uil TG, Krasnykh V, Curiel DT, Nettelbeck DM.** 2004. Mode of transgene expression after fusion to early or late viral genes of a conditionally replicating adenovirus via an optimized internal ribosome entry site in vitro and in vivo. Virology **320:**121-134.
117. **Alemany R.** 2016. Molecular design of oncolytic adenoviruses, p. 319-334, Adenoviral vectors for gene therapy (Second Edition). Elsevier.
118. **Jin F, Kretschmer PJ, Hermiston TW.** 2005. Identification of novel insertion sites in the Ad5 genome that utilize the Ad splicing machinery for therapeutic gene expression. Mol Ther **12:**1052-1063.
119. **Carette JE, Graat HC, Schagen FH, El Hassan MAA, Gerritsen WR, van Beusechem VW.** 2005. Replication-dependent transgene expression from a conditionally replicating adenovirus via alternative splicing to a heterologous splice-acceptor site. J Gene Med **7:**1053-1062.
120. **Sauthoff H, Pipiya T, Heitner S, Chen S, Norman RG, Rom WN, Hay JG.** 2002. Late expression of p53 from a replicating adenovirus improves tumor cell killing and is more tumor cell specific than expression of the adenoviral death protein. Hum Gene Ther **13:**1859-1871.
121. **Funston GM, Kallioinen SE, de Felipe P, Ryan MD, Iggo RD.** 2008. Expression of heterologous genes in oncolytic adenoviruses using picornaviral 2A sequences that trigger ribosome skipping. J Gen Virol **89:**389-396.

122. **Lang FF, Bruner JM, Fuller GN, Aldape K, Prados MD, Chang S, Berger MS, McDermott MW, Kunwar SM, Junck LR.** 2003. Phase I trial of adenovirus-mediated p53 gene therapy for recurrent glioma: biological and clinical results. J Clin Oncol **21:**2508-2518.
123. **Sauthoff H, Hu J, Maca C, Goldman M, Heitner S, Yee H, Pipiya T, Rom WN, Hay JG.** 2003. Intratumoral spread of wild-type adenovirus is limited after local injection of human xenograft tumors: virus persists and spreads systemically at late time points. Hum Gene Ther **14:**425-433.
124. **Smith E, Breznik J, Lichty BD.** 2011. Strategies to enhance viral penetration of solid tumors. Hum Gene Ther **22:**1053-1060.
125. **Ganly I, Kirn D, Eckhardt SG, Rodriguez GI, Soutar DS, Otto R, Robertson AG, Park O, Gulley ML, Heise C.** 2000. A phase I study of Onyx-015, an E1B attenuated adenovirus, administered intratumorally to patients with recurrent head and neck cancer. Clin Cancer Res **6:**798-806.
126. **Choi I, Lee Y, Yoo J, Yoon A, Kim H, Kim D, Seidler D, Kim J, Yun C.** 2010. Effect of decorin on overcoming the extracellular matrix barrier for oncolytic virotherapy. Gene ther **17:**190.
127. **Ganesh S, Gonzalez Edick M, Idamakanti N, Abramova M, VanRoey M, Robinson M, Yun C-O, Jooss K.** 2007. Relaxin-expressing, fiber chimeric oncolytic adenovirus prolongs survival of tumor-bearing mice. Cancer Res **67:**4399.
128. **Guedan S, Rojas JJ, Gros A, Mercade E, Cascallo M, Alemany R.** 2010. Hyaluronidase expression by an oncolytic adenovirus enhances its intratumoral spread and suppresses tumor growth. Mol Ther **18:**1275-1283.
129. **Kim J-H, Lee Y-S, Kim H, Huang J-H, Yoon AR, Yun C-O.** 2006. Relaxin expression from tumor-targeting adenoviruses and its intratumoral spread, apoptosis induction, and efficacy. J Natl Cancer Inst **98:**1482-1493.
130. **Vera B, Martínez-Vélez N, Xipell E, Acanda de la Rocha A, Patiño-García A, Saez-Castresana J, Gonzalez-Huarriz M, Cascallo M, Alemany R, Alonso MM.** 2016. Characterization of the antiglioma effect of the oncolytic adenovirus VCN-01. PLoS One **11:**e0147211.
131. **Gros A, Guedan S.** 2010. Adenovirus release from the infected cell as a key factor for adenovirus oncolysis. Open Gene Ther J **3:**24-30.
132. **Del Papa J, Parks RJ.** 2017. Adenoviral vectors armed with cell fusion-inducing proteins as anti-cancer agents. Viruses **9:**13.
133. **Lichtenstein DL, Toth K, Doronin K, Tollefson AE, Wold WS.** 2004. Functions and mechanisms of action of the adenovirus E3 proteins. Int Rev Immunol **23:**75-111.
134. **Burgert H-G, Maryanski JL, Kvist S.** 1987. "E3/19K" protein of adenovirus type 2 inhibits lysis of cytolytic T lymphocytes by blocking cell-surface expression of histocompatibility class I antigens. Proc Natl Acad Sci U S A 84:1356-1360.
135. **Benedict CA, Norris PS, Prigozy TI, Bodmer J-L, Mahr JA, Garnett CT, Martinon F, Tschopp J, Gooding LR, Ware CF.** 2001. Three adenovirus E3 proteins cooperate to evade apoptosis by tumor necrosis factor-related apoptosis-inducing ligand receptor-1 and-2. J Biol Chem 276:3270-3278.
136. **Elsing A, Burgert H-G.** 1998. The adenovirus E3/10.4 K–14.5 K proteins down-modulate the apoptosis receptor Fas/Apo-1 by inducing its internalization. Proc Natl Acad Sci U S A 95:10072-10077.

137. **Tollefson AE, Hermiston TW, Lichtenstein DL, Colle CF, Tripp RA, Dimitrov T, Toth K, Wells CE, Doherty PC, Wold WS.** 1998. Forced degradation of Fas inhibits apoptosis in adenovirus-infected cells. Nature 392:726.
138. **Gooding L, Sofola I, Tollefson A, Duerksen-Hughes P, Wold W.** 1990. The adenovirus E3-14.7 K protein is a general inhibitor of tumor necrosis factor-mediated cytolysis. J Immunol 145:3080-3086.
139. **Danielsson A, Dzojic H, Nilsson B, Essand M.** 2008. Increased therapeutic efficacy of the prostate-specific oncolytic adenovirus Ad [I/PPT-E1A] by reduction of the insulator size and introduction of the full-length E3 region. Cancer Gene Ther **15:**203.
140. **Yu D-C, Chen Y, Seng M, Dilley J, Henderson DR.** 1999. The addition of adenovirus type 5 region E3 enables calydon virus 787 to eliminate distant prostate tumor xenografts. Cancer Res **59:**4200-4203.
141. **Zhu M, Bristol JA, Xie Y, Mina M, Ji H, Forry-Schaudies S, Ennist DL.** 2005. Linked tumor-selective virus replication and transgene expression from E3-containing oncolytic adenoviruses. J Virol **79:**5455-5465.
142. **Suzuki K, Alemany R, Yamamoto M, Curiel DT.** 2002. The presence of the adenovirus E3 region improves the oncolytic potency of conditionally replicative adenoviruses. Clin Cancer Res **8:**3348-3359.
143. **Scaria A, Tollefson AE, Saha SK, Wold WS.** 1992. The E3-11.6 K protein of adenovirus is an Asn-glycosylated integral membrane protein that localizes to the nuclear membrane. Virology **191:**743-753.
144. **Tollefson AE, Ryerse JS, Scaria A, Hermiston TW, Wold WS.** 1996. The E3-11.6-kDa adenovirus death protein (ADP) is required for efficient cell death: characterization of cells infected with adp mutants. Virology **220:**152-162.
145. **Doronin K, Toth K, Kuppuswamy M, Krajcsi P, Tollefson AE, Wold WS.** 2003. Overexpression of the ADP (E3-11.6 K) protein increases cell lysis and spread of adenovirus. Virology **305:**378-387.
146. **Ramachandra M, Rahman A, Zou A, Vaillancourt M, Howe JA, Antelman D, Sugarman B, Demers GW, Engler H, Johnson D, Shabram P.** 2001. Re-engineering adenovirus regulatory pathways to enhance oncolytic specificity and efficacy. Nat Biotechnol **19:**1035.
147. **Yun C-O, Kim E, Koo T, Kim H, Lee Y-s, Kim J-H.** 2004. ADP-overexpressing adenovirus elicits enhanced cytopathic effect by induction of apoptosis. Cancer Gene Ther **12:**61.
148. **Krabbe T, Altomonte J.** 2018. Fusogenic Viruses in Oncolytic Immunotherapy. Cancers **10:**216.
149. **Bateman AR, Harrington KJ, Kottke T, Ahmed A, Melcher AA, Gough MJ, Linardakis E, Riddle D, Dietz A, Lohse CM.** 2002. Viral fusogenic membrane glycoproteins kill solid tumor cells by nonapoptotic mechanisms that promote cross presentation of tumor antigens by dendritic cells. Cancer Res **62:**6566-6578.
150. **Hoffmann D, Bayer W, Grunwald T, Wildner O.** 2007. Intratumoral expression of respiratory syncytial virus fusion protein in combination with cytokines encoded by adenoviral vectors as in situ tumor vaccine for colorectal cancer. Mol Cancer Ther **6:**1942-1950.
151. **Li H, Haviv YS, Derdeyn CA, Lam J, Coolidge C, Hunter E, Curiel DT, Blackwell JL.** 2001. Human immunodeficiency virus type 1-mediated syncytium formation is

compatible with adenovirus replication and facilitates efficient dispersion of viral gene products and de novo-synthesized virus particles. Hum Gene Ther **12:**2155-2165.

152. **Errington F, Jones J, Merrick A, Bateman A, Harrington K, Gough M, O'donnell D, Selby P, Vile R, Melcher A.** 2006. Fusogenic membrane glycoprotein-mediated tumour cell fusion activates human dendritic cells for enhanced IL-12 production and T-cell priming. Gene Ther **13:**138.
153. **Ebert O, Shinozaki K, Kournioti C, Park M-S, García-Sastre A, Woo SL.** 2004. Syncytia induction enhances the oncolytic potential of vesicular stomatitis virus in virotherapy for cancer. Cancer Res **64:**3265-3270.
154. **Fu X, Tao L, Jin A, Vile R, Brenner MK, Zhang X.** 2003. Expression of a fusogenic membrane glycoprotein by an oncolytic herpes simplex virus potentiates the viral antitumor effect. Mol Ther **7:**748-754.
155. **Gainey MD, Manuse MJ, Parks GD.** 2008. A hyperfusogenic F protein enhances the oncolytic potency of a paramyxovirus simian virus 5 P/V mutant without compromising sensitivity to type I interferon. J Virol **82:**9369-9380.
156. **Le Boeuf F, Diallo J-S, McCart JA, Thorne S, Falls T, Stanford M, Kanji F, Auer R, Brown CW, Lichty BD.** 2010. Synergistic interaction between oncolytic viruses augments tumor killing. Mol Ther **18:**888-895.
157. **Takaoka H, Takahashi G, Ogawa F, Imai T, Iwai S, Yura Y.** 2011. A novel fusogenic herpes simplex virus for oncolytic virotherapy of squamous cell carcinoma. Virol J **8:**294.
158. **Dewar RL, Natarajan V, Vasudevachari MB, Salzman NP.** 1989. Synthesis and processing of human immunodeficiency virus type 1 envelope proteins encoded by a recombinant human adenovirus. J Virol **63:**129-136.
159. **Gómez-Treviño A, Castel S, López-Iglesias C, Cortadellas N, Comas-Riu J, Mercade E.** 2003. Effects of adenovirus-mediated SV5 fusogenic glycoprotein expression on tumor cells. J Gene Med **5:**483-492.
160. **Guedan S, Grases D, Rojas J, Gros A, Vilardell F, Vile R, Mercade E, Cascallo M, Alemany R.** 2012. GALV expression enhances the therapeutic efficacy of an oncolytic adenovirus by inducing cell fusion and enhancing virus distribution. Gene Ther **19:**1048.
161. **Guedan S, Gros A, Cascallo M, Vile R, Mercade E, Alemany R.** 2008. Syncytia formation affects the yield and cytotoxicity of an adenovirus expressing a fusogenic glycoprotein at a late stage of replication. Gene Ther **15:**1240.
162. **Hoffmann D, Bayer W, Wildner O.** 2007. In situ tumor vaccination with adenovirus vectors encoding measles virus fusogenic membrane proteins and cytokines. World J Gastroenterol **13:**3063.
163. **Hoffmann D, Bayer W, Wildner O.** 2007. Therapeutic immune response induced by intratumoral expression of the fusogenic membrane protein of vesicular stomatitis virus and cytokines encoded by adenoviral vectors. Int J Mol Med **20:**673-681.
164. **Harrison SC.** 2008. Viral membrane fusion. Nat Struct Mol Biol **15:**690.
165. **Allen C, McDonald C, Giannini C, Peng KW, Rosales G, Russell SJ, Galanis E.** 2004. Adenoviral vectors expressing fusogenic membrane glycoproteins activated via matrix metalloproteinase cleavable linkers have significant antitumor potential in the gene therapy of gliomas. J Gene Med **6:**1216-1227.
166. **Ciechonska M, Duncan R.** 2014. Reovirus FAST proteins: virus-encoded cellular fusogens. Trends Microbiol **22:**715-724.

167. **Dawe S, Corcoran JA, Clancy EK, Salsman J, Duncan R.** 2005. Unusual topological arrangement of structural motifs in the baboon reovirus fusion-associated small transmembrane protein. J Virol **79:**6216-6226.
168. **Corcoran JA, Duncan R.** 2004. Reptilian reovirus utilizes a small type III protein with an external myristylated amino terminus to mediate cell-cell fusion. J Virol **78:**4342-4351.
169. **Salsman J, Top D, Boutilier J, Duncan R.** 2005. Extensive syncytium formation mediated by the reovirus FAST proteins triggers apoptosis-induced membrane instability. J Virol **79:**8090-8100.
170. **Le Boeuf F, Gebremeskel S, McMullen N, He H, Greenshields AL, Hoskin DW, Bell JC, Johnston B, Pan C, Duncan R.** 2017. Reovirus FAST protein enhances vesicular stomatitis virus oncolytic virotherapy in primary and metastatic tumor models. Mol Ther Oncolytics **6:**80-89.
171. **Stojdl DF, Lichty BD, Paterson JM, Power AT, Knowles S, Marius R, Reynard J, Poliquin L, Atkins H, Brown EG.** 2003. VSV strains with defects in their ability to shutdown innate immunity are potent systemic anti-cancer agents. Cancer cell **4:**263-275.
172. **Wong C, Nash L, Del Papa J, Poulin K, Falls T, Bell J, Parks R.** 2016. Expression of the fusogenic p14 FAST protein from a replication-defective adenovirus vector does not provide a therapeutic benefit in an immunocompetent mouse model of cancer. Cancer Gene Ther **23:**355.
173. **Wong CM, Poulin KL, Tong G, Christou C, Kennedy MA, Falls T, Bell JC, Parks RJ.** 2016. Adenovirus-mediated expression of the p14 fusion-associated small transmembrane protein promotes cancer cell fusion and apoptosis in vitro but does not provide therapeutic efficacy in a xenograft mouse model of cancer. PLoS One **11:**e0151516.
174. **Del Papa J, Petryk J, Bell JC, Parks RJ.** 2018. Expression of the p14 fusion-associated small transmembrane protein improves the oncolytic efficacy of a conditionally replicating adenovirus. Submitted.
175. **Graham FL, Smiley J, Russell W, Nairn R.** 1977. Characteristics of a human cell line transformed by DNA from human adenovirus type 5. J Gen Virol **36:**59-72.
176. **Graham F.** 1987. Growth of 293 cells in suspension culture. J Gen Virol **68:**937-940.
177. **Giard DJ, Aaronson SA, Todaro GJ, Arnstein P, Kersey JH, Dosik H, Parks WP.** 1973. In vitro cultivation of human tumors: establishment of cell lines derived from a series of solid tumors. J Natl Cancer Inst **51:**1417-1423.
178. **Chartier C, Degryse E, Gantzer M, Dieterle A, Pavirani A, Mehtali M.** 1996. Efficient generation of recombinant adenovirus vectors by homologous recombination in Escherichia coli. J Virol **70:**4805-4810.
179. **Cascante A, Abate-Daga D, Garcia-Rodriguez L, Gonzalez J, Alemany R, Fillat C.** 2007. GCV modulates the antitumoural efficacy of a replicative adenovirus expressing the Tat8-TK as a late gene in a pancreatic tumour model. Gene Ther **14:**1471.
180. **García-Castro J, Martínez-Palacio J, Lillo R, García-Sánchez F, Alemany R, Madero L, Bueren JA, Ramírez M.** 2005. Tumor cells as cellular vehicles to deliver gene therapies to metastatic tumors. Cancer Gene Ther **12:**341.
181. **Wong CM.** 2015. Improving adenovirus efficacy with p14 fusion associated small transmembrane protein expression for cancer treatment. PhD thesis. Université d'Ottawa / University of Ottawa.
182. **Poulin KL, Lanthier RM, Smith AC, Christou C, Quiroz MR, Powell KL, O'Meara RW, Kothary R, Lorimer IA, Parks RJ.** 2010. Retargeting of adenovirus vectors through

genetic fusion of a single-chain or single-domain antibody to capsid protein IX. J Virol **84:**10074-10086.

183. **Kim JH, Lee S-R, Li L-H, Park H-J, Park J-H, Lee KY, Kim M-K, Shin BA, Choi S-Y.** 2011. High cleavage efficiency of a 2A peptide derived from porcine teschovirus-1 in human cell lines, zebrafish and mice. PLoS One **6:**e18556.
184. **Ross JP, Parks RJ.** 2009. Construction and characterization of adenovirus vectors. Cold Spring Harbor Protocols **2009:**pdb.prot5011.
185. **Mittereder N, March KL, Trapnell BC.** 1996. Evaluation of the concentration and bioactivity of adenovirus vectors for gene therapy. J Virol **70:**7498-7509.
186. **Horwitz MS, Scharff MD, Maizel Jr JV.** 1969. Synthesis and assembly of adenovirus 2: I. Polypeptide synthesis, assembly of capsomeres, and morphogenesis of the virion. Virology **39:**682-694.
187. **Velicer LF, Ginsberg H.** 1970. Synthesis, transport, and morphogenesis of type 5 adenovirus capsid proteins. J Virol **5:**338-352.
188. **Villanueva E, Martí-Solano M, Fillat C.** 2016. Codon optimization of the adenoviral fiber negatively impacts structural protein expression and viral fitness. Sci rep **6:**27546.
189. **Baer A, Kehn-Hall K.** 2014. Viral concentration determination through plaque assays: using traditional and novel overlay systems. J Vis Exp :e52065-e52065.
190. **Simpson GR, Han Z, Liu B, Wang Y, Campbell G, Coffin RS.** 2006. Combination of a fusogenic glycoprotein, prodrug activation, and oncolytic herpes simplex virus for enhanced local tumor control. Cancer Res **66:**4835-4842.
191. **Ramke M, Lee JY, Dyer DW, Seto D, Rajaiya J, Chodosh J.** 2017. The 5′UTR in human adenoviruses: leader diversity in late gene expression. Sci Rep **7:**618.
192. **Chai L, Liu S, Mao Q, Wang D, Li X, Zheng X, Xia H.** 2012. A novel conditionally replicating adenoviral vector with dual expression of IL-24 and arresten inserted in E1 and the region between E4 and fiber for improved melanoma therapy. Cancer Gene Ther **19:**247.
193. **Corcoran JA, Clancy EK, Duncan R.** 2011. Homomultimerization of the reovirus p14 fusion-associated small transmembrane protein during transit through the ER–Golgi complex secretory pathway. J Gen Virol **92:**162-166.
194. **Zou A, Atencio I, Huang W-M, Horn M, Ramachandra M.** 2004. Overexpression of adenovirus E3-11.6 K protein induces cell killing by both caspase-dependent and caspase-independent mechanisms. Virology **326:**240-249.
195. **Ryan MD, King AM, Thomas GP.** 1991. Cleavage of foot-and-mouth disease virus polyprotein is mediated by residues located within a 19 amino acid sequence. J Gen Virol **72:**2727-2732.
196. **Donnelly ML, Luke G, Mehrotra A, Li X, Hughes LE, Gani D, Ryan MD.** 2001. Analysis of the aphthovirus 2A/2B polyprotein 'cleavage'mechanism indicates not a proteolytic reaction, but a novel translational effect: a putative ribosomal 'skip'. J Gen Virol **82:**1013-1025.
197. **Szymczak-Workman AL, Vignali KM, Vignali DA.** 2012. Design and construction of 2A peptide-linked multicistronic vectors. Cold Spring Harbor Protocols **2012:**pdb.ip067876.
198. **Garanina E, Mukhamedshina Y, Salafutdinov I, Kiyasov A, Lima L, Reis H, Palotás A, Islamov R, Rizvanov A.** 2016. Construction of recombinant adenovirus containing

picorna-viral 2A-peptide sequence for the co-expression of neuro-protective growth factors in human umbilical cord blood cells. Spinal Cord **54:**423.

199. **Tan Y, Liang H, Chen A, Guo X.** 2010. Coexpression of double or triple copies of the rabies virus glycoprotein gene using a 'self-cleaving'2A peptide-based replication-defective human adenovirus serotype 5 vector. Biologicals **38:**586-593.
200. **Wold W, Cladaras C, Magie SC, Yacoub N.** 1984. Mapping a new gene that encodes an 11,600-molecular-weight protein in the E3 transcription unit of adenovirus 2. J Virol **52:**307-313.
201. **Tollefson A, Scaria A, Saha SK, Wold W.** 1992. The 11,600-MW protein encoded by region E3 of adenovirus is expressed early but is greatly amplified at late stages of infection. J Virol **66:**3633-3642.
202. **Liu Z, Chen O, Wall JBJ, Zheng M, Zhou Y, Wang L, Vaseghi HR, Qian L, Liu J.** 2017. Systematic comparison of 2A peptides for cloning multi-genes in a polycistronic vector. Sci Rep **7:**2193.
203. **Tollefson AE, Scaria A, Ying B, Wold WS.** 2003. Mutations within the ADP (E3-11.6 K) protein alter processing and localization of ADP and the kinetics of cell lysis of adenovirus-infected cells. J Virol **77:**7764-7778.
204. **de Felipe P, Ryan MD.** 2004. Targeting of proteins derived from self-processing polyproteins containing multiple signal sequences. Traffic **5:**616-626.
205. **Clancy EK, Duncan R.** 2009. Reovirus FAST protein transmembrane domains function in a modular, primary sequence-independent manner to mediate cell-cell membrane fusion. J Virol **83:**2941-2950.
206. **Toth K, Djeha H, Ying B, Tollefson AE, Kuppuswamy M, Doronin K, Krajcsi P, Lipinski K, Wrighton CJ, Wold WS.** 2004. An oncolytic adenovirus vector combining enhanced cell-to-cell spreading, mediated by the ADP cytolytic protein, with selective replication in cancer cells with deregulated wnt signaling. Cancer Res **64:**3638-3644.

CONTRIBUTION OF COLLABORATORS

Certain plasmids listed in the appendix were cloned by Dr. Robin Parks or previous students of the Parks lab. The FAST protein cDNA was obtained from the pVSV-FAST plasmid provided by Dr. John Bell (Ottawa Hospital Research Institute, Ottawa, ON).

Ryan Clarkin

EDUCATION

Sept. 2016 – Oct. 2018 **Master of Science**
Biochemistry – Specialization in Human and Molecular Genetics
University of Ottawa, Ottawa, ON

Sept. 2011 – May 2016 **Honours Bachelor of Science**
Biopharmaceutical Sciences – (Genomics option) (Co-op) (Cum laude)
University of Ottawa, Ottawa, ON

ACADEMIC RESEARCH EXPERIENCE

Sept. 2016 – Oct. 2018

Graduate Research Student
Ottawa Hospital Research Institute, Ottawa, ON
Regenerative Medicine Program – Dr. Robin Parks Laboratory

- Used traditional and Rec-A mediated molecular cloning to develop adenoviral vector DNA constructs, including replication-defective gene therapy vectors and replication-competent oncolytic vectors.
- Generated large-scale purified virus stocks using standard virological techniques.
- Cultured and maintained mammalian cell culture in Biosafety Level 2 environment.
- Evaluated anti-cancer efficacy of oncolytic adenovirus vectors armed with therapeutic transgenes in cancer cell culture through biochemical, molecular biological, and virological techniques (i.e. immunoblotting, microscopy, cellular metabolic activity assay, cytopathic effect assay, plaque assay).
- Prepared 2 manuscripts for publication.

Sept. 2015 – May 2016

Undergraduate Research Student
University of Ottawa, Ottawa, ON
Department of Biology – Dr. Linda Bonen Laboratory

- Completed Honours project on mapping mRNA termini and RNA editing of mitochondrial mRNAs in plants.
- Techniques used include DNA/RNA purification, molecular cloning, PCR, agarose gel electrophoresis, DNA/cDNA sequence analysis.

LABORATORY SKILLS

- Cellular metabolic activity assay (MTS)
- Cytopathic effect assay (crystal violet staining)
- DNA sequence analysis
- Immunoblotting
- Mammalian cell culture
- Microscopy (phase-contrast, bright-field, fluorescence)
- Molecular cloning
- Polymerase chain reaction
- SDS-PAGE
- Virus propagation, purification, transduction
- Viral plaque assay

SCHOLARSHIPS & AWARDS

Graduate awards:

- Excellence Scholarship, uOttawa (2016-2018)
- Queen Elizabeth II Graduate Scholarship in Science and Technology (2016-2017)
- Ontario Graduate Scholarship (2017-2018)
- Ranked 2nd place in MSc Biochemistry category for oral presentation at BMI Seminar Day (2018).

Undergraduate awards:

- Dean's Honour List for the Faculty of Science 2013-2014, 2014-2015, and 2015-2016.

CONFERENCES

- 4th Ottawa International Conference on Neuromuscular Disease and Biology (Ottawa, ON, Canada – September 2017).
- BMI Scientific Symposium (Montebello, QC, Canada – May 2018).
- CSV 2018: the 2nd symposium of the Canadian Society for Virology (Halifax, NS, Canada - June 2018).

POSTER PRESENTATIONS

- Ryan Clarkin, Josh Del Papa, and Robin J. Parks. *Enhancing oncolytic adenovirus efficacy by improving viral spread*. Presented at CSV 2018: the 2nd symposium of the Canadian Society for Virology, June 2018. (Halifax, NS, Canada).
- Ryan Clarkin, Josh Del Papa, and Robin J. Parks. *Enhancing oncolytic adenovirus efficacy by improving viral spread*. Presented at The Ottawa Hospital Department of Medicine Research Day, June 2017. (Ottawa, ON, Canada).
- Ryan Clarkin and Robin J. Parks. *Enhancing adenovirus replication for treatment of cancer.* Presented at Ottawa Hospital Research Institute Research Day, November 2017. (Ottawa, ON, Canada).
- Ryan Clarkin and Robin J. Parks. *Enhancing adenovirus replication for treatment of cancer*. Presented at The Ottawa Hospital Department of Medicine Research Day, June 2017. (Ottawa, ON, Canada).
- Ryan Clarkin and Robin J. Parks. *Enhancing adenovirus replication for treatment of cancer.* Presented at uOttawa BMI Poster Day, May 2017. (Ottawa, ON, Canada).

ORAL PRESENTATIONS

- *Enhancing oncolytic adenovirus efficacy by improving viral spread.* Presented at uOttawa BMI Scientific Symposium, May 2018. (Montebello, QC, Canada).
- *Enhancing oncolytic adenovirus efficacy by improving viral spread*. Presented at uOttawa BMI Seminar Day, February 2018. (Ottawa, ON, Canada).

EMPLOYMENT

May 2016 – Aug. 2016

Biosafety Risk Analyst (FSWEP work-term)
Centre for Biosecurity, Public Health Agency of Canada

- Worked within the Biosafety Risk Assessment team in the Centre for Biosecurity.
- Contributed to the development of pathogen risk assessments on various microorganisms, including bacteria, viruses, fungi, protozoa/protists, parasites, and other biological agents, such as cell lines.
- Learned and applied knowledge of risk factors such as pathogenicity/virulence, pre- and post-exposure measures, communicability, and host range.
- Contributed to the development of Pathogen Data Safety Sheets; technical documents that describe the hazardous properties of human and animal pathogens and the biosafety recommendations for working with these agents in a laboratory setting.

May 2015 – Aug. 2015

Biosafety Risk Analyst (Co-op work-term)
Centre for Biosecurity, Public Health Agency of Canada

Sept. 2014 – Dec. 2014

Lab Technician (Co-op work-term)
Acarology Lab, Agriculture and Agri-Food Canada

- Research program involves studying the diversity and characterization of plant-feeding mites of North America.
- Assessed diversity, distribution, and host preferences of phytophagous mites through morphological (using dissecting microscope) and molecular-based identification.
- Processed plant samples (extraction and sorting of mite specimens from samples; basic identification of mites to family level).
- Preparation of specimens for DNA extraction.
- Participated in molecular analysis of mite specimens (DNA extraction, PCR, agarose gel electrophoresis, sequence analysis).

Feb. 2014 – Aug. 2014

Product Submission Coordinator (Co-op work-term)
Natural and Non-prescription Health Products Directorate, Health Canada

- Performed licensing/refusal/withdrawal of Natural Health Product (NHP) applications.
- Engaged in correspondence with NHP license applicants (answered inquiries, relayed issues, and issued information requests).
- Updated NHP databases and file tracking programs.
- Supervised and trained new student employees.